HU ISSN 1586–2070

JOURNAL OF COMPUTATIONAL AND APPLIED MECHANICS

An Open Access International Journal

Published by the University of Miskolc

VOLUME 12, NUMBER 1 (2017)

MISKOLC UNIVERSITY PRESS

HU ISSN 1586–2070

JOURNAL OF COMPUTATIONAL AND APPLIED MECHANICS

An Open Access International Journal

Published by the University of Miskolc

VOLUME 12, NUMBER 1 (2017)

MISKOLC UNIVERSITY PRESS

Journal of Computational and Applied Mechanics, Vol. 12, No. 1, (2017), pp. 3–18
DOI: 10.32973/jcam.2017.001

A HALF CIRCULAR BEAM BENDING BY RADIAL LOADS

István Ecsedi and Attila Baksa
Institute of Applied Mechanics, University of Miskolc
H-3515 Miskolc-egyetemváros, Hungary
mechecs@uni-miskolc.hu, mechab@uni-miskolc.hu

[Received: December 13, 2016, Accepted: February 8, 2017]

Abstract. Under the plane strain condition a mixed type boundary value problem of a curved beam with rectangular cross section is investigated. The mixed type boundary value problem describes a bending problem of the curved beam made of linearly elastic polar orthotopic material. A minimum strain energy property is proven for the considered bending problem. The solution is based on Castigliano's principle. One- and two-layered curved beams are analysed. The results obtained are compared with those computed by commercial FEM software (Abaqus).

Mathematical Subject Classification: 74K10, 74S05, 76M10
Keywords: Curved beam, layered beam, FEM

1. Introduction

Figure 1 shows the linearly elastic curved beam of rectangular cross section. The governing equations and boundary conditions are formulated in the cylindrical coordinate system $Or\varphi z$. The plane $z = 0$ is the symmetry plane of the curved beam for the geometrical and loading properties. The space occupied by the curved beam is $\overline{B} = B \cup \partial B$. The points of $\overline{B}$ are given by the prescriptions:

$$B = \left\{(r,\, \varphi,\, z) \,\middle|\, a < r < b,\, 0 < \varphi < \pi,\, -t < z < t\right\}, \qquad \partial B = \bigcup_{\mathrm{i}=1}^{6} \partial B_{\mathrm{i}},$$

$$\partial B_{\mathrm{i}} = \left\{(r,\, \varphi,\, z) \,\middle|\, a \le r \le b,\, \varphi = \varphi_i,\, -t \le z \le t,\, \mathrm{i} = 1, 2,\, \varphi_1 = 0,\, \varphi_2 = \pi\right\},$$

$$\partial B_{\mathrm{i}} = \left\{(r,\, \varphi,\, z) \,\middle|\, r = r_{\mathrm{i}},\, 0 \le \varphi \le \pi,\, -t \le z \le t,\, \mathrm{i} = 3, 4,\, r_3 = a,\, r_4 = b\right\},$$

$$\partial B_{\mathrm{i}} = \left\{(r, \varphi,\, z) \,\middle|\, a \le r \le b,\, 0 \le \varphi \le \pi,\, z = z_{\mathrm{i}},\, \mathrm{i} = 5, 6,\, z_5 = -t,\, z_6 = t\right\}.$$

Unit vectors of the cylindrical coordinate system $Or\varphi z$ are denoted by $\boldsymbol{e}_{\mathrm{r}}$, $\boldsymbol{e}_{\varphi}$ and $\boldsymbol{e}_{\mathrm{z}}$ (Figure 1).

Since the beam is in plane strain the displacement vector is of the form $\boldsymbol{u} = u(r, \varphi)\boldsymbol{e}_{\mathrm{r}} + v(r, \varphi)\boldsymbol{e}_{\varphi}$. It is assumed that the material of the curved beam obeys Hooke's law. Its inverse is given by the equations

$$\varepsilon_{\mathrm{r}} = \frac{\partial u}{\partial r} = S_{11}\sigma_{\mathrm{r}} + S_{12}\sigma_{\varphi}, \tag{1.1}$$

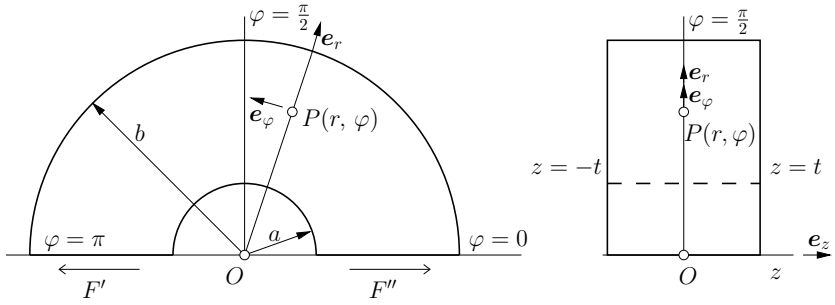

Figure 1. Bending of an orthotropic curved beam of rectangular cross section by radial loads

$$\varepsilon_\varphi = \frac{1}{r}\left(u + \frac{\partial v}{\partial \varphi}\right) = S_{12}\sigma_\mathrm{r} + S_{22}\sigma_\varphi, \tag{1.2}$$

$$\gamma_{\mathrm{r}\varphi} = \frac{1}{r}\left(\frac{\partial u}{\partial \varphi} - v\right) + \frac{\partial v}{\partial r} = S_{66}\tau_{\mathrm{r}\varphi}, \tag{1.3}$$

where ε_r, ε_φ, $\gamma_{\mathrm{r}\varphi}$ are the strains, σ_r, σ_φ, $\tau_{\mathrm{r}\varphi}$ are the stresses and S_{11}, S_{12}, S_{22} and S_{66} are material constants. S_{11}, S_{12}, S_{22} are called reduced flexibility coefficients. Their determination is based on the equations [1, 2]

$$S_{11} = s_{11} - \frac{s_{13}^2}{s_{33}}, \quad S_{12} = s_{12} - \frac{s_{13}s_{23}}{s_{33}}, \quad S_{22} = s_{22} - \frac{s_{23}^2}{s_{33}}$$

in which $s_{11}, \ldots, s_{33}$ are the stiffness components. We would like to emphasize that all quantities, i.e., the displacements, strains and stresses, which appear in equations (1.1), (1.2), (1.3) depend only on the polar coordinates r and φ.

We shall assume that there are no body forces. The considered bending problem is defined by the following boundary conditions (Figure 1)

$$u(r,\,0) = 0, \quad \sigma_\varphi(r,\,0) = 0, \quad a \le r \le b, \tag{1.4}$$

$$u(r,\,\pi) = \frac{\pi}{2}C, \quad \sigma_\varphi(r,\,\pi) = 0, \quad a \le r \le b, \tag{1.5}$$

$$\sigma_\mathrm{r}(a,\,\varphi) = \sigma_\mathrm{r}(b,\,\varphi) = \tau_{\mathrm{r}\varphi}(a,\,\varphi) = \tau_{\mathrm{r}\varphi}(b,\,\varphi) = 0, \quad 0 \le \varphi \le \pi. \tag{1.6}$$

In equation (1.5), C is a given constant ($C \neq 0$).

The stress resultants at the end cross sections $\varphi = 0$ and $\varphi = \pi$ should meet the following conditions:

$$F' = 2t\int_a^b \tau_{\mathrm{r}\varphi}(r,\,\pi)\mathrm{d}r, \qquad F'' = -2t\int_a^b \tau_{\mathrm{r}\varphi}(r,\,0)\mathrm{d}r. \tag{1.7}$$

If the local equilibrium equations are all satisfied are then

$$F' = -F'' = F, \tag{1.8}$$

since there are no body forces and the surface segment $\partial B_3 \cup \partial B_4$ is stress free. It is also obvious that there exists a linear relationship between the stress resultant F and displacement constant C.

2. Minimum strain energy property

We consider a new boundary value problem of curved beams made of orthotopic linearly elastic material. The boundary conditions of the new problem are as follows:

$$\widetilde{u}(r,\,0)=0,\quad \widetilde{\sigma}_{\varphi}(r,\,0)=\widetilde{\sigma}_{\varphi}(r,\,\pi)=0,\qquad a\le r\le b, \tag{2.1}$$

$$F=2t\int\limits_a^b \widetilde{\tau}_{\mathrm{r}\varphi}(r,\,\pi)\mathrm{d}r, \tag{2.2}$$

$$\widetilde{\sigma}_{\mathrm{r}}(a,\,\varphi)=\widetilde{\sigma}_{\mathrm{r}}(b,\,\varphi)=\widetilde{\tau}_{\mathrm{r}\varphi}(a,\,\varphi)=\widetilde{\tau}_{\mathrm{r}\varphi}(b,\,\varphi)=0,\qquad 0\le\varphi\le\pi. \tag{2.3}$$

The radial displacement u at $\varphi=\pi$ is not specified but the stress resultant at the cross section $\varphi=\pi$ is fixed. This boundary value problem has many solutions, it is a relaxed version of the boundary value problem governed by equations (1.4), (1.5), (1.6),(1.7). One solution of the relaxed boundary value problem (2.1), (2.2), (2.3) is $\widetilde{\boldsymbol{u}}=\boldsymbol{u}$, where $\boldsymbol{u}=\boldsymbol{u}(r,\varphi)$ is the unique solution of the bending problem if the boundary conditions are given by equations (1.4), (1.5), (1.6) and (1.7).

Denote U the strain energy of the curved beam. The next theorem formulates a minimum strain energy property of the considered bending problem. Sternberg and Knowles [3] characterized the Saint-Venant extension bending, torsion and flexures problems in terms of certain associated minimum strain energy properties. Here, a similar characterization is formulated for the considered bending problem of the curved beam.

Theorem. For any F $(F\neq 0)$ it holds that

$$U(\boldsymbol{u})\le U(\widetilde{\boldsymbol{u}}), \tag{2.4}$$

where $\widetilde{\boldsymbol{u}}=\widetilde{\boldsymbol{u}}(r,\varphi)$ is an arbitrary solution of the plane strain boundary value problem determined by equations (2.1), (2.2) and (2.3).

Proof. From the definition of the strain energy [4] it follows that

$$U(\widetilde{\boldsymbol{u}})=U(\boldsymbol{u})+U(\widetilde{\boldsymbol{u}}-\boldsymbol{u},\,\boldsymbol{u})+U(\widetilde{\boldsymbol{u}}-\boldsymbol{u}). \tag{2.5}$$

Here, $U(\widetilde{\boldsymbol{u}}-\boldsymbol{u},\,\boldsymbol{u})$ denotes the mixed strain energy defined on the equilibrium displacement fields $\hat{\boldsymbol{u}}=\widetilde{\boldsymbol{u}}-\boldsymbol{u}$ and $\boldsymbol{u}$ (see [4]).

According to Betti's theorem [4] we have

$$\begin{aligned} U(\widetilde{\boldsymbol{u}}-\boldsymbol{u},\,\boldsymbol{u}) &= \frac{\pi}{2}\int\limits_{\partial B_2}\left[\widetilde{\tau}_{\mathrm{r}\varphi}(r,\,\pi)-\tau_{\mathrm{r}\varphi}(r,\,\pi)\right]C\,\mathrm{d}r\,\mathrm{d}z = \\ &= \frac{\pi}{2}\left\{2t\int\limits_a^b\widetilde{\tau}_{\mathrm{r}\varphi}(r,\,\pi)\,\mathrm{d}r-2t\int\limits_a^b\tau_{\mathrm{r}\varphi}(r,\,\pi)\,\mathrm{d}r\right\}C=\frac{\pi}{2}(F-F)C=0. \end{aligned} \tag{2.6}$$

Combination of equation (2.5) with equation (2.6) yields

$$U(\widetilde{\boldsymbol{u}}) = U(\boldsymbol{u}) + U(\widetilde{\boldsymbol{u}} - \boldsymbol{u}). \tag{2.7}$$

Equation (2.7) is the proof of statement (2.4) since the strain energy is always non-negative [4]. Hence $U(\widetilde{\boldsymbol{u}} - \boldsymbol{u}) \geq 0$.

3. Application of Castigliano's principle

The local equilibrium equations for our problem are given by

$$\frac{\partial \sigma_{\mathrm{r}}}{\partial r} + \frac{1}{r}\frac{\partial \tau_{\mathrm{r}\varphi}}{\partial \varphi} + \frac{\sigma_{\mathrm{r}} - \sigma_{\varphi}}{r} = 0, \qquad a < r < b, \quad 0 < \varphi < \pi, \tag{3.1}$$

$$\frac{\partial \tau_{\mathrm{r}\varphi}}{\partial r} + \frac{1}{r}\frac{\partial \sigma_{\varphi}}{\partial \varphi} + \frac{2\tau_{\mathrm{r}\varphi}}{r} = 0, \qquad a < r < b, \quad 0 < \varphi < \pi. \tag{3.2}$$

An equilibrated stress field can be obtained from formulae

$$\sigma_{\mathrm{r}} = \frac{V(r)}{r^2}\sin\varphi, \qquad \sigma_{\varphi} = \frac{1}{r}\frac{\mathrm{d}V}{\mathrm{d}r}\sin\varphi, \qquad \tau_{\mathrm{r}\varphi} = -\frac{V(r)}{r^2}\cos\varphi \tag{3.3}$$

in which $V = V(r)$ is a stress function. Note that the stress boundary conditions $(1.4)_2$, $(1.5)_2$ and the equilibrium equations (3.1), (3.2) are all satisfied. The stress boundary conditions given by (1.6) are also satisfied if

$$V(a) = V(b) = 0\,. \tag{3.4}$$

Then the stress field in terms of $V(r)$ is statically admissible. The total complementary energy of the curved beam can be written in the form [4, 5, 6]

$$\Pi_{\mathrm{c}}(V) = U(V) - W_{\mathrm{u}}, \tag{3.5}$$

where

$$U(V) = \frac{\pi t}{2}\int_a^b \left[S_{11}\left(\frac{V}{r^2}\right)^2 + 2S_{12}\frac{V}{r^3}\frac{\mathrm{d}V}{\mathrm{d}r} + S_{22}\frac{1}{r^2}\left(\frac{\mathrm{d}V}{\mathrm{d}r}\right)^2 + S_{66}\left(\frac{V}{r^2}\right)^2\right] r\,\mathrm{d}r, \tag{3.6}$$

$$W_{\mathrm{u}} = \int_{\partial B_2} u(r,\,\pi)\tau_{\mathrm{r}\varphi}(r,\,\pi)\,\mathrm{d}r\,\mathrm{d}z = C\pi t\int_a^b \frac{V}{r^2}\,\mathrm{d}r. \tag{3.7}$$

According to the well known Castigliano's principle [5, 6]

$$\delta\Pi_{\mathrm{c}} = 0 \tag{3.8}$$

where the stress function $V = V(r)$ is to be varied. We emphasize that the boundary condition (3.4) should also be satisfied.

A detailed computation leads to the following boundary value problem

$$-S_{22}r^2\frac{\mathrm{d}^2V}{\mathrm{d}r^2} + S_{22}r\frac{\mathrm{d}V}{\mathrm{d}r} + (S_{11} + 2S_{12} + S_{66})\,V = C\,r, \qquad a < r < b, \tag{3.9}$$

$$V(a) = 0, \qquad V(b) = 0. \tag{3.10}$$

The general solution of differential equation (3.9) is

$$V(r) = \alpha_1 r^{\lambda_1} + \alpha_2 r^{\lambda_2} + \frac{C}{S_{11} + 2S_{12} + S_{22} + S_{66}}\, r \tag{3.11}$$

where α_1 and α_2 are unknown integration constants and

$$\lambda_1 = 1 + \sqrt{\frac{S_{11} + 2S_{12} + S_{22} + S_{66}}{S_{22}}}, \tag{3.12}$$

$$\lambda_2 = 1 - \sqrt{\frac{S_{11} + 2S_{12} + S_{22} + S_{66}}{S_{22}}}. \tag{3.13}$$

Substitution of equation (3.11) into (3.10) yields

$$\alpha_1 = \frac{ab^{\lambda_2} - ba^{\lambda_2}}{\left(a^{\lambda_2} b^{\lambda_1} - a^{\lambda_1} b^{\lambda_2}\right)\left(S_{11} + 2S_{12} + S_{22} + S_{66}\right)}\, C\,, \tag{3.14}$$

$$\alpha_2 = \frac{a^{\lambda_1} b - ab^{\lambda_1}}{\left(a^{\lambda_2} b^{\lambda_1} - a^{\lambda_1} b^{\lambda_2}\right)\left(S_{11} + 2S_{12} + S_{22} + S_{66}\right)}\, C\,. \tag{3.15}$$

The connection between the displacement constant C and stress resultant F can be derived from the following equation:

$$F = 2t \int_a^b \tau_{r\varphi}(r,\, \pi)\, \mathrm{d}r = 2t \int_a^b \frac{V}{r^2}\, \mathrm{d}r. \tag{3.16}$$

A detailed computation gives

$$\begin{aligned} F = \frac{2tC}{S_{11} + 2S_{12} + S_{22} + S_{66}} \Bigg\{ \ln \frac{b}{a} + \\ + \frac{1}{a^{\lambda_2} b^{\lambda_1} - a^{\lambda_1} b^{\lambda_2}} \Bigg[\frac{\left(ab^{\lambda_2} - a^{\lambda_2} b\right)\left(b^{\lambda_1 - 1} - a^{\lambda_1 - 1}\right)}{\lambda_1 - 1} + \\ + \frac{\left(a^{\lambda_1} b - ab^{\lambda_1}\right)\left(b^{\lambda_2 - 1} - a^{\lambda_2 - 1}\right)}{\lambda_2 - 1} \Bigg] \Bigg\}. \end{aligned} \tag{3.17}$$

Formulae for the stresses are as follows:

$$\sigma_r = \left(\alpha_1 r^{\lambda_1 - 2} + \alpha_2 r^{\lambda_2 - 2} + \frac{C}{\left(S_{11} + 2S_{12} + S_{22} + S_{66}\right) r} \right) \sin\varphi, \tag{3.18}$$

$$\sigma_\varphi = \left(\alpha_1 \lambda_1 r^{\lambda_1 - 2} + \alpha_2 \lambda_2 r^{\lambda_2 - 2} + \frac{C}{\left(S_{11} + 2S_{12} + S_{22} + S_{66}\right) r} \right) \sin\varphi, \tag{3.19}$$

$$\tau_{r\varphi} = -\left(\alpha_1 r^{\lambda_1 - 2} + \alpha_2 r^{\lambda_2 - 2} + \frac{C}{\left(S_{11} + 2S_{12} + S_{22} + S_{66}\right) r} \right) \cos\varphi. \tag{3.20}$$

If the beam is isotropic it holds that

$$S_{11} = S_{22} = \frac{1 - \nu^2}{E}, \qquad S_{12} = -\frac{\nu(1+\nu)}{E}, \qquad S_{66} = \frac{2(1+\nu)}{E}, \tag{3.21}$$

where E is the Young's modulus and ν is the Poisson number. A simple computation gives

$$S_{11} + 2S_{12} + S_{22} + S_{66} = \frac{4(1-\nu^2)}{E} \tag{3.22}$$

$$\lambda_1 = 3, \qquad \lambda_2 = -1. \tag{3.23}$$

Inserting equations (3.22) and (3.23) into expressions (3.18), (3.19) and (3.20) set up for the stresses, we obtain

$$\sigma_{\mathrm{r}} = \left(\alpha_1 r + \frac{\alpha_2}{r^3} + \frac{\alpha_3}{r}\right)\sin\varphi, \tag{3.24}$$

$$\sigma_{\varphi} = \left(3\alpha_1 r - \frac{\alpha_2}{r^3} + \frac{\alpha_3}{r}\right)\sin\varphi, \tag{3.25}$$

$$\tau_{\mathrm{r}\varphi} = -\left(\alpha_1 r + \frac{\alpha_2}{r^3} + \frac{\alpha_3}{r}\right)\cos\varphi, \tag{3.26}$$

where

$$\alpha_3 = \frac{E}{1-\nu^2}\, C. \tag{3.27}$$

Equations (3.24), (3.25) and (3.26) are identical to those which were derived by Timoshenko and Goodier [7], and Lurje [6] for curved beams made of isotropic materials.

4. Two-layered curved beam

Figure 2 shows a two-layered curved beam made of two different linearly elastic orthotopic materials. The boundary conditions for this compound structure are given by equations (1.4), (1.5) and (1.6). The elastic constants for material i (i = 1, 2), which occupies the region B_i, are denoted by $S_{\mathrm{i}11}$, $S_{\mathrm{i}12}$, $S_{\mathrm{i}22}$ and $S_{\mathrm{i}66}$. The region B_i is uniquely determined by the following relations:

$$B_{\mathrm{i}} = \Big\{(r,\,\varphi,\,z)\;\Big|\; a_{\mathrm{i}} < r < b_{\mathrm{i}},\; 0 \le \varphi \le \pi,\; -t \le z \le t;\;\; \mathrm{i} = 1,2;$$
$$a_1 = a,\; b_1 = c;\;\; a_2 = c,\; b_2 = b\Big\}.$$

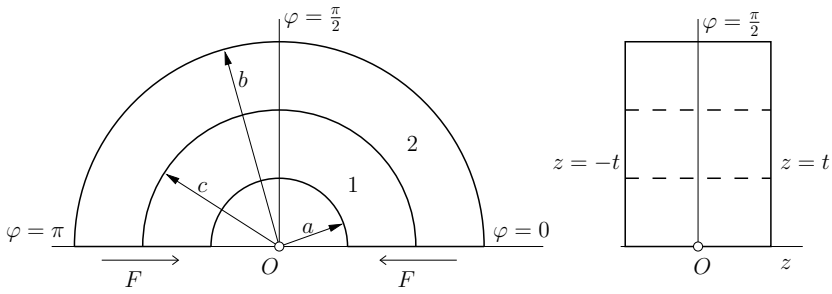

Figure 2. Two-layered curved beam of rectangular cross section.

The connection between the beam components on the common cylindrical surface $r = c$ is perfect, i.e. neither the displacements u, v nor the stresses σ_{r}, $\tau_{\mathrm{r}\varphi}$ have jumps if $r = c$. Consequently

$$u_1(c,\,\varphi) = u_2(c,\,\varphi), \quad v_1(c,\,\varphi) = v_2(c,\,\varphi), \qquad 0 \le \varphi \le \pi, \tag{4.1}$$

$$\sigma_{1\mathrm{r}}(c,\,\varphi) = \sigma_{2\mathrm{r}}(c,\,\varphi), \quad \tau_{1\mathrm{r}\varphi}(c,\,\varphi) = \tau_{2\mathrm{r}\varphi}(c,\,\varphi), \qquad 0 \le \varphi \le \pi. \tag{4.2}$$

We can obtain a solution to the boundary value problem constituted by equations (1.4), (1.5), (1.6), (4.1) and (4.2) if we apply again the principle of minimum complementary energy. Let us denote the stress function for region B_{i} by $V_{\mathrm{i}} = V_{\mathrm{i}}(r)$ ($\mathrm{i} = 1, 2$). The statically admissible stress fields should satisfy both the equations of equilibrium (3.1), (3.2) and the stress boundary conditions $(1.4)_1$, $(1.5)_1$, (1.6). It is obvious that the traction continuity conditions given by equations (4.2) should also be fulfilled. Formulae for the statically admissible stresses are as follows:

$$\sigma_{\mathrm{ir}} = \frac{V_{\mathrm{i}}(r)}{r^2}\,\sin\varphi, \qquad \sigma_{\mathrm{i}\varphi} = \frac{1}{r}\frac{\mathrm{d}V_{\mathrm{i}}}{\mathrm{d}r}\,\sin\varphi, \qquad \tau_{\mathrm{ir}\varphi} = -\frac{V_{\mathrm{i}}(r)}{r^2}\,\cos\varphi, \qquad (\mathrm{i} = 1, 2), \tag{4.3}$$

where

$$V_1(a) = 0, \qquad V_2(b) = 0 \qquad V_1(c) = V_2(c). \tag{4.4}$$

The total complementary energy for the curved two-layered beam is of the form:

$$\begin{aligned}
&\Pi_{\mathrm{c}}(V_1,\,V_2) = \\
&= \frac{\pi t}{2}\left\{\int_a^c \left[S_{111}\left(\frac{V_1}{r^2}\right)^2 + 2S_{112}\frac{V_1}{r^3}\frac{\mathrm{d}V_1}{\mathrm{d}r} + S_{122}\frac{1}{r^2}\left(\frac{\mathrm{d}V_1}{\mathrm{d}r}\right)^2 + S_{166}\left(\frac{V_1}{r^2}\right)^2\right] r\,\mathrm{d}r + \right.\\
&\quad \left. + \int_c^b \left[S_{211}\left(\frac{V_2}{r^2}\right)^2 + 2S_{212}\frac{V_2}{r^3}\frac{\mathrm{d}V_2}{\mathrm{d}r} + S_{222}\frac{1}{r^2}\left(\frac{\mathrm{d}V_2}{\mathrm{d}r}\right)^2 + S_{266}\left(\frac{V_2}{r^2}\right)^2\right] r\,\mathrm{d}r - \right\}\\
&\qquad\qquad - C\pi t\left\{\int_a^c \frac{V_1}{r^2}\,\mathrm{d}r + \int_c^b \frac{V_2}{r^2}\,\mathrm{d}r\right\}.
\end{aligned} \tag{4.5}$$

By means of Castigliano's principle [5, 6] we get from equation (4.5) that

$$\delta\Pi_c = 0 \tag{4.6}$$

where the stress functions $V_1 = V_1(r)$ and $V_2 = V_2(r)$ should be varied under conditions (4.4). After some paper and pencil calculations (details are omitted), equation (4.6) results in the following stationary conditions:

$$\begin{aligned}
&-S_{\mathrm{i}22}r^2\frac{\mathrm{d}^2V_{\mathrm{i}}}{\mathrm{d}r^2} + S_{\mathrm{i}22}r\frac{\mathrm{d}V_{\mathrm{i}}}{\mathrm{d}r} + (S_{\mathrm{i}11} + 2S_{\mathrm{i}12} + S_{\mathrm{i}66})\,V_{\mathrm{i}} = Cr,\\
&\qquad a_{\mathrm{i}} \le r \le b_{\mathrm{i}}, \quad (\mathrm{i} = 1, 2), \quad a_1 = a,\ b_1 = c;\ a_2 = c,\ b_2 = b,
\end{aligned} \tag{4.7}$$

$$S_{122}\frac{1}{c}\left(\frac{\mathrm{d}V_1}{\mathrm{d}r}\right)_{r=c}+S_{112}\frac{V_1(c)}{c^2}-S_{222}\frac{1}{c}\left(\frac{\mathrm{d}V_2}{\mathrm{d}r}\right)_{r=c}-S_{212}\frac{V_2(c)}{c^2}=0. \tag{4.8}$$

The general solution of the differential equation (4.6) is

$$V_{\mathrm{i}}(r)=\alpha_{\mathrm{i}1}r^{\lambda_{\mathrm{i}1}}+\alpha_{\mathrm{i}2}r^{\lambda_{\mathrm{i}2}}+C_{\mathrm{i}}\,r, \tag{4.9}$$

where $(\mathrm{i}=1,2)$ and

$$C_{\mathrm{i}}=\frac{C}{S_{\mathrm{i}11}+2S_{\mathrm{i}12}+S_{\mathrm{i}22}+S_{\mathrm{i}66}}, \tag{4.10}$$

$$\lambda_{\mathrm{i}1}=1+\sqrt{\frac{S_{\mathrm{i}11}+2S_{\mathrm{i}12}+S_{\mathrm{i}22}+S_{\mathrm{i}66}}{S_{\mathrm{i}22}}}, \tag{4.11}$$

$$\lambda_{\mathrm{i}2}=1-\sqrt{\frac{S_{\mathrm{i}11}+2S_{\mathrm{i}12}+S_{\mathrm{i}22}+S_{\mathrm{i}66}}{S_{\mathrm{i}22}}}. \tag{4.12}$$

The unknown integration constants in the expressions for the stress functions can be computed from the following system of linear equations, which are based on boundary conditions (4.4) and (4.8):

$$\begin{bmatrix} a_{11} & a_{12} & a_{13} & a_{14}\\ a_{21} & a_{22} & a_{23} & a_{24}\\ a_{31} & a_{32} & a_{33} & a_{34}\\ a_{41} & a_{42} & a_{43} & a_{44}\end{bmatrix}\begin{bmatrix}\alpha_1\\ \alpha_2\\ \alpha_3\\ \alpha_4\end{bmatrix}=\begin{bmatrix}\beta_1\\ \beta_2\\ \beta_3\\ \beta_4\end{bmatrix}. \tag{4.13}$$

Here

$$\alpha_1=\alpha_{11},\quad \alpha_2=\alpha_{12},\quad \alpha_3=\alpha_{21},\quad \alpha_4=\alpha_{22} \tag{4.14}$$

$$\begin{aligned}&\beta_1=-C_1a,\quad \beta_2=(C_2-C_1)c,\\ &\beta_3=[C_2(S_{212}+S_{222})-C_1(S_{112}+S_{122})]c,\quad \beta_4=-C_2b,\end{aligned} \tag{4.15}$$

$$a_{11}=a^{\lambda_{11}},\quad a_{12}=a^{\lambda_{12}},\quad a_{13}=a_{14}=0, \tag{4.16}$$

$$a_{21}=c^{\lambda_{11}},\quad a_{22}=c^{\lambda_{12}},\quad a_{23}=-c^{\lambda_{21}},\quad a_{24}=-c^{\lambda_{22}}, \tag{4.17}$$

$$\begin{aligned}&a_{31}=(S_{112}+\lambda_{11}S_{122})c^{\lambda_{11}},\quad a_{32}=(S_{112}+\lambda_{12}S_{122})c^{\lambda_{12}},\\ &a_{33}=-(S_{212}+\lambda_{21}S_{222})c^{\lambda_{21}},\quad a_{34}=-(S_{212}+\lambda_{22}S_{222})c^{\lambda_{22}},\end{aligned} \tag{4.18}$$

$$a_{41}=a_{42}=0,\quad a_{43}=b^{\lambda_{21}},\quad a_{44}=b^{\lambda_{22}}. \tag{4.19}$$

The determination of the connection between the stress resultant F and displacement constant C can be obtained from

$$F=2t\left[\int_a^c\tau_{1\mathrm{r}\varphi}(r,\,\pi)\mathrm{d}r+\int_c^b\tau_{2\mathrm{r}\varphi}(r,\,\pi)\mathrm{d}r\right]=2t\left[\int_a^c\frac{V_1}{r^2}\mathrm{d}r+\int_c^b\frac{V_2}{r^2}\mathrm{d}r\right]. \tag{4.20}$$

A combination of equations (4.9), (4.14) with equation (4.20) gives the final formula for the stress resultant:

$$F=2t\left[\frac{\alpha_1}{\lambda_{11}-1}\left(c^{\lambda_{11}-1}-a^{\lambda_{11}-1}\right)+\frac{\alpha_2}{\lambda_{12}-1}\left(c^{\lambda_{12}-1}-a^{\lambda_{12}-1}\right)+C_1\ln\frac{c}{a}+\right.$$

$$+\frac{\alpha_3}{\lambda_{21}-1}\left(b^{\lambda_{21}-1}-c^{\lambda_{21}-1}\right)+\frac{\alpha_4}{\lambda_{22}-1}\left(b^{\lambda_{22}-1}-c^{\lambda_{22}-1}\right)+C_2\ln\frac{b}{c}\Bigg]. \quad (4.21)$$

Formulae for stresses σ_{ir}, $\sigma_{\mathrm{i}\varphi}$ and $\tau_{\mathrm{ir}\varphi}$ $(\mathrm{i}=1,2)$ are as follows:

$$\sigma_{\mathrm{ir}}=\left(\alpha_{\mathrm{i}1}r^{\lambda_{\mathrm{i}1}-2}+\alpha_{\mathrm{i}2}r^{\lambda_{\mathrm{i}2}-2}+\frac{C_{\mathrm{i}}}{r}\right)\sin\varphi, \quad (4.22)$$

$$\sigma_{\mathrm{i}\varphi}=\left(\alpha_{\mathrm{i}1}\lambda_{\mathrm{i}1}r^{\lambda_{\mathrm{i}1}-2}+\alpha_{\mathrm{i}2}\lambda_{\mathrm{i}2}r^{\lambda_{\mathrm{i}2}-2}+\frac{C_{\mathrm{i}}}{r}\right)\sin\varphi, \quad (4.23)$$

$$\tau_{\mathrm{ir}\varphi}=-\left(\alpha_{\mathrm{i}1}r^{\lambda_{\mathrm{i}1}-2}+\alpha_{\mathrm{i}2}r^{\lambda_{\mathrm{i}2}-2}+\frac{C_{\mathrm{i}}}{r}\right)\cos\varphi. \quad (4.24)$$

Following the method presented here we can generalize the two-layered solution for the case of more than two layers.

5. Analysis of the displacement continuity conditions at the interface

There are two independent continuity conditions the displacements should fulfill on the common cylindrical boundary surface of the two curved beam components. By the use of the displacement continuity conditions (4.1) we can derive two independent new continuity conditions that can be expressed in terms of strains and stresses. It follows from equation (1.2) that

$$\varepsilon_{1\varphi}(c,\,\varphi)=\varepsilon_{2\varphi}(c,\,\varphi),\qquad 0\le\varphi\le\pi, \quad (5.1)$$

that is

$$c\,S_{112}\,\sigma_{1\mathrm{r}}(c,\,\varphi)+c\,S_{122}\,\sigma_{1\varphi}(c,\,\varphi)=c\,S_{212}\,\sigma_{2\mathrm{r}}(c,\,\varphi)+c\,S_{222}\,\sigma_{2\varphi}(c,\,\varphi). \quad (5.2)$$

By using (4.3) we can rewrite this equation in terms of the stress functions V_1, V_2:

$$S_{112}\frac{V_1(c)}{c}+S_{122}\left(\frac{\mathrm{d}V_1}{\mathrm{d}r}\right)_{r=c}-S_{212}\frac{V_2(c)}{c}-S_{222}\left(\frac{\mathrm{d}V_2}{\mathrm{d}r}\right)_{r=c}=0. \quad (5.3)$$

We remark that this equation is one of the stationarity conditions for the total complementary energy – see equation (4.8).

The exact solutions should satisfy the two independent displacement continuity condition if $r=c$. Next, we formulate a new displacement continuity conditions in terms of stresses. Starting from equations (1.1), (1.2) we can write

$$\frac{\partial^2 v}{\partial r\partial\varphi}=\frac{\partial}{\partial r}\left[r\left(S_{12}\,\sigma_{\mathrm{r}}+S_{22}\,\sigma_{\varphi}\right)\right]-S_{11}\,\sigma_{\mathrm{r}}-S_{12}\,\sigma_{\varphi}. \quad (5.4)$$

It follows from equation (1.3) that

$$\frac{\partial^2 v}{\partial r\partial\varphi}=S_{66}\frac{\partial\tau_{\mathrm{r}\varphi}}{\partial\varphi}-\frac{1}{r}\left(\frac{\partial^2 u}{\partial\varphi^2}-\frac{\partial v}{\partial\varphi}\right). \quad (5.5)$$

A combination of equation (4.19) with equation (5.5) yields

$$q(r,\,\varphi)=\frac{1}{r}\left(\frac{\partial^2 u}{\partial\varphi^2}-\frac{\partial v}{\partial\varphi}\right)=S_{66}\frac{\partial\tau_{r\varphi}}{\partial\varphi}-\frac{\partial}{\partial r}\left[r\left(S_{12}\,\sigma_{\mathrm{r}}+S_{22}\,\sigma_{\varphi}\right)\right]+S_{11}\,\sigma_{\mathrm{r}}+S_{12}\,\sigma_{\varphi}. \tag{5.6}$$

If equation (4.1) is satisfied at every point on the common cylindrical boundary surface of the curved beam components then it follows that

$$q_1(c,\,\varphi)=\frac{1}{c}\left(\frac{\partial^2 u_1}{\partial\varphi^2}-\frac{\partial v_1}{\partial\varphi}\right)\bigg|_{r=c}=q_2(c,\,\varphi)=\frac{1}{c}\left(\frac{\partial^2 u_2}{\partial\varphi^2}-\frac{\partial v_2}{\partial\varphi}\right)\bigg|_{r=c} \tag{5.7}$$

in which $0\le\varphi\le\pi$.

Substitute the stress functions $V_1=V_1(r)$ and $V_2=V_2(r)$ into equation (5.7) by utilizing equations (4.7) and (5.6). After some manipulations we get

$$-\left[S_{122}\frac{1}{c}\left(\frac{\mathrm{d}V_1}{\mathrm{d}r}\right)_{r=c}+S_{112}\frac{V_1(c)}{c^2}\right]+\frac{C}{c}=-\left[S_{222}\frac{1}{c}\left(\frac{\mathrm{d}V_2}{\mathrm{d}r}\right)_{r=c}+S_{212}\frac{V_2(c)}{c^2}\right]+\frac{C}{c}. \tag{5.8}$$

or

$$S_{112}\frac{V_1(c)}{c}+S_{122}\left(\frac{\mathrm{d}V_1}{\mathrm{d}r}\right)_{r=c}-S_{212}\frac{V_2(c)}{c}-S_{222}\left(\frac{\mathrm{d}V_2}{\mathrm{d}r}\right)_{r=c}=0, \tag{5.9}$$

Hence we have proved that two independent displacement continuity conditions (5.1), (5.7) are all satisfied since they can be transformed into equation (4.8) which follows from the stationary condition (4.6).

6. Examples

6.1. **Example 1.** The geometrical and material data of the considered single curved beam are as follows:

$$a=35\,\mathrm{mm},\qquad b=70\,\mathrm{mm},\qquad t=10\,\mathrm{mm};$$

$$S_{11}=0.5525\cdot10^{-5}\,\frac{1}{\mathrm{MPa}},$$

$$S_{12}=S_{21}=-0.1547\cdot10^{-5}\,\frac{1}{\mathrm{MPa}},$$

$$S_{22}=0.9709\cdot10^{-5}\,\frac{1}{\mathrm{MPa}},$$

$$S_{66}=0.1359\cdot10^{-5}\,\frac{1}{\mathrm{MPa}}.$$

The displacement constant $C=-1\,\mathrm{mm}$. The force resultant which belongs to C is $F=-53.59065\,\mathrm{kN}$. This value is obtained by the application of formula (3.17).

The stresses are calculated by using equations (3.18), (3.19), (3.20). They can also be obtained from a FEM solution which is based on the application of the commercial program Abaqus. The results are listed in Table 1.

Table 1. Stresses in single curved beam. Comparison of theoretical and FEM solutions.

Position		σ_r [MPa]		σ_φ [MPa]		$\tau_{r\varphi}$ [MPa]	
r [mm]	φ [rad]	Eq. (3.18)	FEM	Eq. (3.19)	FEM	Eq. (3.20)	FEM
35.0	0.0	0.0000	0.0178	0.0000	0.0843	0.0000	0.5754
40.0	0.0	0.0000	0.0094	0.0000	-0.0089	90.4089	90.6799
50.0	0.0	0.0000	0.0084	0.0000	-0.0046	115.5556	115.676
60.0	0.0	0.0000	0.0080	0.0000	-0.0025	66.9516	67.0311
70.0	0.0	0.0000	0.0124	0.0000	0.0939	0.0000	-0.0049
35.0	0.7854	0.0000	-0.4065	-683.5371	-683.1990	0.0000	0.4068
40.0	0.7854	-63.9287	-64.1205	-425.3195	-425.3140	63.9287	64.1204
50.0	0.7854	-81.7101	-81.7951	-68.1447	-68.1905	81.7101	81.7950
60.0	0.7854	-47.3419	-47.3982	169.8475	169.8050	47.3419	47.3982
70.0	0.7854	0.0000	0.0000	341.7685	341.8760	0.0000	-0.0355
35.0	2.3562	0.0000	-0.4065	-683.5371	-683.1990	0.0000	-0.4068
40.0	2.3562	-63.9287	-64.1205	-425.3195	-425.3140	-63.9287	-64.1204
50.0	2.3562	-81.7101	-81.7951	-68.1447	-68.1905	-81.7101	-81.7950
60.0	2.3562	-47.3419	-47.3982	169.8475	169.8050	-47.3419	-47.3982
70.0	2.3562	0.0000	0.0000	341.7685	341.8760	0.0000	-0.0035
35.0	3.1416	0.0000	0.0178	0.0000	0.0843	0.0000	-0.5754
40.0	3.1416	0.0000	0.0094	0.0000	-0.0089	-90.4089	-90.6799
50.0	3.1416	0.0000	0.0084	0.0000	-0.0046	-115.5556	-115.6760
60.0	3.1416	0.0000	0.0080	0.0000	-0.0025	-66.9516	-67.0311
70.0	3.1416	0.0000	0.0124	0.0000	0.0939	0.0000	0.0049

6.2. **Example 2.** Two-layered curved beam. The geometrical and material data of the considered two-layered curved beam made of two different materials are as follows:

$$a = 35\,\text{mm}, \qquad b = 70\,\text{mm}, \qquad c = 50\,\text{mm}, \qquad t = 10\,\text{mm};$$

$$S_{111} = 0.5525 \cdot 10^{-5}\,\frac{1}{\text{MPa}}, \qquad S_{211} = 7.14 \cdot 10^{-5}\,\frac{1}{\text{MPa}},$$

$$S_{112} = S_{121} = -0.1547 \cdot 10^{-5}\,\frac{1}{\text{MPa}}, \qquad S_{212} = S_{221} = -3.19 \cdot 10^{-5}\,\frac{1}{\text{MPa}},$$

$$S_{122} = 0.9709 \cdot 10^{-5}\,\frac{1}{\text{MPa}}, \qquad S_{222} = 43.76 \cdot 10^{-5}\,\frac{1}{\text{MPa}},$$

$$S_{166} = 0.1359 \cdot 10^{-5}\,\frac{1}{\text{MPa}}, \qquad S_{266} = 50.70 \cdot 10^{-5}\,\frac{1}{\text{MPa}},$$

The displacement constant is again $C = -1\,\text{mm}$. The force resultant for C is $F = -17.525\,\text{kN}$. For calculating F we have applied formula (4.21).

The stresses calculated with equations (4.22), (4.23), (4.24) are compared to those of a FEM solution obtained by using the commercial program Abaqus. The results are listed in Table 2.

Table 2. Stresses in two-layered curved beam. Comparison of theoretical and FEM solutions.

Position		σ_r [MPa]		σ_φ [MPa]		$\tau_{r\varphi}$ [MPa]	
r [mm]	φ [rad]	Eq. (4.22)	FEM	Eq. (4.23)	FEM	Eq. (4.24)	FEM
35.0	0.0000	0.0000	0.0163	0.0000	0.0477	0.0000	0.4494
40.0	0.0000	0.0000	0.0108	0.0000	-0.0069	40.6747	0.0409
50.0	0.0000	0.0000	0.0113	0.0000	0.0440	6.5699	6.6233
50.0	0.0000	0.0000	0.0079	0.0000	0.0026	6.5699	6.5695
60.0	0.0000	0.0000	0.0004	0.0000	0.0000	2.9508	2.9528
70.0	0.0000	0.0000	0.0005	0.0000	0.0036	0.0005	-0.0007
35.0	0.7854	0.0000	-0.3167	-383.7897	-383.4140	0.0000	0.3177
40.0	0.7854	-28.7614	-28.9218	-124.6154	-124.5690	28.7614	28.9216
50.0	0.7854	-4.6456	-4.6862	237.5746	237.7650	4.6456	4.6834
50.0	0.7854	-4.6456	-4.6454	2.4758	4.9515	4.6456	4.6453
60.0	0.7854	-2.0865	-2.0879	6.9181	9.6141	2.0865	2.0879
70.0	0.7854	0.0000	0.0004	10.3726	13.2767	0.0000	-0.0004
35.0	2.3562	0.0000	-0.3167	-383.7897	-383.4140	0.0000	0.3177
40.0	2.3562	-28.7614	-28.9218	-124.6154	-124.5690	-28.7614	-28.9216
50.0	2.3562	-4.6456	-4.6862	237.5746	237.7650	-4.6456	-4.6834
50.0	2.3562	-4.6456	-4.6454	2.4758	4.9515	-4.6456	-4.6453
60.0	2.3562	-2.0865	-2.0879	6.9181	9.6141	-2.0865	-2.0879
70.0	2.3562	0.0000	0.0004	10.3726	13.2767	0.0000	0.0004
35.0	3.1416	0.0000	0.0163	0.0000	0.0477	0.0000	-0.449
40.0	3.1416	0.0000	0.0108	0.0000	-0.0069	-40.6747	-40.9013
50.0	3.1416	0.0000	0.0113	0.0000	0.0440	-6.5699	-6.6233
50.0	3.1416	0.0000	0.0079	0.0000	0.0026	-6.5699	-6.5695
60.0	3.1416	0.0000	0.0004	0.0000	0.0000	-2.9508	-2.9528
70.0	3.1416	0.0000	0.0005	0.0000	0.0036	0.0000	0.0007

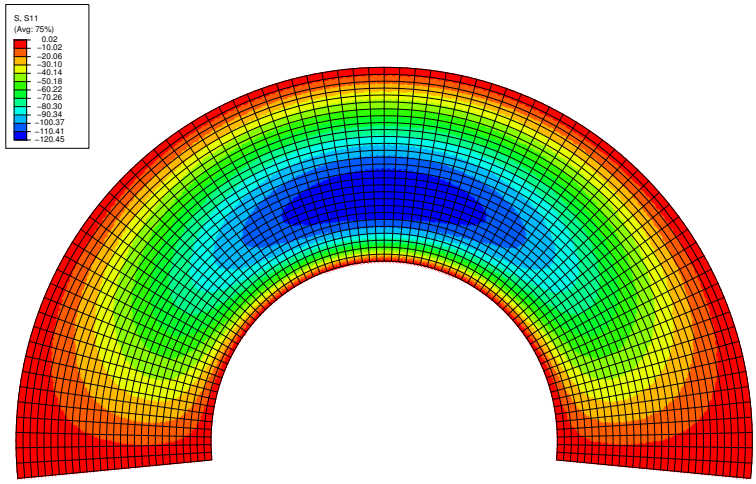

Figure 3. Stress σ_r in a curved beam of rectangular cross section (one layer)

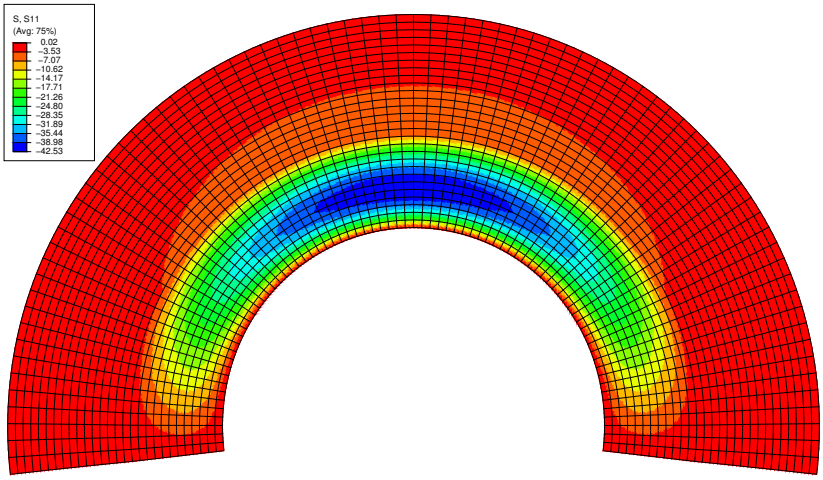

Figure 4. Stress σ_{r} in a curved beam of rectangular cross section (two-layered)

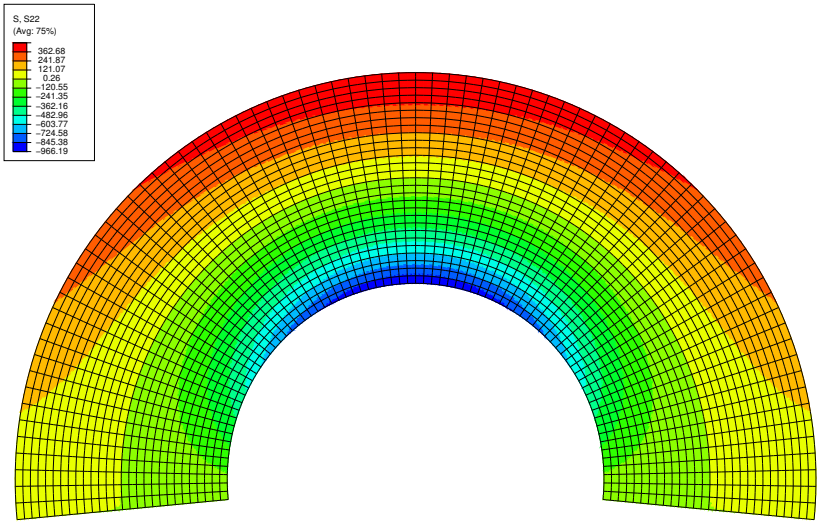

Figure 5. Stress σ_{φ} in a curved beam of rectangular cross section (one layer)

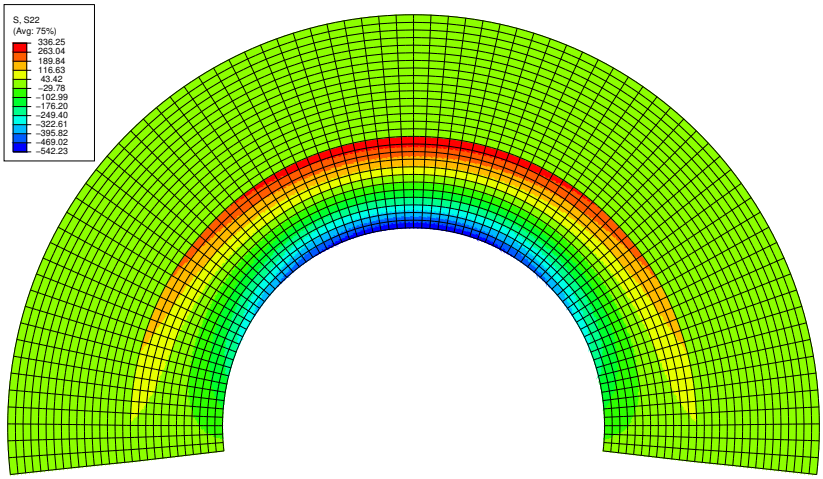

Figure 6. Stress σ_φ in a curved beam of rectangular cross section (two-layered)

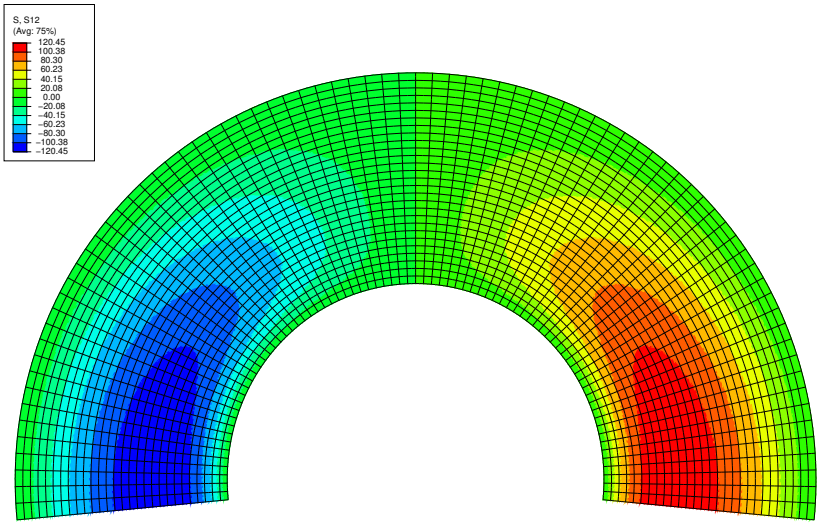

Figure 7. Stress $\tau_{r\varphi}$ in a curved beam of rectangular cross section (one layer)

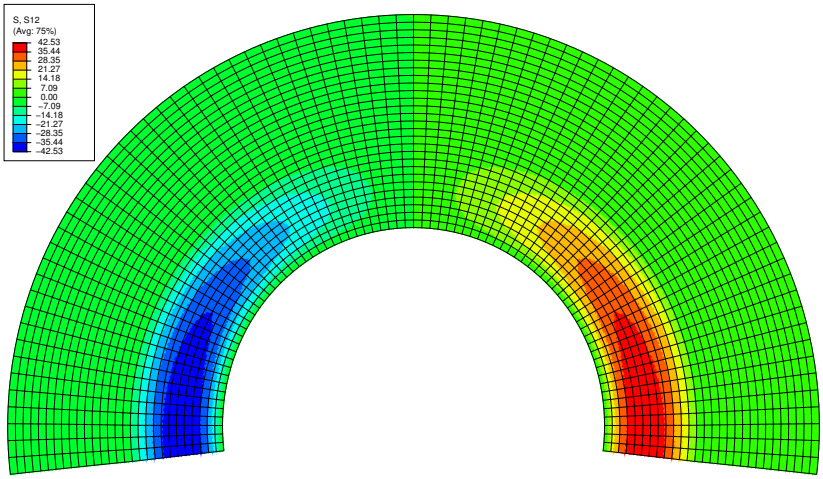

Figure 8. Stress $\tau_{r\varphi}$ in a curved beam of rectangular cross section (two-layered)

Figures 3 and 4 depict a single curved beam and a beam with two layers. Both figures show the stress distribution of the normal stress σ_R. Observe that the computed σ_φ stress distribution is discontinuous, as is expected, only on the two-layered curved beam (see Figures 5 and 6 for details).

The computed stress distribution $\tau_{r\varphi}$ is illustrated for the single curved beam in Figure 7, and for the two-layered beam in Figure 8.

According to results shown in Tables 1 and 2 the theoretical and FEM solutions are in good agreement in both examples.

7. Conclusions

Under the plane strain conditions a mixed type boundary value problem of a curved beam with rectangular cross section is analysed. One- and two-layered curved beams made of polar orthotopic materials are considered. The mixed type boundary value problems are bending problems. For isotropic, homogeneous curved beams this problem was first solved by Golovin [8].

The present paper applies a minimum strain energy property for finding the equations of the considered bending problem. Formulae for the stresses are obtained by means of Castigliano's principle. A detailed analysis is presented for the displacement continuity conditions on the common cylindrical boundary surface of the two-layered curved beam. By applying the method presented in the paper the solutions for the two-layered beam can easily be generalized for the case of beams with more than two

layers. The results of the theoretical computations are in good agreement with the FEM solution.

Acknowledgement. This research was (partially) carried out in the framework of the Center of Excellence of Innovative Engineering Design and Technologies at the University of Miskolc and supported by the National Research, Development and Innovation Office (NKFIH), Grant No. K115701.

References

1. Herakovich, C. T.: *Mechanics of Fibrous Composites*. John Wiley, New York, 1998.
2. Kaw, A. K.: *Mechanics of Composite Materials*. CRC Press, New York, 1997.
3. Sternberg, E. and Knowles, J. K.: Minimum energy characterizations of Saint-Venant's solution to the relaxed Saint-Venant problem. *Arch. Rational Mech. Anal.*, **85**, (1966), 295–310.
4. Gurtin, M. E.: The Linear Theory of Elasticity, In *Handbuch der Physik*, vol. VIa/2. Springer, Berlin-Heidelbert-New York, 1972.
5. Washizu, K.: *Variational Methods in Elasticity and Plasticity*. Pergamon Press, Oxford, 1968.
6. Lurje, A. I.: *Theory of Elasticity*. Izd. Nauka, Moscow, 1970. In Russian.
7. Timoshenko, S. P. and Goodier, J. N.: *Theory of Elasticity*. 3rd edition. McGraw Hill, New York, 1970.
8. Golovin, K. S.: One problem in statics of an elastic body. *Izvestiya St.Peterburg Prakt. Tekhnol. Inst.*, **3**, (1881), 373–410. In Russian.

Journal of Computational and Applied Mechanics, Vol. 12, No. 1, (2017), pp. 19–41
DOI: 10.32973/jcam.2017.002

GREEN'S FUNCTIONS FOR NONHOMOGENEOUS CURVED BEAMS WITH APPLICATIONS TO VIBRATION PROBLEMS

László Péter Kiss
Institute of Applied Mechanics, University of Miskolc
H-3515 Miskolc-Egyetemváros
mechkiss@uni-miskolc.hu

[Received: March 11, 2017; Accepted: April 12, 2017]

Abstract. In the open literature we have found no report on the Green function matrices of curved beams except papers [1, 2, 3] by Szeidl at al. These works assume that the material of the beam is homogeneous and isotropic. In the present paper we assume that the beam is made of heterogeneous material in such a way that the material properties depend on the cross-sectional coordinates. Under this condition we have the following aims: (1) we would like to determine the Green function matrices in a closed-form for (a) fixed-fixed, (b) pinned-pinned and (c) pinned-fixed circular beams. (2) With the knowledge of the Green function matrices we can reduce those eigenvalue problems which provide the natural frequencies of the free vibrations to eigenvalue problems governed by homogeneous Fredholm integral equations. Our goal in this respect is to solve the latter eigenvalue problems numerically and compare the results obtained with the results of finite element (FE) computations. Our numerical solutions show a good agreement with the commercial FE computations.

Mathematical Subject Classification: 74G60, 74B15
Keywords: Circular beam, nonhomogeneous material, Green function matrices, problem of free vibrations

1. Introduction

Curved beams are often used as various structural elements because of their favourable load-carrying capabilities. We mention, for instance, arch bridges and the role of curved beams as stiffener elements in roof- and shell structures. Nowadays, it is gradually getting cheaper to manufacture nonhomogeneous (heterogeneous or inhomogeneous) curved beams, such as composites, laminates and sandwich structures. The benefits of such structural members can be the reduced weight and the higher strength. A class of inhomogeneity (heterogeneity) is called cross-sectional inhomogeneity which means that the material parameters (the Young modulus E and the Poisson number) are functions of the cross-sectional coordinates – these material parameters can change continuously on the cross-section, or can be constant over each segment of the cross-section.

In the present paper we will focus on the free vibrations of heterogeneous curved beams using a Green function matrix technique.

As regards the preliminaries it is worthy to mention that Den Hartog [4] is known to be the first to have dealt with the free vibrations of curved beams. Other early but relevant results, considering the inextensibility of the centerline, were achieved in [5, 6, 7]. A more recent research by Qatu and Elsharkawy [8] presents an exact model and numerical solutions for the free vibrations of laminated arches. With the differential quadrature method, Kang et al. [9] determine the eigenfrequencies for the in- and out-of-plane vibrations of circular Timoshenko arches with rotatory inertia and shear deformations included. Tüfekçi and Arpaci [10] obtain exact solutions for the differential equations which describe the in-plane free harmonic vibrations of extensible curved beams. Krishnan and Suresh [11] tackle the very same issue with a shear-deformable finite element (FE) model. Paper [12] by Ecsedi and Dluhi analyse some dynamic features of nonhomogeneous curved beams and closed rings assuming cross-sectional heterogeneity. Elastic foundation is taken into account in [13]. Survey paper [14] by Hajianmaleki and Qatu collects a bunch of references up until the early 2010s in the topic investigated. Kovács [15] considers layered arches with both perfect and even imperfect bonding between any two adjacent layers. Article [16] by Juna et al. uses the trigonometric shear deformation theory. The dynamic stiffness matrix is obtained from the exact solutions of the related differential equations.

It seems that, meanwhile the Green function is commonly used for various straight beam problems [17, 18, 19, 20, 21], it is somehow not preferred for the free vibrations of curved beams. There are really a few exceptions. Szeidl in his PhD [1] investigates how the extensibility of the centerline affects the free vibrations of planar, radially loaded circular beams. One of the developed numerical techniques is based on the use of the Green function matrix since its knowledge makes it possible to transform the eigenvalue problem set up for the eigenfrequencies into an eigenvalue problem governed by a system of homogeneous Fredholm integral equations where the Green function matrix is the kernel. Similarly in [2], the authors determine the natural frequencies of pinned-pinned and fixed-fixed circular arches under distributed load. Kelemen [3] seeks how the natural frequencies are related to a constant distributed external force system.

On the base of all that has been said the present paper has two main objectives. First, to determine the Green function matrices for heterogeneous curved beams for three support arrangements, i.e., for (a) fixed-fixed, (b) pinned-pinned and (c) pinned-fixed circular beams. Then to investigate the vibratory behaviour of such beams. The paper is organized into seven sections. After the introduction, the most important hypotheses and assumptions are presented with the governing equations of the vibratory issue. Then, the properties and the definition of the Green function matrices are given in Section 3. This is followed by the numerical results and evaluation. The article is closed by some conclusions, an appendix and the list of references. The appendix contains the Green function matrices in closed-form.

2. Kinematical, constitutive and motion equations

Here we summarize the most important hypotheses and governing equations of the model we have established to tackle the vibratory problem. A thorough description is available, e.g., in [22, 23, 24].

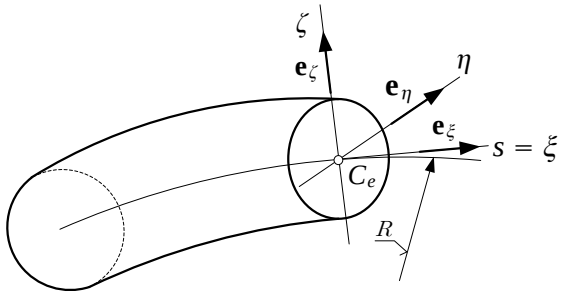

Figure 1. Coordinate system

We use a curvilinear coordinate system whose orthogonal unit vectors $\mathbf{e}_\xi; \mathbf{e}_\eta; \mathbf{e}_\zeta$ are attached to the E-weighted centerline which intersects the cross-section at the point C_e. R is the initial (constant) radius of the centerline and the included angle of the beam is $\bar{\vartheta} = 2\vartheta$. The infinitesimal line element is $\mathrm{d}s = R\mathrm{d}\varphi$ where φ is the angle coordinate. The cross-sections are uniform and symmetric with respect to the axis η not only in the geometry but also in the material composition. Hence, the Young modulus fulfills the condition $E(\eta, \zeta) = E(-\eta, \zeta)$. It is obvious that the axis ζ is a principal axis of inertia. The axis η is selected in such a way that the E-weighted first moment with respect to this axis vanishes:

$$Q_{e\eta} = \int_A E(\eta, \zeta)\zeta \mathrm{d}A = 0.$$

Under the conditions of the Euler-Bernoulli hypothesis the axial strain [8, 25] is given by

$$\varepsilon_\xi = \frac{R}{R+\zeta}\left(\varepsilon_{o\xi} + \zeta\kappa_o\right), \tag{1}$$

where

$$\varepsilon_{o\xi} = \frac{\mathrm{d}u_o}{\mathrm{d}s} + \frac{w_o}{R}, \qquad \psi_{o\eta} = \frac{u_o}{R} - \frac{\mathrm{d}w_o}{\mathrm{d}s} \quad \text{and} \quad \kappa_o = \frac{\mathrm{d}\psi_{o\eta}}{\mathrm{d}s}. \tag{2}$$

In these equations $\varepsilon_{o\xi}$, u_o and w_o are the axial strain as well as the tangential and normal displacement components on the centerline. Besides, $\psi_{o\eta}$ and κ_o are the rotation and the curvature of the centerline.

The material is linearly elastic, isotropic and, by assumption, it holds that $\sigma_\xi \gg \sigma_\eta, \sigma_\zeta$. Thus, the constitutive equation is Hooke's law in the following form: $\sigma_\xi = E(\eta, \zeta)\varepsilon_\xi$. Making use of Hooke's law and the kinematic relations (1)-(2) we can set up the following equations for the axial force N and the bending moment M – as

regards the details the reader is referred to [22, 23]:

$$N = \int_A \sigma_\xi \mathrm{d}A = \frac{I_{e\eta}}{R^2} m\varepsilon_{o\xi} - \frac{M}{R}, \qquad M = \int_A \sigma_\xi \zeta \mathrm{d}A = -I_{e\eta}\left(\frac{\mathrm{d}^2 w_o}{\mathrm{d}s^2} + \frac{w_o}{R^2}\right). \quad (3)$$

Here [12]

$$A_e = \int_A E(\eta,\zeta)\,\mathrm{d}A\,, \qquad I_{e\eta} = \int_A E(\eta,\zeta)\,\zeta^2 \mathrm{d}A; \quad m = \frac{A_e R^2}{I_{e\eta}} - 1 \quad (4)$$

are the E-weighted area and the E-weighted moment of inertia. Moreover, m is a dimensionless geometry-heterogeneity parameter.

The equilibrium equations can be obtained from the principle of virtual work [22]. It can be given in the following form:

$$\int_V \sigma_\xi \delta\varepsilon_\xi \mathrm{d}V = \int_{\mathcal{L}} (f_n \delta w_o + f_t \delta u_o)\,\mathrm{d}s. \quad (5)$$

Here the virtual quantities are denoted by the symbol δ while f_n, f_t are distributed loads in the normal and tangential direction. The principle of virtual work yields two non-linear equilibrium equations [23]:

$$\frac{\mathrm{d}}{\mathrm{d}s}\left(N + \frac{M}{R}\right) - \frac{1}{R}\left(N + \frac{M}{R}\right)\psi_{o\eta} + f_t = 0\,, \quad (6)$$

$$\frac{\mathrm{d}}{\mathrm{d}s}\left[\frac{\mathrm{d}M}{\mathrm{d}s} - \left(N + \frac{M}{R}\right)\psi_{o\eta}\right] - \frac{N}{R} + f_n = 0\,. \quad (7)$$

Let us drop the non-linear terms and substitute $(3)_{1,2}$ for N and M then $(2)_1$ for $\varepsilon_{o\xi}$. If, in addition to this, we introduce the dimensionless displacements

$$U_o = \frac{u_o}{R}\,, \qquad W_o = \frac{w_o}{R}$$

we get the following differential equations [22, 24]:

$$\begin{bmatrix} 0 & 0 \\ 0 & 1 \end{bmatrix}\begin{bmatrix} U_o \\ W_o \end{bmatrix}^{(4)} + \begin{bmatrix} -m & 0 \\ 0 & 2 \end{bmatrix}\begin{bmatrix} U_o \\ W_o \end{bmatrix}^{(2)} + \\ + \begin{bmatrix} 0 & -m \\ m & 0 \end{bmatrix}\begin{bmatrix} U_o \\ W_o \end{bmatrix}^{(1)} + \begin{bmatrix} 0 & 0 \\ 0 & m+1 \end{bmatrix}\begin{bmatrix} U_o \\ W_o \end{bmatrix}^{(0)} = \frac{R^3}{I_{e\eta}}\begin{bmatrix} f_t \\ f_n \end{bmatrix}. \quad (8)$$

Here and now on, the n-th derivative of a quantity $(\ldots)$ in terms of φ is denoted by $(\ldots)^{(n)}$. For the problem of free vibrations the distributed loads are forces of inertia. Thus

$$f_t = -\rho_a A \frac{\partial^2 u_o}{\partial t^2}; \quad f_n = -\rho_a A \frac{\partial^2 w_o}{\partial t^2}, \quad (9)$$

where ρ_a is the average density over the cross-section of area A and t denotes time.

For time-harmonic and undamped vibrations equation system (8) assumes the following form:

$$\begin{bmatrix} 0 & 0 \\ 0 & 1 \end{bmatrix} \begin{bmatrix} \hat{U} \\ \hat{W} \end{bmatrix}^{(4)} + \begin{bmatrix} -m & 0 \\ 0 & 2 \end{bmatrix} \begin{bmatrix} \hat{U} \\ \hat{W} \end{bmatrix}^{(2)} + \\ + \begin{bmatrix} 0 & -m \\ m & 0 \end{bmatrix} \begin{bmatrix} \hat{U} \\ \hat{W} \end{bmatrix}^{(1)} + \begin{bmatrix} 0 & 0 \\ 0 & m+1 \end{bmatrix} \begin{bmatrix} \hat{U} \\ \hat{W} \end{bmatrix}^{(0)} = \lambda \begin{bmatrix} \hat{U} \\ \hat{W} \end{bmatrix} \quad (10)$$

where $\hat{U}$ and $\hat{W}$ are the dimensionless vibration amplitudes and

$$\lambda = \rho_a A \frac{R^3}{I_{e\eta}} \alpha^2 \quad (11)$$

is the unknown eigenvalue which belongs to the eigenfrequency α of the free vibrations. As regards the left side of equation (10), the effect of cross-sectional heterogeneity appears through the parameter m.

3. The Green function matrix

This section presents the definition of the Green function matrix for a class of boundary value problems governed by a system of degenerated ordinary differential equations. The definition is taken from a thesis – see [1] or paper [3] for details. First, we shall rewrite equation (10) into the following matrix form:

$$\mathbf{K}(\mathbf{y}) = \sum_{\nu=0}^{4} \overset{\nu}{\mathbf{P}}(\varphi)\mathbf{y}^{(\nu)}(\varphi) = \mathbf{r}(\varphi) = \\ = \underbrace{\begin{bmatrix} 0 & 0 \\ 0 & 1 \end{bmatrix}}_{\overset{4}{\mathbf{P}}} \underbrace{\begin{bmatrix} \hat{U} \\ \hat{W} \end{bmatrix}^{(4)}}_{\mathbf{y}^{(4)}} + \underbrace{\begin{bmatrix} -m & 0 \\ 0 & 2 \end{bmatrix}}_{\overset{2}{\mathbf{P}}} \underbrace{\begin{bmatrix} \hat{U} \\ \hat{W} \end{bmatrix}^{(2)}}_{\mathbf{y}^{(2)}} + \underbrace{\begin{bmatrix} 0 & -m \\ m & 0 \end{bmatrix}}_{\overset{1}{\mathbf{P}}} \underbrace{\begin{bmatrix} \hat{U} \\ \hat{W} \end{bmatrix}^{(1)}}_{\mathbf{y}^{(1)}} + \\ + \underbrace{\begin{bmatrix} 0 & 0 \\ 0 & m+1 \end{bmatrix}}_{\overset{0}{\mathbf{P}}} \underbrace{\begin{bmatrix} \hat{U} \\ \hat{W} \end{bmatrix}}_{\mathbf{y}^{(0)}} = \underbrace{\lambda \begin{bmatrix} \hat{U} \\ \hat{W} \end{bmatrix}}_{\mathbf{r}} \qquad \overset{3}{\mathbf{P}} = \begin{bmatrix} 0 & 0 \\ 0 & 0 \end{bmatrix}. \quad (12)$$

Remark 1.: Differential equation (12) is called degenerated since the matrix $\overset{3}{\mathbf{P}}$ has no inverse.

Remark 2.: For equilibrium problems, the right side $\mathbf{r}$ is given by equation (10) which means that $\mathbf{r}$ represents a dimensionless distributed load.

We shall assume that (12) is associated with homogeneous linear boundary conditions of the form

$$\mathbf{U}_\mu(\mathbf{y}) = \sum_{\nu=0}^{3} \left[\mathbf{A}_{\nu\mu}\mathbf{y}^{(\nu)}(-\vartheta) + \mathbf{B}_{\nu\mu}\mathbf{y}^{(\nu)}(\vartheta) \right] = \\ = \sum_{\nu=0}^{3} \left\{ \begin{bmatrix} \overset{11}{A}_{\nu\mu} & \overset{12}{A}_{\nu\mu} \\ \overset{21}{A}_{\nu\mu} & \overset{22}{A}_{\nu\mu} \end{bmatrix} \begin{bmatrix} y_1(-\vartheta) \\ y_2(-\vartheta) \end{bmatrix}^{(v)} + \begin{bmatrix} \overset{11}{B}_{\nu\mu} & \overset{12}{B}_{\nu\mu} \\ \overset{21}{B}_{\nu\mu} & \overset{22}{B}_{\nu\mu} \end{bmatrix} \begin{bmatrix} y_1(\vartheta) \\ y_2(\vartheta) \end{bmatrix}^{(v)} \right\} = \begin{bmatrix} 0 \\ 0 \end{bmatrix} \quad (13)$$

where $\mu = 1, \ldots, 4$. The constant matrices $A_{\nu\mu}$ and $B_{\nu\mu}$ fulfill the conditions

$$\overset{11}{A}_{\nu\mu} = \overset{21}{A}_{\nu\mu} = \overset{11}{B}_{\nu\mu} = \overset{21}{B}_{\nu\mu} = 0.$$

For equilibrium problems equations (12), (13) constitute a boundary value problem. With the knowledge of the Green function matrix the solution sought can be given by the integral:

$$\mathbf{y}(\varphi) = \int_{-\vartheta}^{\vartheta} \mathbf{G}(\varphi, \gamma)\mathbf{r}(\gamma)\mathrm{d}\gamma \tag{14}$$

in which $\mathbf{G}(\varphi, \gamma)$ is the Green function matrix and φ, γ are angle coordinates. The Green function matrix is defined by the following four properties [1, 23]:

1. $\mathbf{G}(\varphi, \gamma)$ is a continuous function of the angle coordinates φ and γ in each of the triangular domains $-\vartheta \le \varphi \le \gamma \le \vartheta$ and $-\vartheta \le \gamma \le \varphi \le \vartheta$. Moreover,

   $$G_{11}(\varphi, \gamma), G_{12}(\varphi, \gamma) \;\; [G_{21}(\varphi, \gamma), G_{22}(\varphi, \gamma)]$$

   are 2 [4] times continuously differentiable with respect to φ. The derivatives

   $$\frac{\partial^\nu \mathbf{G}(\varphi, \gamma)}{\partial \varphi^\nu} = \mathbf{G}^{(\nu)}(\varphi, \gamma) \qquad (\nu = 1, 2)$$
   $$\frac{\partial^\nu G_{2i}(\varphi, \gamma)}{\partial \varphi^\nu} = G_{2i}^{(\nu)}(\varphi, \gamma) \qquad (\nu = 1, 2, \ldots, 4;\ i = 1, 2)$$

   are also continuous in φ and γ.
2. For any γ in $-\vartheta, \ldots, \vartheta$ the derivatives

   $$G_{11}(\varphi, \gamma);\;\; G_{12}^{(1)}(\varphi, \gamma);\;\; G_{21}^{(\nu)}(\varphi, \gamma) \qquad (\nu = 1, 2, 3);\;\; G_{22}^{(\nu)}(\varphi, \gamma) \qquad (\nu = 1, 2)$$

   are continuous at $\varphi = \gamma$, except $G_{11}^{(1)}(\varphi, \gamma)$ and $G_{22}^{(3)}(\varphi, \gamma)$ – these later two have a jump that is

   $$\lim_{\varepsilon \to 0} \left[G_{11}^{(1)}(\varphi + \varepsilon, \varphi) - G_{11}^{(1)}(\varphi - \varepsilon, \varphi) \right] = \overset{1}{P}{}_{11}^{-1}(\varphi), \tag{15a}$$

   $$\lim_{\varepsilon \to 0} \left[G_{22}^{(3)}(\varphi + \varepsilon, \varphi) - G_{22}^{(3)}(\varphi - \varepsilon, \varphi) \right] = \overset{4}{P}{}_{22}^{-1}(\varphi). \tag{15b}$$

3. Let $\boldsymbol{\alpha}$ be an arbitrary constant vector. Then, for any γ, $\mathbf{G}(\varphi, \gamma)\boldsymbol{\alpha}$ as a function of φ $(\varphi \neq \gamma)$ satisfies the equation

   $$\mathbf{K}\left[\mathbf{G}(\varphi, \gamma)\boldsymbol{\alpha}\right] = \mathbf{0}.$$

4. The vector $\mathbf{G}(\varphi, \gamma)\boldsymbol{\alpha}$ as function of φ should satisfy the boundary conditions as well:

   $$\mathbf{U}_\mu\left[\mathbf{G}(\varphi, \gamma)\boldsymbol{\alpha}\right] = \mathbf{0}, \quad \mu = 1, \ldots, 4.$$

If the Green function matrix exists (an existence proof can be found in [1]) the column vector (14) satisfies differential equation (12) and the boundary conditions (13), i.e., integral (14) is really the solution of the boundary value problem (12), (13).

The general solution to the homogeneous part of equation (12) is given by the equation

$$\mathbf{y} = \left[\sum_{i=1}^{4} \underset{(2\times 2)}{\mathbf{Y}}{}_{i} \underset{(2\times 2)}{\mathbf{C}}{}_{i} \right] \underset{(2\times 1)}{\mathbf{e}} \tag{16}$$

where $\mathbf{C}_i$ is a constant non-singular matrix, $\mathbf{e}$ is a constant column matrix and

$$\mathbf{Y}_1 = \begin{bmatrix} \cos\varphi & 0 \\ \sin\varphi & 0 \end{bmatrix}, \qquad \mathbf{Y}_2 = \begin{bmatrix} -\sin\varphi & 0 \\ \cos\varphi & 0 \end{bmatrix}, \tag{17a}$$

$$\mathbf{Y}_3 = \begin{bmatrix} -\sin\varphi + \varphi\cos\varphi & (m+1)\varphi \\ \varphi\sin\varphi & -m \end{bmatrix}, \qquad \mathbf{Y}_4 = \begin{bmatrix} -\cos\varphi - \varphi\sin\varphi & 1 \\ \varphi\cos\varphi & 0 \end{bmatrix}. \tag{17b}$$

It follows from Property 3 that the Green function matrix has the following mathematical form:

$$\mathbf{G}(\varphi,\gamma) = \sum_{i=1}^{4} \mathbf{Y}_i(\varphi)\left[\mathbf{A}_i(\gamma) + \mathbf{B}_i(\gamma)\right] \qquad \varphi \le \gamma, \tag{18a}$$

$$\mathbf{G}(\varphi,\gamma) = \sum_{i=1}^{4} \mathbf{Y}_i(\varphi)\left[\mathbf{A}_i(\gamma) - \mathbf{B}_i(\gamma)\right] \qquad \varphi \ge \gamma. \tag{18b}$$

Here $\mathbf{A}_i(\gamma)$ and $\mathbf{B}_i(\gamma)$ are 2×2 matrices. We remark that the coefficients $\mathbf{B}_i(\gamma)$ can be determined by using Properties 1 and 2 of the definition while the coefficients $\mathbf{A}_i(\gamma)$ can be obtained by using Property 4 of the definition, i.e., the boundary conditions

$$\mathbf{U}_\mu \left[\sum_{i=1}^{4} \mathbf{Y}_i(\varphi)\mathbf{A}_i(\gamma)\boldsymbol{\alpha} \right] = \mp \mathbf{U}_\mu \left[\sum_{i=1}^{4} \mathbf{Y}_i(\varphi)\mathbf{B}_i(\gamma)\boldsymbol{\alpha} \right] . \tag{19}$$

Calculation of the Green function matrix and the results of the calculations for fixed-fixed, pinned-pinned and pinned-fixed beams are presented in Appendix A.1 and A.4.

Consider now the system of differential equations

$$\mathbf{K}[\mathbf{y}] = \lambda \mathbf{y} \tag{20}$$

where λ is a parameter (the unknown eigenvalue). Assume that differential equations (20) are associated with the homogeneous linear boundary conditions (13). Equations (20) and (13) constitute an eigenvalue problem with λ as the eigenvalue. Since the eigenvalue problem (20) and (13) is self-adjoint [1, 23] it follows that the Green function matrix is cross-symmetric [1]:

$$\mathbf{G}(\varphi,\gamma) = \mathbf{G}^T(\gamma,\varphi).$$

Recalling (14) the eigenvalue problem (20), (13) can be replaced by the homogeneous Fredholm integral equation

$$\mathbf{y}(\varphi) = \lambda \int_{-\vartheta}^{\vartheta} \mathbf{G}(\varphi,\gamma)\mathbf{y}(\gamma)\mathrm{d}\gamma\,. \tag{21}$$

Eigenvalue problem (21) can be solved numerically if we follow the solution procedure detailed in [23, 26].

4. Numerical results – free vibrations

We have developed a Fortran 90 program for solving numerically the algebraic eigenvalue problem derived from eigenvalue problem (21). Three support arrangements were considered: (a) fixed-fixed beams, (b) pinned-pinned beams and (c) pinned-fixed beams. The results are the same as those in thesis [22] obtained under the condition that the central force acting on the beam is equal to zero.

Table 1. Typical values of $C_{i,\mathrm{char}}$

	$i=1$	$i=2$	$i=3$	$i=4$
Fixed-fixed beams	2.266	6.243	12.23	20.25
Pinned-pinned beams	1	4	9	16
Pinned-fixed beams	1.556	5.078	10.541	17.97

Consider a straight beam with the same length ℓ as that of the curved beam we deal with. The eigenfrequencies $\alpha_{i\ \mathrm{str.}}$ $(i=1,2,...)$ of the straight beam are well-known – see for instance [1, 22] – and are given by

$$\alpha_{i\ \mathrm{str.}} = \frac{C_{i,\,\mathrm{char}}\pi^2}{\sqrt{\frac{\rho_a A}{I_{e\eta}}}\ell^2}\,. \tag{22}$$

The constant $C_{i,\,\mathrm{char}}$ depends on the ordinal number of the frequency – see Table 1 — and $\ell = 2R\vartheta$ is the length of the beam. Recalling now equation (11), as detailed in [23], we get

$$C_{i,\mathrm{char}}\frac{\alpha_i}{\alpha_{i\ \mathrm{str.}}} = \frac{\frac{\sqrt{\lambda_i}}{\sqrt{\frac{\rho_a A}{I_{e\eta}}}R^2}}{\frac{\pi^2}{\sqrt{\frac{\rho_a A}{I_{e\eta}}}\ell^2}} = \frac{\bar{\vartheta}^{\,2}\sqrt{\lambda_i}}{\pi^2}. \tag{23}$$

This quotient is plotted in the next three diagrams for the above mentioned three support conditions. The eigenfrequencies of the curved beams we have considered are therefore compared to the first eigenfrequency of straight beams with the same length and same material composition. It is worth emphasizing that the material composition is incorporated into the model via the parameter m.

4.1. **Fixed-fixed supports.** The quotient (23) is plotted in Figure 2 against the central angle $\bar{\vartheta}$ of the beam. The picked values of m are 750, 1 000, 1 300, 1 750, 2 400, 3 400, 5 000, 7 500, 12 000, 20 000, 35 000, 60 000, 100 000 and 200 000. The outcomes are identical to those of [1] valid for homogeneous beams. Thus, it turns out that the ratio of the even frequencies do not depend on m. Another important property is that a frequency shift can be observed: in terms of magnitude, the first/third frequency becomes the second/fourth one if the central angle is sufficiently great.

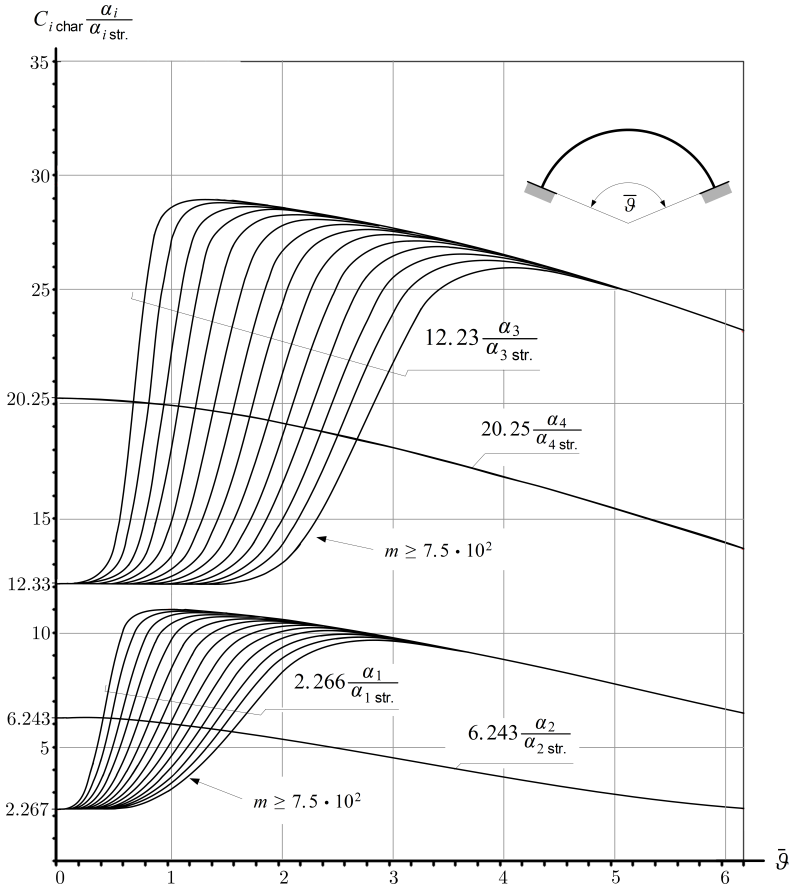

Figure 2. Eigenfrequencies for fixed-fixed beams [27]

Table 2. FE verifications, fixed-fixed beams, $m = 1\,200$, $R/b = 10$

ϑ	$\frac{\alpha_{1\ \text{New model}}}{\alpha_{1\ \text{Abaqus}}}$	$\frac{\alpha_{2\ \text{New model}}}{\alpha_{2\ \text{Abaqus}}}$	$\frac{\alpha_{3\ \text{New model}}}{\alpha_{3\ \text{Abaqus}}}$	$\frac{\alpha_{4\ \text{New model}}}{\alpha_{4\ \text{Abaqus}}}$
0.5	1.019	1.115	1.193	1.314
1	1.031	1.037	1.021	1.075
1.5	1.014	1.025	1.039	1.037
2	1.008	1.015	1.022	1.032
2.5	0.971	1.010	1.015	1.022

Some finite element computations were carried out for verification reasons using the commercial software Abaqus. In Abaqus 6.7 we used the Linear Perturbation, Frequency Step. The model consisted of $B22$ (3-node Timoshenko beam) elements. Further, we chose $E = 2 \cdot 10^{11}$ Pa and $\rho_a = 7800$ kg/m^3. R/b is the

centerline radius/cross-sectional height ratio. The frequency ratios of the new model ($\alpha_{i\,\text{New model}}$) and Abaqus ($\alpha_{i\,\text{Abaqus}}$) are gathered in Tables 2 and 3. Generally, there is a very good agreement.

Table 3. FE verifications, fixed-fixed beams, $m = 10\,800$, $R/b = 30$

ϑ	$\frac{\alpha_{1\ \text{New model}}}{\alpha_{1\ \text{Abaqus}}}$	$\frac{\alpha_{2\ \text{New model}}}{\alpha_{2\ \text{Abaqus}}}$	$\frac{\alpha_{3\ \text{New model}}}{\alpha_{3\ \text{Abaqus}}}$	$\frac{\alpha_{4\ \text{New model}}}{\alpha_{4\ \text{Abaqus}}}$
0.5	1.014	1.007	1.018	1.039
1	1.004	1.006	1.010	1.014
1.5	1.002	1.003	1.006	1.009
2	1.001	1.002	1.003	1.005
2.5	1.000	1.001	1.002	1.004
3	1.000	1.001	1.002	1.004

Recalling the results gathered in Tables 1 and 4 in article [10], we can make some additional comparisons as shown in Tables 4 and 5. We assume a rectangular cross-section ($A = 0.01$ m^2; $I_\eta = 8.33 \cdot 10^{-6}$ m^4) and that $E = 2 \cdot 10^{11}$ Pa, $\rho_a = 7\,800$ kg/m^3. In Tables 4 and 5 Ref. [10] col. 1 and Ref. [28] consider axial extension and rotatory inertia effects, while in Ref. [10] col. 2, none of these is incorporated. Moreover, Ref. [10] col 5. is the most accurate model: axial extension, rotatory inertia and transverse shear effects are all assumed. In general, the agreement is quite good between the current and even with the most accurate model.

Table 4. Comparison of the eigenfrequencies, $2\vartheta = \pi/2$, fixed-fixed supports

m		Ref. [28]	Ref. [10] col. 1	Ref. [10] col. 2	Ref. [10] col. 5	New model
10 000	α_1	63.07	63.06	63.16	62.62	63.1
10 000	α_2	117.22	117.19	120.76	115.85	117.5
10 000	α_3	217.13	217.08	218.41	213.28	218.2
10 000	α_4	249.26	345.21	322.26	247.96	249.8
2 500	α_1	251	251	252.66	244.24	251.89
2 500	α_2	399.68	399.65	483.04	390.09	401.16
2 500	α_3	613.25	613.33	873.64	600.7	617.25
2 500	α_4	847.24	847.07	1289.06	795.82	859.02

Table 5. Comparison of the eigenfrequencies, $2\vartheta = \pi$, fixed-fixed supports

m		Ref. [28]	Ref. [10] col. 1	Ref. [10] col. 2	Ref. [10] col. 5	New model
10 000	α_1	12.23	12.23	12.24	12.21	12.24
10 000	α_2	26.89	26.89	26.95	26.80	26.92
10 000	α_3	49.93	49.93	50.03	49.70	50.07
10 000	α_4	76.43	76.44	76.84	75.95	76.85
2 500	α_1	48.87	48.86	48.96	48.51	48.9
2 500	α_2	106.85	106.85	107.78	105.53	107.1
2 500	α_3	198.57	198.51	200.13	194.94	199.5
2 500	α_4	299.61	299.59	307.37	292.46	302.13

4.2. **Pinned-pinned supports.** In Figure 3 the ratio (23) is plotted against the central angle $\bar{\vartheta}$ of the circular beam. The curves run similarly as for fixed-fixed beams and the character of the curves plotted are the same. The quotients are generally smaller for the same parameters meaning that the pinned supports are softer.

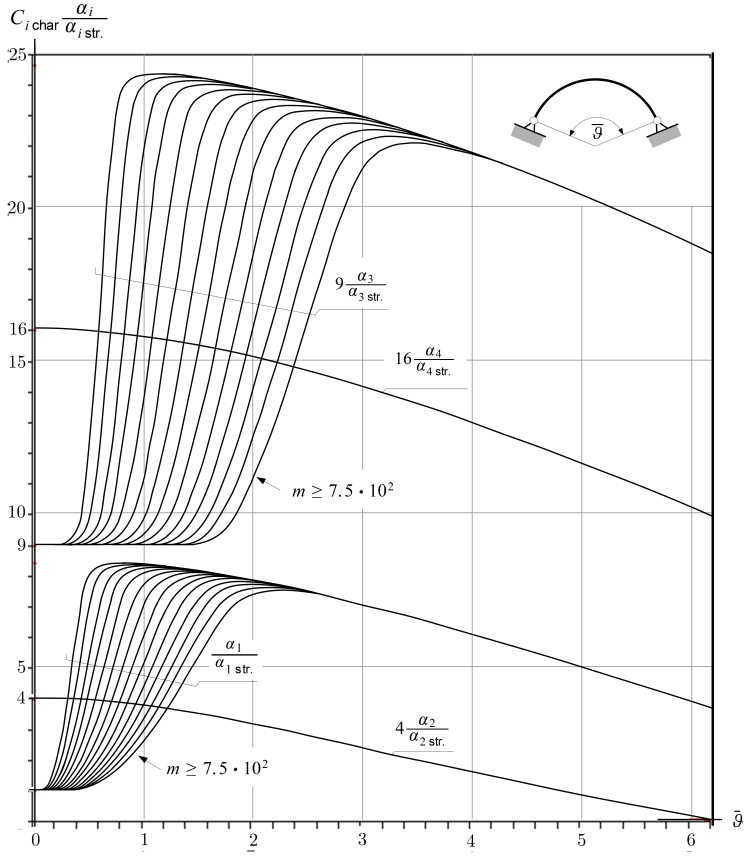

Figure 3. Eigenfrequencies for pinned-pinned beams [26]

Table 6. FE verifications, $R/b = 10$; $m = 1\ 200$

ϑ	$\frac{\alpha_{1\ \text{New model}}}{\alpha_{1\ \text{Abaqus}}}$	$\frac{\alpha_{2\ \text{New model}}}{\alpha_{2\ \text{Abaqus}}}$	$\frac{\alpha_{3\ \text{New model}}}{\alpha_{3\ \text{Abaqus}}}$	$\frac{\alpha_{4\ \text{New model}}}{\alpha_{4\ \text{Abaqus}}}$
0.5	1.001	1.053	1.109	1.179
1	1.014	1.029	1.004	1.053
1.5	1.007	1.014	1.028	1.006
2	1.004	1.008	1.014	1.022
2.5	1.003	1.005	1.010	1.015

When comparing these numerical results to the Abaqus computations (the settings were the same as mentioned in relation with fixed-fixed beam) once again, we find a really good agreement. See Tables 6 and 7 for the computational results.

Table 7. FE verifications, $R/b = 30$, $m = 10\,800$

ϑ	$\frac{\alpha_{1\text{ New model}}}{\alpha_{1\text{ Abaqus}}}$	$\frac{\alpha_{2\text{ New model}}}{\alpha_{2\text{ Abaqus}}}$	$\frac{\alpha_{3\text{ New model}}}{\alpha_{3\text{ Abaqus}}}$	$\frac{\alpha_{4\text{ New model}}}{\alpha_{4\text{ Abaqus}}}$
0.5	1.006	1.010	1.005	1.025
1	1.002	1.004	1.007	1.011
1.5	1.001	1.002	1.003	1.006
2	1.000	1.001	1.002	1.003
2.5	1.000	1.001	1.002	1.003
3	1.001	1.001	1.001	1.002

Some further comparisons with Tables 5 and 8 in [10] are provided hereinafter. The data are the same as for fixed-fixed members. The results are presented in Tables 8 and 9.

Table 8. Comparison of the eigenfrequencies, $2\vartheta = \pi/2$, pinned-pinned supports

m		Ref. [28]	Ref. [10] col. 1	Ref. [10] col. 2	Ref. [10] col. 5	New model
10 000	α_1	38.38	38.38	38.42	38.28	38.41
10 000	α_2	89.57	89.56	90.46	89.08	89.77
10 000	α_3	171.42	171.41	172.17	169.75	172.18
10 000	α_4	244.96	244.94	269.26	243.05	245.82
2 500	α_1	152.93	152.93	153.7	151.45	153.48
2 500	α_2	343.01	342.76	361.85	336.46	345.31
2 500	α_3	552.15	552.17	688.7	549.84	552.28
2 500	α_4	675.71	675.83	1077.01	651.82	685.38

Table 9. Comparison of the eigenfrequencies, $2\vartheta = \pi$, pinned-pinned supports

m		Ref. [28]	Ref. [10] col. 1	Ref. [10] col. 2	Ref. [10] col. 5	New model
10 000	α_1	6.33	6.33	6.33	6.32	6.33
10 000	α_2	19.31	19.31	19.33	19.28	19.32
10 000	α_3	38.98	38.97	39.02	38.87	39.05
10 000	α_4	63.53	63.53	63.71	63.29	63.79
2 500	α_1	25.28	25.28	25.31	25.21	25.3
2 500	α_2	77.01	76.99	77.31	76.57	77.18
2 500	α_3	155.24	155.25	156.09	153.75	155.96
2 500	α_4	251.86	251.82	254.83	248.12	253.81

4.3. **Pinned-fixed supports.** The curves are similar to the two previous cases and the frequencies are always between the typical values valid for pinned-pinned and fixed-fixed members. Abaqus computations [29] verified the validity of these numerical results just for the two previous support arrangements.

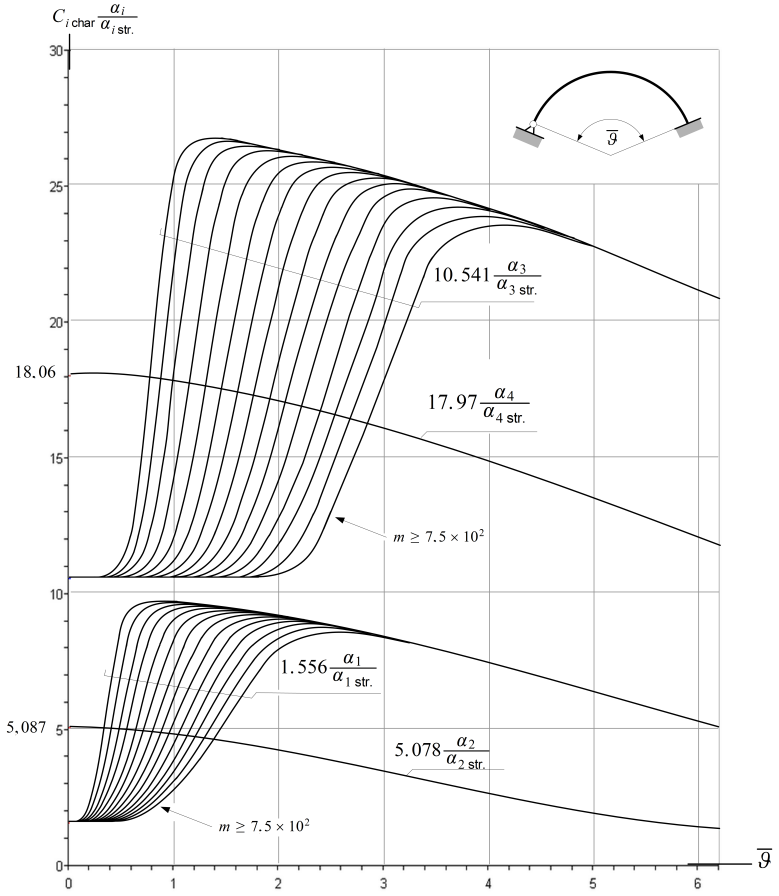

Figure 4. Eigenfrequencies for pinned-fixed beams [23]

5. Conclusions

We list our conclusions below:

1. We have investigated the free vibrations of circular beams with cross-sectional heterogeneity. For the three support arrangements, i.e., for fixed-fixed, pinned-pinned and pinned-fixed curved beams we have determined the Green function matrices in closed form.

2. With the knowledge of the Green function matrices we have reduced the self-adjoint eigenvalue problems, the solution of which results in the natural frequencies sought, to eigenvalue problems governed by homogeneous Fredholm integral equations. These integral equations were solved numerically.
3. It has turned out that, for any support arrangement, the even natural frequencies are independent of the heterogeneity-geometry parameter m while the odd ones do depend on it for smaller central angles.
4. The numerical results were verified by commercial finite element calculations and by comparing them to other models from the literature. A good agreement is found.
5. Let $\mathbf{r}$ be a dimensionless distributed load of the beams. With the knowledge of the Green function matrices the corresponding equilibrium problems can be solved in a closed form which is given by equation (14).

Acknowledgement. This research was supported by the National Research, Development and Innovation Office - NKFIH, K115701.

Appendix A. Elements of the Green function matrix

The definition of the Green function matrix in Section 3 was published in thesis [1]. It is worth mentioning that Lin [30] introduced the concept of a generalized Green function for a class of ordinary differential equations for finding particular solutions to nonhomogeneous boundary value problems (equilibrium problems). In contrast to this work, integral (14) provides the complete solution to the boundary value problem considered if we know the corresponding Green function matrix. In the sequel we detail its calculation.

Recalling (18) and (17) we can give the Green function matrix in the following form:

$$\begin{aligned}\underbrace{\mathbf{G}(\varphi,\gamma)}_{(2\times 2)} = &\begin{bmatrix} \cos\varphi & 0 \\ \sin\varphi & 0 \end{bmatrix} \left\{ \begin{bmatrix} \overset{1}{A}_{11} & \overset{1}{A}_{12} \\ 0 & 0 \end{bmatrix} \pm \begin{bmatrix} \overset{1}{B}_{11} & \overset{1}{B}_{12} \\ 0 & 0 \end{bmatrix} \right\} + \\ &\begin{bmatrix} -\sin\varphi & 0 \\ \cos\varphi & 0 \end{bmatrix} \left\{ \begin{bmatrix} \overset{2}{A}_{11} & \overset{2}{A}_{12} \\ 0 & 0 \end{bmatrix} \pm \begin{bmatrix} \overset{2}{B}_{11} & \overset{2}{B}_{12} \\ 0 & 0 \end{bmatrix} \right\} + \\ &\begin{bmatrix} -\sin\varphi + \varphi\cos\varphi & (m+1)\varphi \\ \varphi\sin\varphi & -m \end{bmatrix} \left\{ \begin{bmatrix} \overset{3}{A}_{11} & \overset{3}{A}_{12} \\ \overset{2}{A}_{21} & \overset{2}{A}_{22} \end{bmatrix} \pm \begin{bmatrix} \overset{3}{B}_{11} & \overset{3}{B}_{12} \\ \overset{3}{B}_{21} & \overset{3}{B}_{22} \end{bmatrix} \right\} + \\ &\begin{bmatrix} -\cos\varphi - \varphi\sin\varphi & 1 \\ \varphi\cos\varphi & 0 \end{bmatrix} \left\{ \begin{bmatrix} \overset{3}{A}_{11} & \overset{3}{A}_{12} \\ \overset{3}{A}_{21} & \overset{3}{A}_{22} \end{bmatrix} \pm \begin{bmatrix} \overset{3}{B}_{11} & \overset{3}{B}_{12} \\ \overset{3}{B}_{21} & \overset{3}{B}_{22} \end{bmatrix} \right\}. \end{aligned}$$

The sign is [positive](negative) if $[\varphi \le \psi]\,(\varphi \ge \psi)$.

A.1. **Solutions for the matrices $\mathbf{B}_i$.** Fulfillment of Properties 1 and 2 yields the unknown elements of the matrices $\mathbf{B}_i$. The discontinuities are taken from a comparison of (12) and (15a). The equation system to be solved is obviously independent of the boundary conditions:

$$\begin{bmatrix} \cos\gamma & -\sin\gamma & -\sin\gamma+\gamma\cos\gamma & (1+m)\gamma & -\cos\gamma-\gamma\sin\gamma & 1 \\ \sin\gamma & \cos\gamma & \gamma\sin\gamma & -m & \gamma\cos\gamma & 0 \\ -\sin\gamma & -\cos\gamma & -\gamma\sin\gamma & 1+m & -\gamma\cos\gamma & 0 \\ \cos\gamma & -\sin\gamma & \gamma\cos\gamma+\sin\gamma & 0 & -\gamma\sin\gamma+\cos\gamma & 0 \\ -\sin\gamma & -\cos\gamma & -\gamma\sin\gamma+2\cos\gamma & 0 & -\gamma\cos\gamma-2\sin\gamma & 0 \\ -\cos\gamma & \sin\gamma & -\gamma\cos\gamma-3\sin\gamma & 0 & \gamma\sin\gamma-3\cos\gamma & 0 \end{bmatrix} \begin{bmatrix} \overset{1}{B}_{11} & \overset{1}{B}_{12} \\ \overset{2}{B}_{11} & \overset{2}{B}_{12} \\ \overset{3}{B}_{11} & \overset{3}{B}_{12} \\ \overset{3}{B}_{21} & \overset{3}{B}_{22} \\ \overset{4}{B}_{11} & \overset{4}{B}_{12} \\ \overset{4}{B}_{21} & \overset{4}{B}_{22} \end{bmatrix} = \begin{bmatrix} 0 & 0 \\ 0 & 0 \\ \dfrac{1}{2m} & 0 \\ 0 & 0 \\ 0 & 0 \\ 0 & -\dfrac{1}{2} \end{bmatrix}. \tag{24}$$

The solutions are given by the following equations:

$$\begin{aligned} \overset{1}{B}_{11} &= \frac{1}{2}\sin\gamma - \frac{1}{4}\gamma\cos\gamma & \qquad \overset{1}{B}_{12} &= -\frac{1}{4}\cos\gamma - \frac{1}{4}\gamma\sin\gamma \\ \overset{2}{B}_{11} &= \frac{1}{4}\gamma\sin\gamma + \frac{1}{2}\cos\gamma & \qquad \overset{2}{B}_{12} &= \frac{1}{4}\sin\gamma - \frac{1}{4}\gamma\cos\gamma \\ \overset{3}{B}_{11} &= \frac{1}{4}\cos\gamma & \qquad \overset{3}{B}_{12} &= \frac{1}{4}\sin\gamma \\ \overset{3}{B}_{21} &= \frac{1}{2m} & \text{and} \qquad \overset{3}{B}_{22} &= 0 \\ \overset{4}{B}_{11} &= -\frac{1}{4}\sin\gamma & \qquad \overset{4}{B}_{12} &= \frac{1}{4}\cos\gamma \\ \overset{4}{B}_{21} &= -\frac{1}{2}(1+m)\frac{\gamma}{m} & \qquad \overset{4}{B}_{21} &= \frac{1}{2}. \end{aligned} \tag{25}$$

In what follows, let us introduce simplified notations as shown

$$a = \overset{1}{B}_{1i};\quad b = \overset{2}{B}_{1i};\quad c = \overset{3}{B}_{1i};\quad d = \overset{3}{B}_{2i};\quad e = \overset{4}{B}_{1i};\quad f = \overset{4}{B}_{2i}.$$

A.2. **The matrices $\mathbf{A}_i$ – fixed-fixed supports.** The boundary conditions are of the form

$$\hat{U}\Big|_{\pm\vartheta} = \hat{W}\Big|_{\pm\vartheta} = \hat{W}^{(1)}\Big|_{\pm\vartheta} = 0$$

thus, Property 3 yields the equations

$$\begin{bmatrix} \cos\vartheta & \sin\vartheta & \sin\vartheta-\vartheta\cos\vartheta & -(m+1)\vartheta & -\cos\vartheta-\vartheta\sin\vartheta & 1 \\ \cos\vartheta & -\sin\vartheta & -\sin\vartheta+\vartheta\cos\vartheta & (m+1)\vartheta & -\cos\vartheta-\vartheta\sin\vartheta & 1 \end{bmatrix} \begin{bmatrix} {}^{1}_{}A_{1i} \\ {}^{2}_{}A_{1i} \\ {}^{3}_{}A_{1i} \\ {}^{3}_{}A_{2i} \\ {}^{4}_{}A_{1i} \\ {}^{4}_{}A_{2i} \end{bmatrix} =$$

$$= \begin{bmatrix} -a\cos\vartheta - b\sin\vartheta - c\,(\sin\vartheta-\vartheta\cos\vartheta) + d(m+1)\vartheta + e\,(\cos\vartheta+\vartheta\sin\vartheta) - f \\ a\cos\vartheta - b\sin\vartheta + c\,(-\sin\vartheta+\vartheta\cos\vartheta) + d(m+1)\vartheta + e\,(-\cos\vartheta-\vartheta\sin\vartheta) + f \end{bmatrix},$$

$$\begin{bmatrix} -\sin\vartheta & \cos\vartheta & \vartheta\sin\vartheta & -m & -\vartheta\cos\vartheta & 0 \\ \sin\vartheta & \cos\vartheta & \vartheta\sin\vartheta & -m & \vartheta\cos\vartheta & 0 \end{bmatrix} \begin{bmatrix} {}^{1}_{}A_{1i} \\ {}^{2}_{}A_{1i} \\ {}^{3}_{}A_{1i} \\ {}^{3}_{}A_{2i} \\ {}^{4}_{}A_{1i} \\ {}^{4}_{}A_{2i} \end{bmatrix} =$$

$$= \begin{bmatrix} a\sin\vartheta - b\cos\vartheta - c\vartheta\sin\vartheta + dm + e\vartheta\cos\vartheta \\ a\sin\vartheta + b\cos\vartheta + c\vartheta\sin\vartheta - dm + e\vartheta\cos\vartheta \end{bmatrix},$$

$$\begin{bmatrix} \cos\vartheta & \sin\vartheta & -\sin\vartheta-\vartheta\cos\vartheta & 0 & \cos\vartheta-\vartheta\sin\vartheta & 0 \\ \cos\vartheta & -\sin\vartheta & \sin\vartheta+\vartheta\cos\vartheta & 0 & \cos\vartheta-\vartheta\sin\vartheta & 0 \end{bmatrix} \begin{bmatrix} {}^{1}_{}A_{1i} \\ {}^{2}_{}A_{1i} \\ {}^{3}_{}A_{1i} \\ {}^{3}_{}A_{2i} \\ {}^{4}_{}A_{1i} \\ {}^{4}_{}A_{2i} \end{bmatrix} =$$

$$= \begin{bmatrix} -a\cos\vartheta - b\sin\vartheta + c\,(\sin\vartheta+\vartheta\cos\vartheta) - e\,(\cos\vartheta-\vartheta\sin\vartheta) \\ a\cos\vartheta - b\sin\vartheta + c\,(\sin\vartheta+\vartheta\cos\vartheta) + e\,(\cos\vartheta-\vartheta\sin\vartheta) \end{bmatrix}.$$

Hence, the equation system to be solved is

$$\begin{bmatrix} \cos\vartheta & \sin\vartheta & \sin\vartheta-\vartheta\cos\vartheta & -(m+1)\vartheta & -\cos\vartheta-\vartheta\sin\vartheta & 1 \\ \cos\vartheta & -\sin\vartheta & -\sin\vartheta+\vartheta\cos\vartheta & (m+1)\vartheta & -\cos\vartheta-\vartheta\sin\vartheta & 1 \\ -\sin\vartheta & \cos\vartheta & \vartheta\sin\vartheta & -m & -\vartheta\cos\vartheta & 0 \\ \sin\vartheta & \cos\vartheta & \vartheta\sin\vartheta & -m & \vartheta\cos\vartheta & 0 \\ \cos\vartheta & \sin\vartheta & -\sin\vartheta-\vartheta\cos\vartheta & 0 & \cos\vartheta-\vartheta\sin\vartheta & 0 \\ \cos\vartheta & -\sin\vartheta & \sin\vartheta+\vartheta\cos\vartheta & 0 & \cos\vartheta-\vartheta\sin\vartheta & 0 \end{bmatrix} \begin{bmatrix} \overset{1}{A}_{1i} \\ \overset{2}{A}_{1i} \\ \overset{3}{A}_{1i} \\ \overset{3}{A}_{2i} \\ \overset{4}{A}_{1i} \\ \overset{4}{A}_{2i} \end{bmatrix} =$$

$$= \begin{bmatrix} -a\cos\vartheta-b\sin\vartheta-c\left(\sin\vartheta-\vartheta\cos\vartheta\right)+d(m+1)\vartheta+e\left(\cos\vartheta+\vartheta\sin\vartheta\right)-f \\ a\cos\vartheta-b\sin\vartheta+c\left(-\sin\vartheta+\vartheta\cos\vartheta\right)+d(m+1)\vartheta-e\left(\cos\vartheta+\vartheta\sin\vartheta\right)+f \\ a\sin\vartheta-b\cos\vartheta-c\vartheta\sin\vartheta+dm+e\vartheta\cos\vartheta \\ a\sin\vartheta+b\cos\vartheta+c\vartheta\sin\vartheta-dm+e\vartheta\cos\vartheta \\ -a\cos\vartheta-b\sin\vartheta+c\left(\sin\vartheta+\vartheta\cos\vartheta\right)-e\left(\cos\vartheta-\vartheta\sin\vartheta\right) \\ a\cos\vartheta-b\sin\vartheta+c\left(\sin\vartheta+\vartheta\cos\vartheta\right)+e\left(\cos\vartheta-\vartheta\sin\vartheta\right) \end{bmatrix}.$$

By introducing the notations

$$D_1 = \vartheta\cos^2\vartheta-\sin\vartheta\cos\vartheta+\vartheta\sin^2\vartheta = \vartheta-\sin\vartheta\cos\vartheta \tag{26a}$$

and

$$D_2 = m\sin\vartheta\left(\vartheta\cos\vartheta-2\sin\vartheta\right)+(1+m)\,\vartheta^2+\vartheta\cos\vartheta\sin\vartheta \tag{26b}$$

the solutions are as follows:

$$\overset{1}{A}_{1i} = \frac{1}{D_1}\left[-b\cos^2\vartheta+c\vartheta^2+dm\left(\cos\vartheta-\vartheta\sin\vartheta\right)\right], \tag{27a}$$

$$\overset{2}{A}_{1i} = \frac{1}{D_2}\left[a\left(1+m\right)\vartheta\sin^2\vartheta+2am\sin\vartheta\cos\vartheta-2em\vartheta+ \right.$$
$$\left. +e\left(1+m\right)\vartheta^3+fm\left(\vartheta\cos\vartheta+\sin\vartheta\right)\right], \tag{27b}$$

$$\overset{3}{A}_{1i} = \frac{1}{D_2}\left[a\left(1+m\right)\vartheta+e\left(1+m\right)\vartheta\cos^2\vartheta-2em\sin\vartheta\cos\vartheta+fm\sin\vartheta\right], \tag{27c}$$

$$\overset{3}{A}_{2i} = \frac{1}{D_2}\left[2a\sin\vartheta-2e\vartheta\cos\vartheta+f\left(\vartheta+\sin\vartheta\cos\vartheta\right)\right], \tag{27d}$$

$$\overset{4}{A}_{1i} = \frac{1}{D_1}\left(b-c\sin^2\vartheta-dm\cos\vartheta\right), \tag{27e}$$

$$\overset{4}{A}_{2i} = \frac{1}{D_1}\left[2b\cos\vartheta-2c\vartheta\sin\vartheta+d\left(1+m\right)\vartheta^2-d\left(1+m\right)\vartheta\sin\vartheta\cos\vartheta-2dm\cos^2\vartheta\right]. \tag{27f}$$

A.3. **The matrices $\mathbf{A}_i$ – pinned-pinned supports.** The boundary conditions are

$$\hat{U}\Big|_{\pm\vartheta} = \hat{W}\Big|_{\pm\vartheta} = \hat{W}^{(2)}\Big|_{\pm\vartheta} = 0.$$

Since only the last two boundary conditions are different in contrast to the case of the fixed-fixed beams, the equation system to be solved is

$$\begin{bmatrix} \cos\vartheta & \sin\vartheta & \sin\vartheta - \vartheta\cos\vartheta & -(m+1)\vartheta & -\cos\vartheta - \vartheta\sin\vartheta & 1 \\ \cos\vartheta & -\sin\vartheta & -\sin\vartheta + \vartheta\cos\vartheta & (m+1)\vartheta & -\cos\vartheta - \vartheta\sin\vartheta & 1 \\ -\sin\vartheta & \cos\vartheta & \vartheta\sin\vartheta & -m & -\vartheta\cos\vartheta & 0 \\ \sin\vartheta & \cos\vartheta & \vartheta\sin\vartheta & -m & \vartheta\cos\vartheta & 0 \\ \sin\vartheta & -\cos\vartheta & 2\cos\vartheta - \vartheta\sin\vartheta & 0 & 2\sin\vartheta + \vartheta\cos\vartheta & 0 \\ -\sin\vartheta & -\cos\vartheta & 2\cos\vartheta - \vartheta\sin\vartheta & 0 & -2\sin\vartheta - \vartheta\cos\vartheta & 0 \end{bmatrix} \begin{bmatrix} \overset{1}{A}_{1i} \\ \overset{2}{A}_{1i} \\ \overset{3}{A}_{1i} \\ \overset{3}{A}_{2i} \\ \overset{4}{A}_{1i} \\ \overset{4}{A}_{2i} \end{bmatrix}$$

$$= \begin{bmatrix} -a\cos\vartheta - b\sin\vartheta - c(\sin\vartheta - \vartheta\cos\vartheta) + d(m+1)\vartheta + e(\cos\vartheta + \vartheta\sin\vartheta) - f \\ a\cos\vartheta - b\sin\vartheta + c(-\sin\vartheta + \vartheta\cos\vartheta) + d(m+1)\vartheta - e(\cos\vartheta + \vartheta\sin\vartheta) + f \\ a\sin\vartheta - b\cos\vartheta - c\vartheta\sin\vartheta + dm + e\vartheta\cos\vartheta \\ a\sin\vartheta + b\cos\vartheta + c\vartheta\sin\vartheta - dm + e\vartheta\cos\vartheta \\ -a\sin\vartheta + b\cos\vartheta - c(2\cos\vartheta - \vartheta\sin\vartheta) - e(2\sin\vartheta + \vartheta\cos\vartheta) \\ -a\sin\vartheta - b\cos\vartheta + c(2\cos\vartheta - \vartheta\sin\vartheta) - e(2\sin\vartheta + \vartheta\cos\vartheta) \end{bmatrix}.$$

If we define D_1 and D_2 by the equations

$$D_1 = \sin^2\vartheta \tag{28a}$$

and

$$D_2 = m\vartheta + 2(1+m)\vartheta\cos^2\vartheta - 3m\sin\vartheta\cos\vartheta \tag{28b}$$

the solutions are

$$\overset{1}{A}_{1i} = \frac{1}{2D_1}\left[2b\sin\vartheta\cos\vartheta + 2c\vartheta - dm(2\sin\vartheta + \vartheta\cos\vartheta)\right], \tag{29a}$$

$$\overset{2}{A}_{1i} = \frac{1}{D_2}\left[a\left(2(1+m)\vartheta\sin\vartheta\cos\vartheta - m\sin^2\vartheta + 2m\cos^2\vartheta\right) + \right.$$
$$\left. + e\left(3m\vartheta^2 + 2\vartheta^2 - 2m\right) - fm(\vartheta\sin\vartheta - 2\cos\vartheta)\right], \tag{29b}$$

$$\overset{3}{A}_{1i} = \frac{1}{D_2}\left(am - e\left(m\cos^2\vartheta - 2m\sin^2\vartheta + 2(1+m)\vartheta\sin\vartheta\cos\vartheta\right) + fm\cos\vartheta\right), \tag{29c}$$

$$\overset{3}{A}_{2i} = \frac{2}{D_2}\left[a\cos\vartheta + e(\vartheta\sin\vartheta - \cos\vartheta) + f\cos^2\vartheta\right], \tag{29d}$$

$$\overset{4}{A}_{1i} = \frac{1}{2D_1}\left(-2c\sin\vartheta\cos\vartheta + dm\sin\vartheta\right), \tag{29e}$$

$$\overset{4}{A}_{2i} = \frac{1}{2D_1}\left[-2b\sin\vartheta - 2c(\sin\vartheta + \vartheta\cos\vartheta) + \right.$$
$$\left. + d\left(m\vartheta\cos^2\vartheta + 3m\sin\vartheta(\cos\vartheta + \vartheta\sin\vartheta) + 2\vartheta\sin^2\vartheta\right)\right]. \tag{29f}$$

A.4. **The matrices $\mathbf{A}_i$ – pinned-fixed supports.** Finally, for the third support arrangements

$$\hat{U}\Big|_{\pm\vartheta} = \hat{W}\Big|_{\pm\vartheta} = \hat{W}^{(1)}\Big|_{\vartheta} = \hat{W}^{(2)}\Big|_{-\vartheta} = 0$$

are the boundary conditions. Hence

$$\begin{bmatrix} \cos\vartheta & \sin\vartheta & \sin\vartheta-\vartheta\cos\vartheta & -(m+1)\vartheta & -\cos\vartheta-\vartheta\sin\vartheta & 1 \\ \cos\vartheta & -\sin\vartheta & -\sin\vartheta+\vartheta\cos\vartheta & (m+1)\vartheta & -\cos\vartheta-\vartheta\sin\vartheta & 1 \\ -\sin\vartheta & \cos\vartheta & \vartheta\sin\vartheta & -m & -\vartheta\cos\vartheta & 0 \\ \sin\vartheta & \cos\vartheta & \vartheta\sin\vartheta & -m & \vartheta\cos\vartheta & 0 \\ \sin\vartheta & -\cos\vartheta & 2\cos\vartheta-\vartheta\sin\vartheta & 0 & 2\sin\vartheta+\vartheta\cos\vartheta & 0 \\ \cos\vartheta & -\sin\vartheta & \sin\vartheta+\vartheta\cos\vartheta & 0 & \cos\vartheta-\vartheta\sin\vartheta & 0 \end{bmatrix} \begin{bmatrix} \overset{1}{A}_{1i} \\ \overset{2}{A}_{1i} \\ \overset{3}{A}_{1i} \\ \overset{3}{A}_{2i} \\ \overset{4}{A}_{1i} \\ \overset{4}{A}_{2i} \end{bmatrix} =$$

$$= \begin{bmatrix} -a\cos\vartheta - b\sin\vartheta - c(\sin\vartheta-\vartheta\cos\vartheta) + d(m+1)\vartheta + e(\cos\vartheta+\vartheta\sin\vartheta) - f \\ a\cos\vartheta - b\sin\vartheta + c(-\sin\vartheta+\vartheta\cos\vartheta) + d(m+1)\vartheta - e(\cos\vartheta+\vartheta\sin\vartheta) + f \\ a\sin\vartheta - b\cos\vartheta - c\vartheta\sin\vartheta + dm + e\vartheta\cos\vartheta \\ a\sin\vartheta + b\cos\vartheta + c\vartheta\sin\vartheta - dm + e\vartheta\cos\vartheta \\ -a\sin\vartheta + b\cos\vartheta - c(2\cos\vartheta-\vartheta\sin\vartheta) - e(2\sin\vartheta+\vartheta\cos\vartheta) \\ a\cos\vartheta - b\sin\vartheta + c(\sin\vartheta+\vartheta\cos\vartheta) + e(\cos\vartheta-\vartheta\sin\vartheta) \end{bmatrix}$$

is the equation system to be solved. With

$$\begin{aligned} D = {} & -4m + 11m\cos^2\vartheta - 7m\cos^4\vartheta - 4m\vartheta\sin\vartheta\cos^3\vartheta - \\ & - 2m\vartheta\sin\vartheta\cos\vartheta + 2\vartheta\cos\vartheta\sin\vartheta - 4\vartheta\cos^3\vartheta\sin\vartheta + 3m\vartheta^2 + 2\vartheta^2 \end{aligned} \tag{30}$$

the solutions are as follows:

$$\begin{aligned} \overset{1}{A}_{1i} = -\frac{1}{D}\Big\{ & a\left[-2\vartheta^2(m+1)\cos^2\vartheta + 2m\vartheta\cos\vartheta\sin\vartheta\right] + \\ & + b\left[-2\vartheta^2 m\sin\vartheta\cos\vartheta - 2\vartheta^2\sin\vartheta\cos\vartheta - m\vartheta\cos^2\vartheta + 4m\vartheta\cos^4\vartheta - \right. \\ & \left. - 7m\sin\vartheta\cos^3\vartheta + 4m\sin\vartheta\cos\vartheta - 2\vartheta\cos^2\vartheta + 4\vartheta\cos^4\vartheta\right] + \\ & c\left[-2\vartheta^3 - 2\vartheta^3(m+1)\cos^2\vartheta - 3\vartheta^3 m + 4m\vartheta\sin^2\vartheta + m\vartheta^2\sin\vartheta\cos\vartheta - 2\vartheta^2\sin\vartheta\cos\vartheta\right] \\ & + d\left[m(m+1)\vartheta^3\cos\vartheta - 4m^2\vartheta\cos\vartheta + m^2\vartheta\cos^3\vartheta + 2\vartheta m\cos\vartheta - \right. \\ & \left. - 4\vartheta m\cos^3\vartheta - 4m^2\sin\vartheta + 7m^2\sin\vartheta\cos^2\vartheta + \right. \\ & \left. + 3m(m+1)\vartheta^2\sin\vartheta\cos^2\vartheta + 2m\vartheta^2\sin\vartheta + 3m^2\vartheta^2\sin\vartheta\right] + \\ & + e\left[-2(m+1)\vartheta^3\sin\vartheta\cos\vartheta - 4\vartheta m\cos\vartheta(\vartheta\cos\vartheta - \sin\vartheta) - 2\vartheta^2\cos^2\vartheta\right] + \\ & + fm\vartheta\cos\vartheta[\vartheta - \sin\vartheta\cos\vartheta]\Big\}, \end{aligned} \tag{31a}$$

$$\begin{aligned} \overset{2}{A}_{1i} = -\frac{1}{D}\Big\{ & a\left[-2\vartheta - m\vartheta + 6\vartheta\cos^2\vartheta - 4(m+1)\vartheta\cos^4\vartheta + 3m\vartheta\cos^2\vartheta - \right. \\ & \left. - 5m\cos\vartheta\sin\vartheta + 7m\sin\vartheta\cos^3\vartheta - 2\vartheta^2(m+1)\sin\vartheta\cos\vartheta\right] + \\ & + b\left[2m\sin^2\vartheta - 2m\vartheta\sin\vartheta\cos\vartheta - 2(m+1)\vartheta^2\sin^2\vartheta\right] + \end{aligned}$$

$$+c\left[4m\vartheta\sin\vartheta\cos\vartheta+2m\cos^2\vartheta-2\vartheta^2\cos^2\vartheta-2mc-\right.$$
$$\left.2\left(m+1\right)\vartheta^3\sin\vartheta\cos\vartheta+2m\vartheta^2-4m\vartheta^2\cos^2\vartheta+2\vartheta^2\right]+$$
$$+d\left[m\vartheta^2\cos\vartheta\sin^2\vartheta+2m^2\vartheta^2\cos\vartheta\sin^2\vartheta-m^2\vartheta\sin\vartheta\sin^2\vartheta-\right.$$
$$\left.-m^2\cos\vartheta\sin^2\vartheta+m\left(m+1\right)\vartheta^3\sin\vartheta\right]+$$
$$+e\left[6m\vartheta-5m\vartheta^3+2\vartheta^2\sin\vartheta\cos\vartheta+2m\vartheta^3\cos^2\vartheta-4\vartheta^3-\right.$$
$$-2m\sin\vartheta\cos\vartheta+3m\vartheta^2\cos\vartheta\sin\vartheta-4m\vartheta\cos^2\vartheta+2\vartheta^3\cos^2\vartheta\Big]+$$
$$\left.+f\left[-2m\sin\vartheta+4m\sin\vartheta\cos^2\vartheta-5m\vartheta\cos\vartheta+3m\vartheta\cos^3\vartheta+\vartheta^2m\sin\vartheta\right]\right\},\quad(31b)$$

$$\overset{3}{A}_{1i}=\frac{1}{D}\left\{a\left[2\vartheta-2\vartheta\left(m+1\right)\cos^2\vartheta-m\cos\vartheta\sin\vartheta+3m\vartheta\right]+\right.$$
$$+b\left[2m\sin^2\vartheta-2\left(m+1\right)\vartheta\sin\vartheta\cos\vartheta\right]+$$
$$+c\left[4m\vartheta\sin\vartheta\cos\vartheta-2m\sin^2\vartheta-2\left(m+1\right)\vartheta^2\cos^2\vartheta+2\vartheta\sin\vartheta\cos\vartheta\right]+$$
$$+d\left[m\left(m+1\right)\vartheta\sin\vartheta\cos^2\vartheta+m\left(m+1\right)\vartheta^2\cos\vartheta-m^2\vartheta\sin\vartheta-m^2\sin^2\vartheta\cos\vartheta\right]+$$
$$+e\left[m\vartheta\cos^2\vartheta-4m\vartheta\cos^4\vartheta-2\left(m+1\right)\vartheta^2\sin\vartheta\cos\vartheta-\right.$$
$$-6m\sin\vartheta\cos\vartheta+7m\sin\vartheta\cos^3\vartheta+2m\vartheta+4\vartheta\cos^2\vartheta\sin^2\vartheta\Big]+$$
$$\left.+f\left[2m\sin\vartheta-3m\sin\vartheta\cos^2\vartheta+m\vartheta\cos\vartheta\right]\right\},\quad(31c)$$

$$\overset{3}{A}_{2i}=\frac{1}{D}\left\{2a\left(-3\sin\vartheta\cos^2\vartheta+2\sin\vartheta+\vartheta\cos\vartheta\right)+2b\left(-\cos\vartheta+\cos^3\vartheta+\vartheta\sin\vartheta\right)+\right.$$
$$+2c\left(-\vartheta\sin\vartheta\cos^2\vartheta+\vartheta^2\cos\vartheta-\vartheta\sin\vartheta-\cos^3\vartheta+\cos\vartheta\right)-$$
$$-dm\left(\vartheta^2-\cos^2\vartheta+\cos^4\vartheta\right)+2e\left(3\vartheta\cos^3\vartheta-4\vartheta\cos\vartheta+\vartheta^2\sin\vartheta+\sin\vartheta\cos^2\vartheta\right)+$$
$$\left.+2f\left(-2\sin\vartheta\cos^3\vartheta+\sin\vartheta\cos\vartheta+\vartheta\right)\right\},\quad(31d)$$

$$\overset{4}{A}_{1i}=\frac{1}{D}\left\{-2a\left(-m\sin^2\vartheta+\left(1+m\right)\vartheta\sin\vartheta\cos\vartheta\right)+\right.$$
$$+b\left(2m\vartheta\cos^2\vartheta-3m\sin\vartheta\cos\vartheta+m\vartheta+2\vartheta\cos^2\vartheta\right)-$$
$$-c\left[m\vartheta-7m\sin^3\vartheta\cos\vartheta+3m\vartheta\cos^2\vartheta-4m\vartheta\cos^4\vartheta+\right.$$
$$\left.+2\left(m+1\right)\vartheta^2\sin\vartheta\cos\vartheta+4\vartheta\cos^2\vartheta\sin^2\vartheta\right]+$$
$$+dm\left(\vartheta\cos\vartheta-2m\sin\vartheta+5m\sin\vartheta\cos^2\vartheta+\left(m+1\right)\vartheta^2\sin\vartheta-3\left(m+1\right)\vartheta\cos^3\vartheta\right)+$$
$$+2e\left(-\vartheta^2\sin^2\vartheta+2m\sin^2\vartheta-m\vartheta^2\sin^2\vartheta-\vartheta\sin\vartheta\cos\vartheta-2m\vartheta\sin\vartheta\cos\vartheta\right)+$$
$$\left.+fm\left(\vartheta\sin\vartheta-\cos\vartheta+\cos^3\vartheta\right)\right\},\quad(31e)$$

$$\overset{4}{A}_{2i}=\frac{1}{D}a\left[2m\sin^2\cos\vartheta-2\vartheta^2\left(m+1\right)\cos\vartheta-2\vartheta^2\cos\vartheta+\right.$$
$$+4m\vartheta^2\cos^5\vartheta+2m\vartheta\sin\vartheta-2\left(m+1\right)\vartheta\sin\vartheta\cos^2\vartheta\Big]+$$
$$+b\left[-2\vartheta\cos\vartheta+6b\vartheta\cos^3\vartheta-10m\sin\vartheta\cos^2\vartheta-\right.$$

$$-2m\vartheta^2\sin\vartheta+6m\vartheta\cos^3\vartheta-2\vartheta^2\sin\vartheta+4m\sin\vartheta\big]+$$
$$+c\left[-2\left(m+1\right)\vartheta^3\cos\vartheta-2\vartheta\sin^2\vartheta\cos\vartheta-2\vartheta^2\sin\vartheta-4m\vartheta^2\sin\vartheta+4m\sin\vartheta-\right.$$
$$\left.-4m\sin\vartheta\cos^2\vartheta+8m\vartheta\cos\vartheta\sin^2\vartheta-6\left(m+1\right)\vartheta^2\sin\vartheta\cos^2\vartheta\right]+$$
$$+d\left[2\vartheta^3+4m\vartheta\left(m\vartheta^2-1\right)+6m\vartheta\left(\vartheta^2-m\right)+14m\left(m+1\right)\vartheta\sin^2\vartheta\cos^2\vartheta+\right.$$
$$+12m^2\sin\vartheta\cos^3\vartheta-4\vartheta^2\left(m+1\right)^2\sin\vartheta\cos^3\vartheta+$$
$$\left.+2\left(\vartheta^2m^2-3m^2+\vartheta^2+2m\vartheta^2\right)\cos\vartheta\sin\vartheta\right]+$$
$$+e\left[2\vartheta^3\sin\vartheta+2\left(m+1\right)\vartheta^2\cos^3\vartheta-4\vartheta^2\cos\vartheta+4m\cos\vartheta\sin^2\vartheta-\right.$$
$$\left.-4m\vartheta\sin\vartheta\cos^2\vartheta-2\vartheta\sin\vartheta\cos^2\vartheta+4m\vartheta\sin\vartheta-6m\vartheta^2\cos\vartheta-2\vartheta^3m\sin\vartheta\right]+$$
$$+fm\left(\vartheta^2-\cos^2\vartheta+\cos^4\vartheta\right). \quad (31f)$$

References

1. Szeidl, G.: *The Effect of Change in Length on the Natural Frequencies and Stability of Circular Beams*. Ph.D. thesis, Department of Mechanics, University of Miskolc, Hungary, 1975. (in Hungarian).
2. Szeidl, G., Kelemen, K., and Szeidl, A.: Natural Frequencies of a Circular Arch – Computations by the Use of Green Functions. *Publications of the University of Miskolc, Series D. Natural Sciences, Mathematics*, **38**(1), (1998), 117–132.
3. Kelemen, K.: Vibrations of circular arches subjected to hydrostatic follower loads – computations by the use of the Green functions. *Journal of Computational and Applied Mechanics*, **1**(2), (2000), 167–178.
4. Hartog, J. P. D.: Vibration of frames of electrical machines. *Transactions of the American Society of Mechanical Engineers, Journal of Applied Mechanics*, **50**, (1928), 1–6.
5. Volterra, E. and Morrel, J. D.: Lowest natural frequency of elastic arc for vibrations outside the plane of initial curvature. *Journal of Applied Mechanics*, **12**, (1961), 624–627.
6. Volterra, E. and Morrel, J. D.: On the fundamental frequencies of curved beams. *Bulletin of the Polytechnic Institute of Jassy*, **7**(11), (1961), 1–2.
7. Federhofer, K.: *Dynamik des Bogenträgers und Kreisringes [Dynamics of arches and circular rings]*. Wien Springer Verlag, 1950.
8. Qatu, M. S. and Elsharkawy, A. A.: Vibration of laminated composite arches with deep curvature and arbitrary boundaries. *Computers & Structures*, **47**(2), (1993), 305–311.
9. Kang, K., Bert, C. W., and Striz, A. G.: Vibration analysis of shear deformable circular arches by the differential quadrature method. *Journal of Sound and Vibration*, **181**(2), (1995), 353–360.
10. Tüfekçi, E. and Arpaci, A.: Exact solution of in-plane vibrations of circular arches with account taken of axial extension, transverse shear and rotatory inertia affects. *Journal of Sound and Vibration*, **209**(5), (1998), 845–856.
11. Krishnan, A. and Suresh, Y. J.: A simple cubic linear element for static and free vibration analyses of curved beams. *Computers & Structures*, **68**, (1998), 473–489.

12. Ecsedi, I. and Dluhi, K.: A linear model for the static and dynamic analysis of non-homogeneous curved beams. *Applied Mathematical Modelling*, **29**(12), (2005), 1211–1231.

13. Çalim, F. F.: Forced vibration of curved beams on two-parameter elastic foundation. *Applied Mathematical Modelling*, **36**, (2012), 964–973.

14. Hajianmaleki, M. and Qatu, M. S.: Vibrations of straight and curved composite beams: A review. *Composite Structures*, **100**, (2013), 218–232.

15. Kovács, B.: Vibration analysis of layered curved arch. *Journal of Sound and Vibration*, **332**, (2013), 4223–4240.

16. Jun, L., Guangweia, R., Jina, P., Xiaobina, L., and Weiguoa, W.: Free vibration analysis of a laminated shallow curved beam based on trigonometric shear deformation theory. *Mechanics Based Design of Structures and Machines*, **42**(1), (2014), 111–129.

17. Lueschen, G. G. G., Bergman, L. A., and McFarland, D. M.: Green's functions for uniform Timoshenko beams. *Journal of Sound and Vibration*, **194**, (1996), 93–102.

18. Foda, M. A. and Abduljabbar, Z.: A dynamic Green function formulation for the response of a beam structure to a moving mass. *Journal of Sound and Vibration*, **210**(3), (1997), 295–306.

19. Kukla, S. and Zamojska, I.: Frequency analysis of axially loaded stepped beams by Green's function method. *Journal of Sound and Vibration*, **300**, (2007), 1034–1041.

20. Mehri, B., Davar, A., and Rahmani, O.: Dynamic Green's function solution of beams under a moving load with different boundary contitions. *Scientia Iranica*, **16**, (2009), 273–279.

21. Failla, G. and Santini, A.: On Euler-Bernoulli discontinuous beam solutions via uniform-beam Green's functions. *International Journal of Solids and Structures*, **44**, (2007), 7666-7687.

22. Kiss, L. P.: *Vibrations and Stability of Heterogeneous Curved Beams*. Ph.D thesis, Institute of Applied Mechanics, University of Miskolc, Hungary, 2015. Pp. 142.

23. Kiss, L. P. and Szeidl, G.: Vibrations of pinned-fixed heterogeneous circular beams pre-loaded by a vertical force at the crown point. *Journal of Sound and Vibration*, **393**, (2017), 92–113.

24. Szeidl, G. and Kiss, L. P.: Free vibrations of rotationally restrained nonhomogeneous circular beams by means of the Green function. (Manuscript, under review).

25. Rajasekaran, S.: Static, stability and free vibration analysis of arches using a new differential transformation-based arch element. *International Journal of Mechanical Sciences*, **77**, (2013), 82–97.

26. Kiss, L. and Szeidl, G.: Vibrations of pinned-pinned heterogeneous circular beams subjected to a radial force at the crown point. *Mechanics Based Design of Structures and Machines*, **43**(4), (2015), 424–449.

27. Kiss, L., Szeidl, G., Vlase, S., Gálfi, B. P., Dani, P., Munteanu, I. R., Ionescu, R. D., and Száva, J.: Vibrations of fixed-fixed heterogeneous curved beams loaded by a central force at the crown point. *International Journal for Engineering Modelling*, **27**(3-4), (2014), 85–100.

28. Wolf, J. A.: Natural frequencies of circular arches. *Transactions of the American Society of Civil Engineers, Journal of the Structural Division*, **97**, (1971), 2337–2349.

29. Kiss, L. P.: Free vibrations of heterogeneous curved beams. *GÉP*, **LXIV**(5), (2013), 16–21. (in Hungarian).

30. Lin, S. M.: Exact solutions for extensible circular curved Timoshenko beams with nonhomogeneous elastic boundary conditions. *Acta Mechanica*, **130**, (1998), 67–79.

Journal of Computational and Applied Mechanics, Vol. 12, No. 1, (2017), pp. 43–55
DOI: 10.32973/jcam.2017.003

DYNAMIC ANALYSIS OF COMPOSITE BEAMS WITH WEAK SHEAR CONNECTION SUBJECTED TO AXIAL LOAD

Ákos József Lengyel
Departmrent of Applied Mechanics, University of Miskolc
H-3515 Miskolc-Egyetemváros, Miskolc, Hungary
mechlen@uni-miskolc.hu

[Received: March 26, 2017; Accepted: June 12, 2017]

Abstract. The paper provides a new analytical method for determining the eigenfrequences of composite beams with interlayer slip provided that the beam is subjected to an axial load. Application of the d'Alembert principle yields the equations of motion. The axial and rotary inertia are taken into account. This formulation leads to a general eigenvalue problem whose solution is illustrated by a numerical example.

Mathematical Subject Classification: 74H45, 74H55, 74K10
Keywords: Composite beam, interlayer slip, stability analysis, vibration analysis

1. Introduction

Layered composite structures, especially layered beams, are widely applied in building and bridge engineering since the advantages of the layers made of different elastic materials can be complement each other, while their disadvantages can be reduced or eliminated. Therefore it is very important to understand the mechanical behavior of the layered composite beams and the influence of the connection between the layers for the mechanical properties. In a number of industrial applications the layers of composite beams are joined to each other by different shear connectors such as nails, screws or rivets. Because of the elastic deformation of those connectors two phenomena can occur between the layers. In normal direction the layers can separate (it is called uplift) and in axial direction an interlayer slip can happen. In this paper it is assumed that the connection is perfect in normal direction, viz. uplift is not allowed, whilst the connection is imperfect in axial direction so interlayer slip can appear.

There are a lot of works in connection with composite beams with interlayer slip [1]-[18] The first studies were published in the 1950's [1, 2, 3]. The pioneering and most cited work is Newmark et al. [1]. They elaborated an analytical solution for composite beams with interlayer slip based on the Euler-Bernoulli beam theory. The problem was governed by a linear differential equation of second order in the longitudinal force resisted by the top element, and the other unknowns were the longitudinal force and

the expression for moment along the beam. Girhammar and Gopu [5] proposed a formulation for the exact first- and second-order analyses of composite beam columns with partial shear interaction subjected to transverse and axial loading. Ecsedi and Baksa [6] also deduced the governing equation of the problem in terms of the slip and the vertical displacement.

There exist several works in connection with the dynamic analysis of composite beams with interlayer slip [7, 8, 9, 10, 11]. An exact and an approximate analysis of composite members with partial interaction and subjected to general dynamic loading was presented by Girhammar and Pan [7]. Adam et al. [8] analysed the flexural vibration of composite beams with interlayer slip using the Euler-Bernoulli beam theory. The governing sixth order initial-boundary value problem was solved by separating the dynamic response in a quasi-static and in a complementary dynamic response. Heuer and Adam extended the previous model for composite beams made of piezoelectric materials in [9]. The partial differential equations and general solutions for the deflection and internal actions and the pertaining consistent boundary conditions were presented for composite Euler–Bernoulli members with interlayer slip subjected to general dynamic loading in [10]. Wu et al. [11] derived the governing differential equations of motion for the partial-interaction composite members with axial force. All these works neglected the influence of axial and rotary inertia.

The elastic stability problems of composite beams with weak shear connection were also investigated [12, 13, 14, 15, 16]. Challamel and Girhammar [12] analysed the lateral-torsional stability of vertically layered composite beams with interlayer slip based on a variational approach. An analytical method was presented for the delamination buckling using the Timoshenko beam theory by Chen and Qiao [13]. Grognec et al. [14] utilized the Timoshenko beam theory as well. Schnabl and Planinc [15] presented a detailed analysis of the influence of boundary conditions and axial deformation on the critical buckling loads and the same authors took into account the effect of the transverse shear deformation on buckling [16].

In this paper the free vibration of layered composite beams with interlayer slip is investigated while an axial force is acting on the considered beam. During the formulation of the equations of motion axial and the rotary inertia is also taken into account. The results from papers by Lengyel and Ecsedi [17, 18] are compared with those deriving from the presented method.

2. Equations of motion

The considered two-layer composite beam with interlayer slip is shown in Figure 1. It is assumed that each layer separately follows the Euler-Bernoulli hypothesis and the load-slip relation for the flexible shear connection is a linear relationship. In the reference configuration, the composite beam occupies the 3D region $B = A \times [0, L]$ generated by translating its symmetrical cross section A along a rectilinear axis, orthogonal to the cross section. The cross-section A is divided into two parts A_1 and A_2, that is $A = A_1 \cup A_2$ and the common boundary A_1 and A_2 is denoted by ∂A_{12}. The components B_1 and B_2 are defined as $B_i = A_i \times [0, L]$, $\partial B_i = \partial A_i \times [0, L]$,

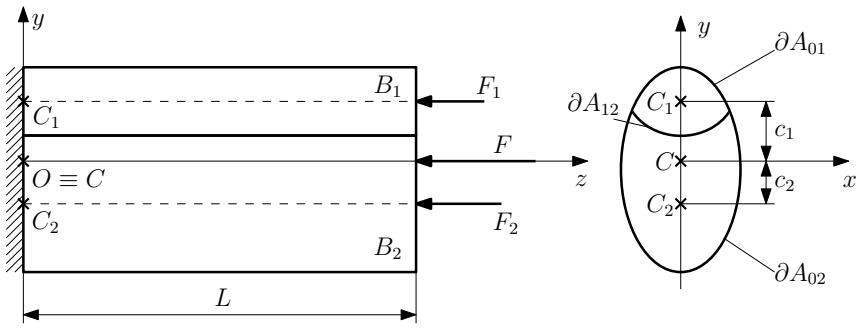

Figure 1. Two-layered beam with weak shear connection

$\partial A_i = \partial A_{0i} \cup \partial A_{12}$, $(i = 1, 2)$ (Figure 1). Here L is the length of the beam and ∂A_{0i} is the 'outer' boundary curve of the cross-section A_i $(i = 1, 2)$. A point P in $\overline{B} = B \cup \partial B$ $(\partial B = (\partial A_{01} \cup \partial A_{02}) \times [0, L])$ is determined by the position vector $\mathbf{r} = x\mathbf{e}_x + y\mathbf{e}_y + z\mathbf{e}_z$, where x, y, z and $\mathbf{e}_x$, $\mathbf{e}_y$, $\mathbf{e}_z$ are referred to the rectangular coordinate system $Oxyz$ shown in Figure 1. The axis z is located in the E-weighted centerline of the whole composite beam and the plane yz is the plane of symmetry for the geometrical and support conditions. The center of A_i is C_i $(i = 1, 2)$ and C is the E-weighted center of the whole cross-section $A = A_1 \cup A_2$ (Figure 1), furthermore

$$c_1 = |\overrightarrow{CC_1}|, \quad c_2 = |\overrightarrow{CC_2}|. \tag{1}$$

According to the Euler-Bernoulli beam theory the displacement field $\mathbf{u} = u\mathbf{e}_x + v\mathbf{e}_y + w\mathbf{e}_z$ has the form [6]

$$\begin{gathered} u = 0, \quad v = v(z,t), \quad \tilde{w}_i(y,z,t) = -\frac{F}{\langle AE \rangle} z + w_i(z,t) - y\frac{\partial v}{\partial z}, \\ (x,y,z) \in B_i, \quad (i = 1,2), \end{gathered} \tag{2}$$

where $\langle AE \rangle = A_1E_1 + A_2E_2$ and t is the time. Application of the strain-displacement relationship of elasticity and Hooke's law gives

$$\sigma_{zi} = E_i\varepsilon_i = E_i\frac{\partial \tilde{w}_i}{\partial z} = E_i\left(-\frac{F}{\langle AE \rangle} + \frac{\partial w_i}{\partial z} - y\frac{\partial^2 v}{\partial z^2}\right), \quad (i = 1,2). \tag{3}$$

The definition of section axial forces provides

$$\begin{aligned} \tilde{N}_i = \int_{A_i} \sigma_{zi}\mathrm{d}A &= -F\frac{A_iE_i}{\langle AE \rangle} + A_iE_i\frac{\partial w_i}{\partial z} + (-1)^i c_iA_iE_i\frac{\partial^2 v}{\partial z^2} = \\ &= -F\frac{A_iE_i}{\langle AE \rangle} + N_i, \quad (i = 1,2). \end{aligned} \tag{4}$$

The mechanical meaning of the first term in the expression of $\tilde{N}_i$ is as follows (see Figure 1)

$$F_i = \frac{A_iE_i}{\langle AE \rangle}F, \quad (i = 1,2), \quad F = F_1 + F_2. \tag{5}$$

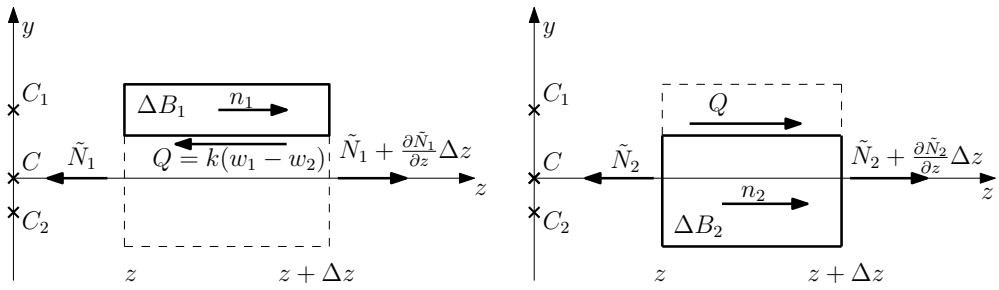

Figure 2. Free body diagram for axial forces

The axial force function in the whole beam

$$N = \tilde{N}_1 + \tilde{N}_2 = -F + N_1 + N_2 = -F. \tag{6}$$

According to this we have

$$N_1 + N_2 = A_1 E_1 \left(\frac{\partial w_1}{\partial z} - c_1 \frac{\partial^2 v}{\partial z^2} \right) + A_2 E_2 \left(\frac{\partial w_2}{\partial z} + c_2 \frac{\partial^2 v}{\partial z^2} \right) = 0. \tag{7}$$

The moment of normal stress σ_z about axis x is expressed as

$$\begin{aligned} M = \tilde{M}_1 + \tilde{M}_2 = \int_{A_1} y\sigma_{z1} \mathrm{d}A + \int_{A_2} y\sigma_{z2} \mathrm{d}A = \\ = E_1 A_1 c_1 \frac{\partial w_1}{\partial z} - E_2 A_2 c_2 \frac{\partial w_2}{\partial z} - \{IE\} \frac{\partial^2 v}{\partial z^2}, \end{aligned} \tag{8}$$

where

$$\{IE\} = I_1 E_1 + I_2 E_2, \quad I_i = \int_{A_i} y^2 \mathrm{d}A, \quad (i = 1, 2). \tag{9}$$

Denote Q the interlayer shear force. The interlayer slip is interpreted as the difference of the axial displacements of the layers $(w_1 - w_2)$ so we have for the interlayer shear force

$$Q = k(w_1 - w_2). \tag{10}$$

Here, k is the so-called slip modulus, which characterizes the rigidity of the connection. When the value of k is equal to zero ($Q = 0$) there is no connection between the layers. If the slip modulus is equal to infinity ($w_1 - w_2 = 0$) the connection among the layers is perfect.

The beam elements ΔB_1 and ΔB_2 assigned by z and $z + \Delta z$ coordinates are shown in Figure 2. The force equilibrium equations in axial direction for beam component ΔB_1 and ΔB_2 can be written in the form

$$\frac{\partial \tilde{N}_1}{\partial z} + n_1 - k(w_1 - w_2) = 0, \tag{11}$$

$$\frac{\partial \tilde{N}_2}{\partial z} + n_2 + k(w_1 - w_2) = 0. \tag{12}$$

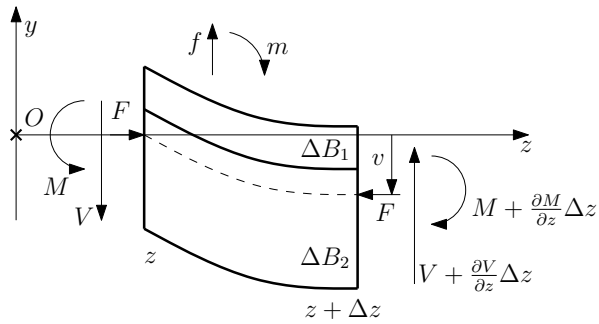

Figure 3. A small beam element $\Delta B_1 \cup \Delta B_2$ with the shear forces and bending moments

The applied line loads in axial direction are denoted by n_1 and n_2. A $\Delta B_1 \cup \Delta B_2$ beam element is illustrated in Figure 3 without the axial forces. According to this beam element the following equilibrium equations can be deduced

$$\frac{\partial V}{\partial z} + f = 0, \quad \frac{\partial M}{\partial z} + F\frac{\partial v}{\partial z} - V + m = 0. \tag{13}$$

In equation (13) $f = f(z,t)$ is the applied line load, $V = V(z,t)$ is the shear force, m is the applied distributed moment. From equation (13) the shear force can be eliminated. In this way we obtain only one equilibrium equation instead of the two in equation (13)

$$\frac{\partial^2 M}{\partial z^2} + F\frac{\partial^2 v}{\partial z^2} + \frac{\partial m}{\partial z} + f = 0. \tag{14}$$

In equations (11), (12), (13) and (14) furthermore in Figures 2 and 3 the d'Alembert forces are introduced in the next form

$$f(z,t) = -(\rho_1 A_1 + \rho_2 A_2)\frac{\partial^2 v}{\partial t^2}, \tag{15}$$

$$n_1(z,t) = -\rho_1 A_1 \frac{\partial^2 w_1}{\partial t^2} + c_1 \rho_1 A_1 \frac{\partial^3 v}{\partial z \partial t^2}, \tag{16}$$

$$n_2(z,t) = -\rho_2 A_2 \frac{\partial^2 w_2}{\partial t^2} - c_2 \rho_2 A_2 \frac{\partial^3 v}{\partial z \partial t^2}, \tag{17}$$

$$m(z,t) = -c_1 \rho_1 A_1 \frac{\partial^2 w_1}{\partial t^2} + c_2 \rho_2 A_2 \frac{\partial^2 w_2}{\partial t^2} + \{\rho I\}\frac{\partial^3 v}{\partial z \partial t^2}. \tag{18}$$

Here, ρ_1 and ρ_2 mean the mass density of beam component B_1 and B_2, respectively, and

$$\{\rho I\} = \rho_1 I_1 + \rho_2 I_2. \tag{19}$$

Combining equations (4), (8), (11), (12) and (14) with equations (15–18) yields the system of motion equations for the two-layered composite beam with interlayer slip

$$E_1 A_1 \frac{\partial^2 w_1}{\partial z^2} - c_1 E_1 A_1 \frac{\partial^3 v}{\partial z^3} - k(w_1 - w_2) - \rho_1 A_1 \frac{\partial^2 w_1}{\partial t^2} + c_1 \rho_1 A_1 \frac{\partial^3 v}{\partial z \partial t^2} = 0, \tag{20}$$

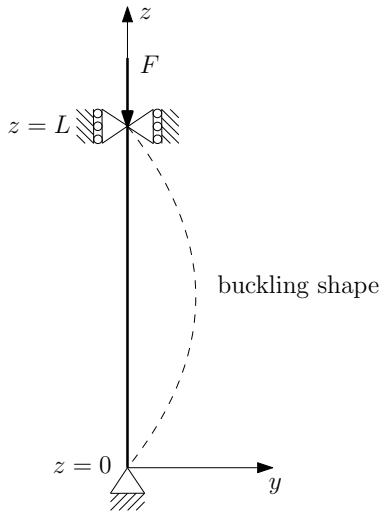

Figure 4. Simply supported column with axial load and its buckling shape

$$E_2A_2\frac{\partial^2 w_2}{\partial z^2}+c_2E_2A_2\frac{\partial^3 v}{\partial z^3}+k(w_1-w_2)-\rho_2A_2\frac{\partial^2 w_2}{\partial t^2}-c_2\rho_2A_2\frac{\partial^3 v}{\partial z\partial t^2}=0, \tag{21}$$

$$\begin{aligned} c_1E_1A_1\frac{\partial^3 w_1}{\partial z^3}-c_2E_2A_2\frac{\partial^3 w_2}{\partial z^3}-\{IE\}\frac{\partial^4 v}{\partial z^4}+F\frac{\partial^2 v}{\partial z^2}-c_1\rho_1A_1\frac{\partial^3 w_1}{\partial z\partial t^2}+\\ +c_2\rho_2A_2\frac{\partial^3 w_2}{\partial z\partial t^2}+\{\rho I\}\frac{\partial^4 v}{\partial z^2\partial t^2}-(\rho_1A_1+\rho_2A_2)\frac{\partial^2 v}{\partial t^2}=0. \end{aligned} \tag{22}$$

3. Simply supported beam-column

The considered simply supported column is shown in Figure 4. In this case the following boundary conditions are valid:

$$N_1(0,t)=N_1(L,t)=0, \quad t>0, \tag{23}$$

$$N_2(0,t)=N_2(L,t)=0, \quad t>0, \tag{24}$$

$$M(0,t)=M(L,t)=0, \quad t>0, \tag{25}$$

$$v(0,t)=v(L,t)=0, \quad t>0. \tag{26}$$

We look for the solution of the boundary value problem (20–22) and (23–26) in the following form:

$$w_1(z,t)=W_{1j}\cos\frac{j\pi}{L}z\cos\omega_j t, \tag{27}$$

$$w_2(z,t)=W_{2j}\cos\frac{j\pi}{L}z\cos\omega_j t, \tag{28}$$

$$v(z,t)=V_j\sin\frac{j\pi}{L}z\cos\omega_j t, \quad (j=1,2,\ldots). \tag{29}$$

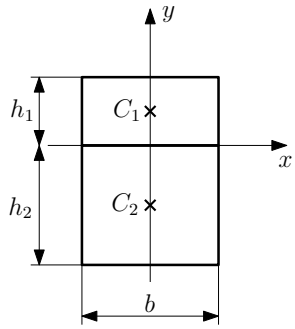

Figure 5. The cross section of the column considered in the example

These functions satisfy the boundary conditions (23–26) for all values of W_{1j}, W_{2j}, V_j. Substituting the functions into equations (20–22) the following linear system of equation can be deduced:

$$\mathbf{C}_j\mathbf{X}_j = \omega_j^2\mathbf{M}_j\mathbf{X}_j, \tag{30}$$

where

$$\mathbf{X}_j = [W_{1j}, W_{2j}, V_j]^T, \tag{31}$$

$$\mathbf{C}_j = \begin{bmatrix} E_1A_1\left(\frac{j\pi}{L}\right)^2 + k & -k & -c_1E_1A_1\left(\frac{j\pi}{L}\right)^3 \\ -k & E_2A_2\left(\frac{j\pi}{L}\right)^2 + k & c_2E_2A_2\left(\frac{j\pi}{L}\right)^3 \\ -c_1E_1A_1\left(\frac{j\pi}{L}\right)^3 & c_2E_2A_2\left(\frac{j\pi}{L}\right)^3 & \{IE\}\left(\frac{j\pi}{L}\right)^4 - F\left(\frac{j\pi}{L}\right)^2 \end{bmatrix}, \tag{32}$$

$$\mathbf{M}_j = \begin{bmatrix} \rho_1A_1 & 0 & -c_1\rho_1A_1\frac{j\pi}{L} \\ 0 & \rho_2A_2 & -c_2\rho_2A_2\frac{j\pi}{L} \\ -c_1\rho_1A_1\frac{j\pi}{L} & -c_2\rho_2A_2\frac{j\pi}{L} & \{\rho I\}\left(\frac{j\pi}{L}\right)^4 + \rho_1A_1 + \rho_2A_2 \end{bmatrix}. \tag{33}$$

The non-trivial solution of equations (30) is sought that means

$$\det\left(\mathbf{C}_j - \omega_j^2\mathbf{M}_j\right) = 0, \quad (j = 1, 2, \ldots). \tag{34}$$

From equation (34) a cubic equation can be formulated for ω_j^2 $(j = 1, 2, \ldots)$ in terms of F, which means that we have three eigenfrequencies for each value of j for arbitrary value of the axial load.

4. Numerical example

In this example the simply supported beam illustrated in Figure 4 is considered and its cross section is shown in Figure 5. The following data were used: $h_1 = 0.02\,\mathrm{m}$, $h_2 = 0.04\,\mathrm{m}$, $b = 0.03\,\mathrm{m}$, $L = 2\,\mathrm{m}$, $E_1 = 10^{10}\,\mathrm{Pa}$, $E_2 = 2 \times 10^{11}\,\mathrm{Pa}$, $k = 10^6\,\mathrm{Pa}$, $\rho_1 = 4000\,\mathrm{kg/m^3}$, $\rho_2 = 7000\,\mathrm{kg/m^3}$.

Substituting the data into equation (34) the eigenfrequencies were investigated for three different value of axial force. The results are shown in Table 1 for $F = 0$, in Table 2 for $F = 40,000\,\mathrm{N}$ and in Table 3 for $F = 80,000\,\mathrm{N}$. According to the results one can see that by increasing the axial load the eigenfrequencies decreases.

Table 1. The eigenfrequencies of simply supported column without axial force ($F = 0$)

j	ω_{j1} $^1/_\mathrm{s}$	ω_{j2} $^1/_\mathrm{s}$	ω_{j3} $^1/_\mathrm{s}$
1	135.42	2566.01	8403.41
2	539.36	5009.04	16796.21
3	1211.79	7478.84	25191.61
4	2151.61	9955.53	33587.91
5	3357.32	12434.99	41984.87
10	13289.8	24844.86	83980.52

Table 2. The eigenfrequencies of simply supported column with axial force $F = 40,000\,\mathrm{N}$

j	ω_{j1} $^1/_\mathrm{s}$	ω_{j2} $^1/_\mathrm{s}$	ω_{j3} $^1/_\mathrm{s}$
1	95.93	2566.01	8403.41
2	504.36	5009.04	16796.21
3	1177.49	7478.84	25191.61
4	2117.52	9955.53	33587.91
5	3323.33	12434.99	41984.87
10	13256.3	24844.86	83980.51

Table 3. The eigenfrequencies of simply supported column with axial force $F = 80,000\,\mathrm{N}$

j	ω_{j1} $^1/_\mathrm{s}$	ω_{j2} $^1/_\mathrm{s}$	ω_{j3} $^1/_\mathrm{s}$
1	8.167	2566.01	8403.41
2	466.78	5009.04	16796.21
3	1142.08	7478.84	25191.61
4	2082.86	9955.53	33587.91
5	3289.01	12434.99	41984.87
10	13222.73	24844.86	83980.51

The relation between the axial force and the square of the eigefrequency is a linear relationship. Applying the presented method a linear function is provided that is illustrated below. Figures 6, 7, 8, 9, 10 and 11 show the connection between the axial force and the square of the eigenfrequency for $j = 1$, $j = 2$, $j = 3$, $j = 4$, $j = 5$ and $j = 10$, respectively. When the axial load is equal to zero the method gives the same eigenfrequencies (Table 1) as in an earlier study by Lengyel and Ecsedi [18]. In [18] the authors proposed an analytical method for the free vibration of a composite beam with interlayer slip without any loading.

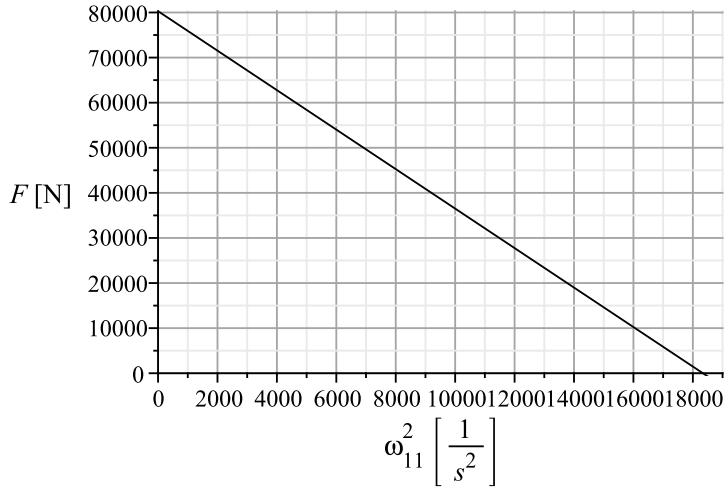

Figure 6. The function of $F = F\left(\omega_{11}^2\right)$

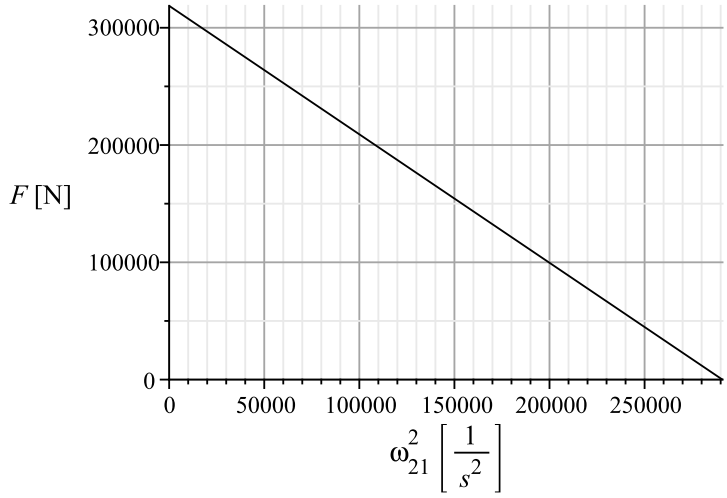

Figure 7. The function of $F = F\left(\omega_{21}^2\right)$

If the j-th eigenfrequency is equal to zero the j-th critical load can be gained from the presented method. Lengyel and Ecsedi in [17] deduced a solution method for determination of the critical buckling load of composite beams with interlayer slip. During the analysis they derived a closed form for the j-th critical load, which is

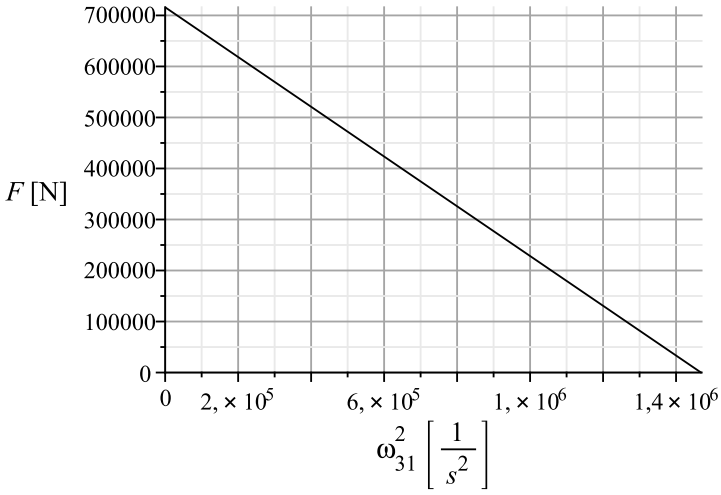

Figure 8. The function of $F = F\left(\omega_{31}^2\right)$

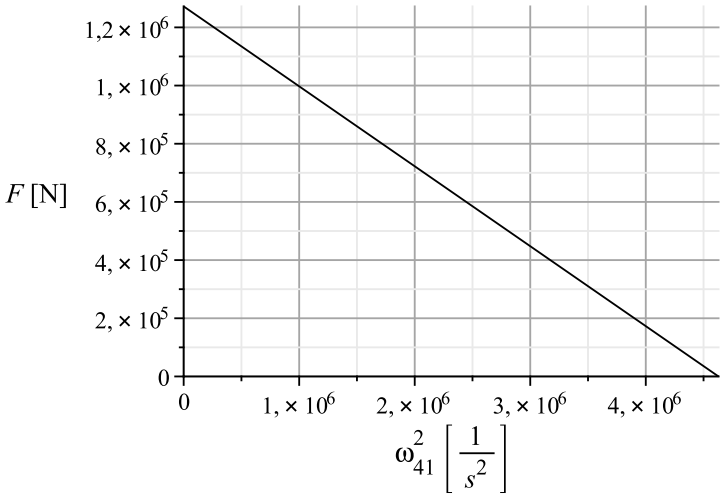

Figure 9. The function of $F = F\left(\omega_{41}^2\right)$

$$F_j^{cr} = \frac{\langle IE\rangle \langle AE\rangle_{-1} \left(\frac{j\pi}{L}\right)^4 + k\{IE\}\left(\frac{j\pi}{L}\right)^2}{\langle AE\rangle_{-1}\left(\frac{j\pi}{L}\right)^2 + k}. \tag{35}$$

Here,

$$\langle AE\rangle_{-1} = \frac{A_1E_1A_2E_2}{A_1E_1 + A_2E_2}, \tag{36}$$

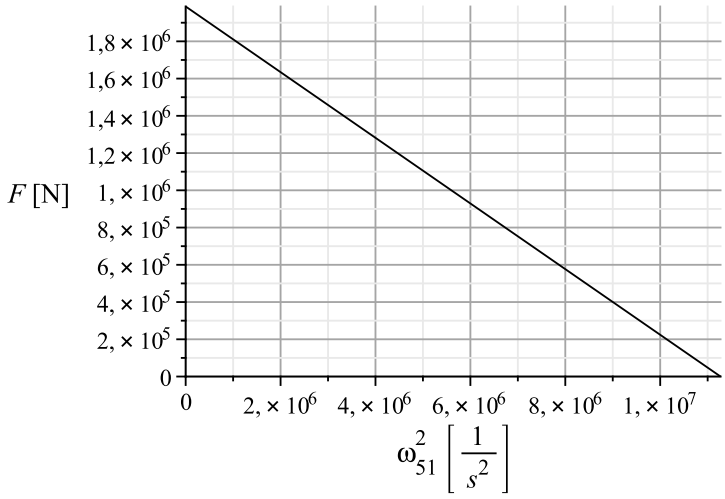

Figure 10. The function of $F = F\left(\omega_{51}^2\right)$

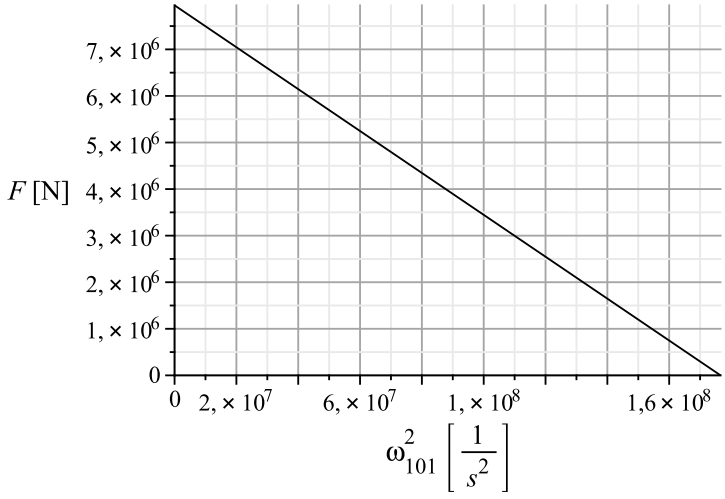

Figure 11. The function of $F = F\left(\omega_{101}^2\right)$

$$\langle IE \rangle = \{IE\} - c^2 \langle AE \rangle_{-1}, \quad c = c_1 + c_2. \tag{37}$$

Table 4 illustrates the j-th critical load from the presented method and computed by equation (35).

Table 4. The critical loads for the simply supported composite beam with interlayer slip.

j	F_j^{cr} [N] from equation (34), $\omega_j = 0$	F_j^{cr} [N] from equation (35)
1	80, 292.038	80, 292.038
2	318, 685.949	318, 685.949
3	715, 945.968	715, 945.968
4	1, 272, 101.169	1, 272, 101.17
5	1, 987, 155.398	1, 987, 155.402
10	7, 945, 930.916	7, 945, 930.923

5. Conclusions

The paper proposes a new analytical method for the analysis of free vibration of composite beams with interlayer slip loaded by axial force. The presented method takes into account the influence of axial and rotary inertia, from which three different eigenfrequencies can be obtained for each value of j. The connection between the axial force and the square of the eigenfrequency is linear. The critical buckling loads and the eigenfrequencies belonging to the composite beam without axial loading are also computed by means of the method and the results are in very good agreement with the results from earlier studies.

Acknowledgement. Supported by the ÚNKP-16-3. New National Excellence Program of the Ministry of Human Capacities.

References

1. Newmark, N. M., Siess, C. P., and Viest, I. M.: Test and analyis of composite beams with incomplete interaction. *Proceedings of the Society of Experimental Stress Analysis*, **9**(1), (1951), 75–92.
2. Stüssi, F.: Zusammengesetzte Vollwandträger. *IABSE Publications*, **8**, (1947), 249–269.
3. Granholm, H.: *On composite beams and columns with particular regard to nailed timber structures.* Transaction No. 88, Chalmers Technical University, Göteborg, Sweden, 1949. (in Swedish).
4. Kovács, B.: Vibration of multi-layered bands with interfacial imperfection. *Journal of Sound and Vibration*, **300**(1–2), (2007), 379–386.
5. Girhammar, U. A. and Gopu, V. K. A.: Composite beam-columns with interlayer slip – exact analysis. *Journal of Structural Engineering*, **119**(4), (1993), 1265–1282.
6. Ecsedi, I. and Baksa, A.: Static analysis of composite beams with weak shear connection. *Applied Mathematical Modelling*, **35**(4), (2011), 1739–1750.
7. Girhammar, U. A. and Pan, D.: Dynamic analysis of composite members with interlayer slip. *International Journal of Solids and Structures*, **30**(6), (1993), 797–823.
8. Adam, C., Heuer, R., and Jeschko, A.: Flexural vibrations of elastic composite beams with interlayer slip. *Acta Mechanica*, **125**(1), (1997), 17–30.

9. Heuer, R. and Adam, C.: Piezoelectric vibrations of composite beams with interlayer slip. *Acta Mechanica*, **140**(3), (2000), 247–263.

10. Girhammar, U. A., Pan, D. H., and Gustafsson, A.: Exact dynamic analysis of composite beams with partial interaction. *International Journal of Mechanical Sciences*, **51**(8), (2009), 565–582.

11. Wu, Y. F., Xu, R., and Chen, W.: Free vibrations of the partial-interaction composite members with axial force. *Journal of Sound and Vibration*, **299**(4–5), (2007), 1074–1093.

12. Challamel, N. and Girhammar, U. A.: Lateral-torsional buckling of vertically layered composite beams with interlayer slip under uniform moment. *Engineering Structures*, **34**(8), (2012), 505–513.

13. Chen, F. and Qiao, P.: Buckling of delaminated bi-layer beam-columns. *International Journal of Solids and Structures*, **48**(18), (2011), 2485–2495.

14. Grognec, P. L., Nguyen, Q. H., and Hjiaj, M.: Exact buckling solution for two-layer Timoshenko beams with interlayer slip. *International Journal of Solids and Structures*, **49**(1), (2012), 143–150.

15. Schnabl, S. and Planinc, I.: The influence of boundary conditions and axial deformability on buckling behavior of two-layer composite columns with interlayer slip. *Engineering Structures*, **32**(10), (2010), 3103–3111.

16. Schnabl, S. and Planinc, I.: The effect of transverse shear deformation on the buckling of two-layer composite columns with interlayer slip. *International Journal of Non-Linear Mechanics*, **46**(3), (2011), 543–553.

17. Lengyel, A. J. and Ecsedi, I.: Elastic stability of columns with weak shear connection. In *MultiScience – XXVIII. microCAD International Multidisciplinary Scientific Conference*, Miskolc, Hungary, University of Miskolc, 2014. Paper no. D-37.

18. Lengyel, A. J. and Ecsedi, I.: Kétrétegű nem tökéletesen kapcsolt kompozit rudak rezgéseinek vizsgálata *GÉP*, **LXV**(1), (2014), 34–38. (in Hungarian).

Journal of Computational and Applied Mechanics, Vol. 12, No. 1, (2017), pp. 57–76
DOI: 10.32973/jcam.2017.004

VIBRATION OF CIRCULAR PLATES SUBJECTED TO CONSTANT RADIAL LOAD IN THEIR PLANE

Nóra Szűcs
Robert Bosch Energy and Body Systems Kft.,
H-3526 Miskolc, Robert Bosch Park 3., Hungary
noraszucs@gmail.com

György Szeidl
Institute of Applied Mechanics, University of Miskolc
H-3515 Miskolc-Egyetemváros, Hungary
gyorgy.szeidl@gmail.com

[Received: October 18, 2016; Accepted: December 12, 2016]

Abstract. The present paper deals with the vibration of circular plates provided that the plates are prestressed in such a way that the stresses due to the in-plane load are constants. We have determined the Green functions of the governing equations. The self adjoint eigenvalue problems giving the natural frequencies are replaced by homogenous Fredholm integral equations for which the symmetric Green functions constitute the kernel. According to the numerical solution the square of the natural frequencies is linear, or approximately linear functions of the constant in plane load.

Mathematical Subject Classification: 74H45, 74H55, 74K20
Keywords: Circular plates, Green functions, natural frequencies, critical load

1. Introduction

It is well known [1] that the natural frequency of a simply supported beam subjected to a compressive axial force – the beam is in a prestressed state – satisfies the equation

$$\frac{\alpha^2}{\alpha_1^2} = 1 - \frac{f}{f_1} \tag{1.1}$$

in which α and α_1 are the first natural frequencies of the loaded and unloaded beam while f and f_1 are the compressive force and its smallest critical value.

Lawther [1] attacks the problem how a prestressed state of the body affects the natural frequencies in a more general form. He studies finite dimensional multiparameter eigenvalue problems and comes to the conclusion that for multiparameter problems, the eigenvalue part of the solution is described by interaction curves in an eigenvalue space, and every such eigenvalue solution has an associated eigenvector. If all points

on a curve have the same eigenvector then the curve is necessarily a straight line, but the converse is far more complex.

Boundary element solutions for the plate buckling problem have been published among others in papers [2, 3, 4, 5, 6]. The authors of the papers cited investigate the buckling phenomenon under various assumptions and use different mechanical models. However, it is a common feature of each paper that the fundamental solutions utilized do not involve the effect of the in-plane stresses directly. The reason for attacking the problem in this way is simple: the model is applicable for any in-plane load exerted on the boundary. The price one has to pay for the generality of the model concerning the in-plane load is the presence of a domain integral which should be handled in some way. However, there are various cases when the stress state due to the in-plane load is a constant one. We also remark that the papers cited above are not concerned with the issue of how the in-plane stresses affect the vibrations of the plate.

Paper [7] is devoted to the issue what vibration characteristics of centrally clamped, variable thickness disks have if they are subjected to rotational and thermal in-plane stresses. This paper contains useful references for the most important earlier results which are not cited here. Pardoen [8] turned his attention to the vibration of prestressed circular orthotropic plates and used a finite element procedure for solving the problem. In [9] Chotova investigated the effect of a uniformly distributed in-plane compressive force system – exerted on the outer boundary of the plate – on the natural frequencies of circular plates assuming axisymmetric behavior. Numerical solutions were found by determining the zeros of the corresponding frequency determinant, which is regarded as a function of the load. It is also important to cite papers [10, 11] by Chen and his co-authors who dealt with the large amplitude vibrations of an initially stressed thick circular plate. They applied energetic methods in order to clarify how the load influences the vibrations. The results achieved are presented graphically. Paper [12] is devoted to the stability of parametric vibrations of circular plates subjected to in-plane forces by using the Liapunov method. Younesian [13] studied the forced vibrations of annular plates under the action of a transverse load rotating on the outer boundary.

The main objective of the present paper is to clarify mathematically – by setting up polynomial relationships – how the constant in plane load influences the vibrations of clamped, simply supported and spring supported circular plates. We attack the problem by determining the Green functions of the prestressed plates, which might also be useful for solving various boundary value problems in a closed form if the plates are subjected to transverse loads. With the knowledge of the Green functions the two parameter eigenvalue problems established for the natural frequencies are reduced to eigenvalue problems governed by homogenous Fredholm integral equations with symmetric kernels. These formulations are basically the same as those of the boundary element methods; however the kernels are not singular. After having set up the eigenvalue problems this way we solve them by the boundary element method.

The paper is organized into seven sections. Section 2 is a collection of the most important notations and notational conventions. Section 3 presents the governing

equations of the problem raised. Section 4 outlines the determination of the Green functions. It is also shown that the third Green function contains the other two at the limit, i.e., if the spring constant tends to zero or infinity. The algorithm of the numerical solutions is considered in Section 5. Computational and analytical (closed form approximate) solutions are presented in Section 6. The last section is a conclusion. We remark that some preliminary results were published earlier in Hungarian [14, 2007].

2. Notations and notational conventions

The table below presents the most important notations and notational conventions.

$\mathcal{A}^{1/2} = \sqrt{\frac{\gamma}{g}\frac{R_o^4}{I_1 E_1}}\alpha$	dimensionless natural frequency
$2b$	thickness of the plate
f	radial load in the mid-plane
$I_1 = 8b^3/12$	moment of inertia
E	Young's modulus
$E_1 = E/(1-\nu^2)$	modified Young's modulus
$\mathcal{F} = R_o^2\frac{f}{I_1 E_1}$	dimensionless in-plane load
$\mathcal{F}_\nu = \frac{\mathcal{F}}{1-\nu}$	modified dimensionless in-plane load
g	gravitational acceleration
$G(\rho,\xi) = G(\xi,\rho)$	Green function
$J_n,\ Y_n\ , I_n\ , K_n\ , n = 0,1,2,\ldots$	Bessel functions
k_γ	spring constant
$\mathcal{K} = \frac{R_o k_\gamma}{I_1 E_1}$	dimensionless spring constant
$\mathcal{K}_\nu = 1 - \frac{\mathcal{K}}{1-\nu}$	modified dimensionless spring constant
$p_z(\rho)$	load in the z direction
$Q_R(\rho)$	shear force
R	radius
R_o	outer radius of the plate
$w(\rho)$	deflection
$\tilde{\Delta} = \frac{\mathrm{d}^2}{\mathrm{d}\rho^2} + \frac{1}{\rho}$	differential operator
α	natural frequency
γ	density
ν	Poisson number
$\rho = R/R_o$	dimensionless independent variable
ξ	dimensionless independent variable

The text contains further notations defined at the place of their first appearance.

3. Governing equations

If a circular plate is subjected to a constant radial load f in its plane then the deflection w due to the load $p_z(\rho)$ acting perpendicularly to the middle plane of the plate should meet the differential equation

$$\tilde{\Delta}\tilde{\Delta}w \pm \mathcal{F}\tilde{\Delta}w = \frac{R_o^4}{I_1 E_1}\, p_z, \qquad \tilde{\Delta} = \frac{\mathrm{d}^2}{\mathrm{d}\rho^2} + \frac{1}{\rho}\frac{\mathrm{d}}{\mathrm{d}\rho} \tag{3.1}$$

if axisymmetric deformations are assumed – the sign preceding $\mathcal{F}$ is positive for compression and negative for tension – Figure 1 shows a compressive load [15, 2003]. Depending on what the supports are equation (3.1) should be associated with appropriate boundary conditions. As regards the outer boundary it is clear from Figure 1 that for a clamped plate

$$w|_{\rho=1} = 0\,, \qquad \left.\frac{\mathrm{d}w}{\mathrm{d}\rho}\right|_{\rho=1} = 0\,, \tag{3.2}$$

are the boundary conditions. If the plate is simply supported then the boundary conditions are of the form

$$w|_{\rho=1} = 0\,, \qquad \left.\left(\frac{\mathrm{d}^2 w}{\mathrm{d}\rho^2} + \frac{\nu}{\rho}\frac{\mathrm{d}w}{\mathrm{d}\rho}\right)\right|_{\rho=1} = 0\,. \tag{3.3}$$

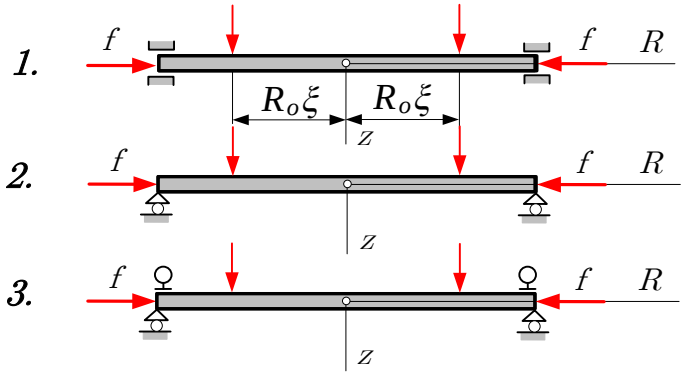

Figure 1.

Finally if the plate is supported by a torsional spring which exerts a bending moment on the boundary of the plate then

$$w = 0\,, \qquad \left.\left(\frac{\mathrm{d}^2 w}{\mathrm{d}\rho^2} + \frac{\nu}{\rho}\frac{\mathrm{d}w}{\mathrm{d}\rho}\right)\right|_{\rho=1} = -\frac{R_o}{I_1 E_1} k_\gamma \left.\frac{\mathrm{d}w}{\mathrm{d}\rho}\right|_{\rho=1} \tag{3.4}$$

are the boundary conditions. It is also clear that the deflection at the center of the plate should meet the conditions

$$w|_{\rho=0} = \text{finite}\,, \qquad \left.\frac{\mathrm{d}w}{\mathrm{d}\rho}\right|_{\rho=0} = 0 \tag{3.5}$$

as well. For our later considerations we remark that the shear force Q_R is related to the deflection via equation

$$Q_R \frac{R_o^3}{I_1 E_1} = \frac{\mathrm{d}}{\mathrm{d}\rho}\left[\frac{\mathrm{d}^2}{\mathrm{d}\rho^2} + \frac{1}{\rho}\frac{\mathrm{d}}{\mathrm{d}\rho} \pm \mathcal{F}\right] w(\rho)\,. \tag{3.6}$$

We remark that the boundary conditions and the formula for the shear force are all taken from Kozák [16].

4. Green functions

4.1. **Definition of the Green function.** Assume that the plate is subjected to a uniform load distributed on the circle with radius $R_o\xi$ (ξ is also a dimensionless coordinate) – see Figure 1. The resultant of the total load is assumed to be 1. The deflection due to the load at ρ is denoted by $G(\rho,\xi)$ and is referred to as the Green function. Observe that the Green function should satisfy the homogenous equation in (3.1) if $0 \le \rho < \xi$ and $\xi < \rho \le 1$.

4.2. **Green functions for a compressive f.**

4.2.1. *General solution.* As is well known the general solution of the homogenous equation in (3.1) assumes the form

$$w(\rho) = c_1 + c_2 \ln\rho + c_3 J_o(\sqrt{\mathcal{F}}\rho) + c_4 Y_o(\sqrt{\mathcal{F}}\rho)\,, \tag{4.1}$$

where c_1, c_2, c_3 and c_4 are undetermined constants of integration.

Since the Green function should meet conditions (3.5) it assumes the form

$$G(\rho,\xi) = A_1 + A_3 J_0(\sqrt{\mathcal{F}}\rho)\,, \qquad 0 \le \rho \le \xi\,, \tag{4.2a}$$

$$G(\rho,\xi) = B_1 + B_2 \ln\rho + B_3 J_0(\sqrt{\mathcal{F}}\rho) + B_4 Y_0(\sqrt{\mathcal{F}}\rho)\,, \qquad \xi \le \rho \le 1\,, \tag{4.2b}$$

where the constants of integration A_1, A_3 and B_1, B_2, B_3, B_4 are to be determined from the continuity and discontinuity conditions prescribed at $\rho = \xi$ and form the boundary conditions which are imposed on the boundary $\rho = 1$.

Observe that the continuity conditions

$$G(\xi - 0, \xi) = G(\xi + 0, \xi)\,, \tag{4.3a}$$

$$G'(\xi - 0, \xi) = G'(\xi + 0, \xi)\,, \tag{4.3b}$$

$$G''(\xi - 0, \xi) = G''(\xi + 0, \xi) \tag{4.3c}$$

and the discontinuity condition

$$2\pi R_o \xi\,[Q_R(\xi + 0) - Q_R(\xi - 0)] = 2\pi R_o \xi Q_R(\xi + 0) = 1\,, \tag{4.4}$$

in which $Q_R(\xi - 0) = 0$ from the vertical equilibrium, are all independent of the supports. Here (a) derivatives with respect to ρ are denoted by primes and (b) it follows from (3.6) that

$$Q_R \frac{R_o^3}{I_1 E_1} = \frac{\mathrm{d}}{\mathrm{d}\rho}\left[\frac{\mathrm{d}^2}{\mathrm{d}\rho^2} + \frac{1}{\rho}\frac{\mathrm{d}}{\mathrm{d}\rho} + \mathcal{F}\right] G(\xi,\rho)\,. \tag{4.5}$$

4.2.2. *Green function for the clamped plate.* If the plate is clamped the continuity and discontinuity conditions are associated with the boundary conditions

$$G(1,\xi)=0\,,\qquad G'(1,\xi)=0\,. \tag{4.6}$$

In what follows we need the derivatives

$$G'(\rho,\xi)=-A_3\sqrt{\mathcal{F}}J_1(\sqrt{\mathcal{F}}\rho)\qquad 0\le\rho\le\xi\,, \tag{4.7a}$$

$$G'(\rho,\xi)=B_2\frac{1}{\rho}-B_3\sqrt{\mathcal{F}}J_1(\sqrt{\mathcal{F}}\rho)-B_4\sqrt{\mathcal{F}}Y_1(\sqrt{\mathcal{F}}\rho)\qquad \xi\le\rho\le 1\,, \tag{4.7b}$$

$$G''(\rho,\xi)=A_3\mathcal{F}\left[\frac{J_1\left(\sqrt{\mathcal{F}}\rho\right)}{\sqrt{\mathcal{F}}\rho}-J_0\left(\sqrt{\mathcal{F}}\rho\right)\right]\qquad 0\le\rho\le\xi\,, \tag{4.8a}$$

$$G''(\rho,\xi)=-B_2\frac{1}{\rho^2}+B_3\mathcal{F}\left[\frac{J_1\left(\sqrt{\mathcal{F}}\rho\right)}{\sqrt{\mathcal{F}}\rho}-J_0\left(\sqrt{\mathcal{F}}\rho\right)\right]+ \tag{4.8b}$$

$$+B_4\mathcal{F}\left(\frac{Y_1\left(\sqrt{\mathcal{F}}\rho\right)}{\sqrt{\mathcal{F}}\rho}-Y_0\left(\sqrt{\mathcal{F}}\rho\right)\right)\quad \xi\le\rho\le 1\,, \tag{4.8c}$$

$$\begin{aligned}G'''(\rho,\xi)&=-A_3\frac{\mathcal{F}^{3/2}}{4}\left[J_3(\sqrt{\mathcal{F}}\rho)-3J_1(\sqrt{\mathcal{F}}\rho)\right]=\\&=A_2\frac{\mathcal{F}^{3/2}}{4}\left[\frac{1}{\sqrt{\mathcal{F}}\rho}J_2(\sqrt{\mathcal{F}}\rho)-J_1\left(\sqrt{\mathcal{F}}\rho\right)\right]\qquad 0\le\rho\le\xi\end{aligned} \tag{4.9a}$$

and

$$\begin{aligned}G'''(\rho,\xi)&=\frac{2}{\rho^3}B_2-B_3\frac{\mathcal{F}^{3/2}}{4}\left[J_3(\sqrt{\mathcal{F}}\rho)-3J_1(\sqrt{\mathcal{F}}\rho)\right]-\\&\quad-B_4\frac{\mathcal{F}^{3/2}}{4}\left[Y_3(\sqrt{\mathcal{F}}\rho)-3Y_1(\sqrt{\mathcal{F}}\rho)\right]=\\&=\frac{2}{\rho^3}B_2+B_3\frac{\mathcal{F}^{3/2}}{4}\left[\frac{1}{\sqrt{\mathcal{F}}\rho}J_2(\sqrt{\mathcal{F}}\rho)-J_1\left(\sqrt{\mathcal{F}}\rho\right)\right]+\\&\quad+B_4\frac{\mathcal{F}^{3/2}}{4}\left[\frac{1}{\sqrt{\mathcal{F}}\rho}Y_2(\sqrt{\mathcal{F}}\rho)-Y_1\left(\sqrt{\mathcal{F}}\rho\right)\right]\qquad \xi\le\rho\le 1\end{aligned} \tag{4.9b}$$

obtained by using relations (A.1).

Substituting the Green function and its derivatives into the continuity conditions (4.3a) and then combining the continuity conditions (4.3b) and (4.3c) we have

$$A_1+A_3J_0(\sqrt{\mathcal{F}}\xi)=B_1+B_2\ln\xi+B_3J_0(\sqrt{\mathcal{F}}\xi)+B_4Y_0(\sqrt{\mathcal{F}}\xi)\,, \tag{4.10a}$$

$$-A_3\sqrt{\mathcal{F}}J_1\left(\sqrt{\mathcal{F}}\xi\right)=B_2\frac{1}{\xi}-B_3\sqrt{\mathcal{F}}J_1\left(\sqrt{\mathcal{F}}\xi\right)-B_4\sqrt{\mathcal{F}}Y_1\left(\sqrt{\mathcal{F}}\xi\right)\,, \tag{4.10b}$$

$$A_3J_0(\sqrt{\mathcal{F}}\xi)=B_3J_0(\sqrt{\mathcal{F}}\xi)+B_4Y_0(\sqrt{\mathcal{F}}\xi)\,. \tag{4.10c}$$

It follows from (4.5) that

$$\begin{aligned}
\frac{R_K^3}{I_1E_1}Q_R(\xi+0) = {} & B_2\frac{d}{d\rho}\left\{-\frac{1}{\rho^2}+\frac{1}{\rho^2}+\mathcal{F}\ln\rho\right\}\Big|_{\rho=\xi} + \\
& + B_3\frac{d}{d\rho}\left\{\left[\frac{\mathcal{F}}{2}\left[J_2(\sqrt{\mathcal{F}}\rho)-J_0(\sqrt{\mathcal{F}}\rho)\right]-\mathcal{F}\frac{J_1(\sqrt{\mathcal{F}}\rho)}{\sqrt{\mathcal{F}}\rho}\right]+\mathcal{F}J_0(\sqrt{\mathcal{F}}\rho)\right\}\Big|_{\rho=\xi} \\
& + B_4\frac{d}{d\rho}\left\{\left[\frac{\mathcal{F}}{2}\left[Y_2(\sqrt{\mathcal{F}}\rho)-Y_0(\sqrt{\mathcal{F}}\rho)\right]-\mathcal{F}\frac{Y_1(\sqrt{\mathcal{F}}\rho)}{\sqrt{\mathcal{F}}\rho}\right]+\mathcal{F}Y_0(\sqrt{\mathcal{F}}\rho)\right\}\Big|_{\rho=\xi} = \\
= {} & B_2\frac{d}{d\rho}\left\{-\frac{1}{\rho^2}+\frac{1}{\rho^2}+\mathcal{F}\ln\rho\right\}\Big|_{\rho=\xi} + \\
& + B_3\frac{d}{d\rho}\underbrace{\left\{\left[\frac{\mathcal{F}}{2}\left[J_2(\sqrt{\mathcal{F}}\rho)+J_0(\sqrt{\mathcal{F}}\rho)\right]-\mathcal{F}\frac{J_1(\sqrt{\mathcal{F}}\rho)}{\sqrt{\mathcal{F}}\rho}\right]\right\}}_{=zero}\Big|_{\rho=\xi} \\
& + B_4\frac{d}{d\rho}\underbrace{\left\{\left[\frac{\mathcal{F}}{2}\left[Y_2(\sqrt{\mathcal{F}}\rho)+Y_0(\sqrt{\mathcal{F}}\rho)\right]-\mathcal{F}\frac{Y_1(\sqrt{\mathcal{F}}\rho)}{\sqrt{\mathcal{F}}\rho}\right]\right\}}_{=zero}\Big|_{\rho=\xi} = B_2\mathcal{F}\frac{1}{\xi}\,.
\end{aligned}$$

Consequently discontinuity condition (4.4) leads to the equation

$$B_2 = \frac{R_o^3}{I_1E_1}\frac{1}{2\pi\xi R_o}\frac{1}{\mathcal{F}}\xi = \frac{R_o^2}{I_1E_1\frac{fR_o^2}{I_1E_1}}\frac{1}{2\pi\xi}\xi = \frac{1}{2\pi f}\,. \tag{4.10d}$$

The last two equations for the integration constants are obtained from the boundary conditions (4.6)

$$B_1 + B_3J_0(\sqrt{\mathcal{F}}) + B_4Y_0(\sqrt{\mathcal{F}}) = 0\,, \tag{4.10e}$$

$$B_2 - B_3\sqrt{\mathcal{F}}J_1(\sqrt{\mathcal{F}}) - B_4\sqrt{\mathcal{F}}Y_1(\sqrt{\mathcal{F}}) = 0\,. \tag{4.10f}$$

Introducing the notations $J_{n\rho} = J_n(\sqrt{\mathcal{F}}\rho)$, $J_{n\xi} = J_n(\sqrt{\mathcal{F}}\xi)$, $J_{n1} = J_n(\sqrt{\mathcal{F}})$ and $Y_{n\rho} = Y_n(\sqrt{\mathcal{F}}\rho)$, $Y_{n\xi} = Y_n(\sqrt{\mathcal{F}}\xi)$, $Y_{n1} = Y_n(\sqrt{\mathcal{F}})$ we can rewrite equations (4.10) in the following form:

$$\begin{bmatrix}
1 & J_{0\xi} & -1 & -\ln\xi & -J_{0\xi} & -Y_{0\xi} \\
0 & -\sqrt{\mathcal{F}}J_{1\xi} & 0 & -\frac{1}{\xi} & \sqrt{\mathcal{F}}J_{1\xi} & \sqrt{\mathcal{F}}Y_{1\xi} \\
0 & J_{0\xi} & 0 & 0 & -J_{0\xi} & -Y_{0\xi} \\
0 & 0 & 0 & 1 & 0 & 0 \\
0 & 0 & 1 & 0 & J_{01} & Y_{01} \\
0 & 0 & 0 & 1 & -\sqrt{\mathcal{F}}J_{11} & -\sqrt{\mathcal{F}}Y_{11}
\end{bmatrix}
\begin{bmatrix} A_1 \\ A_3 \\ B_1 \\ B_2 \\ B_3 \\ B_4 \end{bmatrix} =
\begin{bmatrix} 0 \\ 0 \\ 0 \\ \frac{1}{2\pi f} \\ 0 \\ 0 \end{bmatrix} \tag{4.11}$$

After solving equation system (4.11) and substituting solutions (B.1) given in the Appendix into (4.2) we have

$$G(\rho,\xi)=\frac{J_{11}\ln\xi+\frac{1}{\sqrt{\mathcal{F}}}\left(J_{0\rho}+J_{0\xi}-J_{01}\right)+\frac{\pi}{2}J_{0\rho}\left(J_{0\xi}Y_{11}-Y_{0\xi}J_{11}\right)}{2\pi f J_{11}}$$
$$0\le\rho\le\xi\,, \quad (4.12a)$$

$$G(\rho,\xi)=\frac{J_{11}\ln\rho+\frac{1}{\sqrt{\mathcal{F}}}\left(J_{0\xi}+J_{0\rho}-J_{01}\right)+\frac{\pi}{2}J_{0\xi}\left(J_{0\rho}Y_{11}-Y_{0\rho}J_{11}\right)}{2\pi f J_{11}}$$
$$\xi\le\rho\le 1\,, \quad (4.12b)$$

which is the Green function for the clamped plate. It can be checked with ease that the Green function is symmetric, i.e., $G(\rho,\xi)=G(\xi,\rho)$.

4.2.3. *Green function for the simply supported plate.* If the plate is simply supported the continuity and discontinuity conditions are associated with the following boundary conditions:

$$G(1,\xi)=0\,,\qquad G''(1,\xi)+\frac{\nu}{\rho}G'(1,\xi)=0 \quad (4.13)$$

Observe that only one equation differs from those we used earlier – compare $(4.13)_2$ and $(4.6)_2$. For the sake of brevity we omit the paper and pencil calculations and present the final result only:

$$G(\rho,\xi)=\frac{J_{01}-J_{0\xi}-J_{0\rho}+\frac{\pi}{2}J_{0\xi}J_{0\rho}(\mathcal{F}_\nu Y_{01}-\sqrt{\mathcal{F}}Y_{11})}{2\pi f(\mathcal{F}_\nu J_{01}-\sqrt{\mathcal{F}}J_{11})}+$$
$$+\frac{\ln\xi-\frac{\pi}{2}J_{0\rho}Y_{0\xi}}{2\pi f}\qquad 0\le\rho\le\xi\,, \quad (4.14a)$$

$$G(\rho,\xi)=\frac{J_{01}-J_{0\rho}-J_{0\xi}+\frac{\pi}{2}J_{0\rho}J_{0\xi}\left(\mathcal{F}_\nu Y_{01}-\sqrt{\mathcal{F}}Y_{11}\right)}{4\pi f(\mathcal{F}_\nu J_{01}-\sqrt{\mathcal{F}}J_{11})}+$$
$$+\frac{\ln\rho-\frac{\pi}{2}J_{0\xi}Y_{0\rho}}{2\pi f}\qquad \xi\le\rho\le 1\,. \quad (4.14b)$$

This Green function is also symmetric, i.e., $G(\rho,\xi)=G(\xi,\rho)$.

4.2.4. *Green function for the spring-supported plate.* For the spring-supported plate the continuity and discontinuity conditions are associated with the following boundary conditions:

$$G(1,\xi)=0\,,\qquad G(1,\xi)''+\frac{\nu}{\rho}G(1,\xi)'+\frac{R_o}{I_1E_1}k_\gamma G(1,\xi)'=0\,. \quad (4.15)$$

Without entering into details we have arrived at the following Green function

$$G(\rho,\xi)=\frac{\mathcal{K}_\nu\left(J_{01}-J_{0\xi}-J_{0\rho}\right)+\frac{\pi}{2}J_{0\rho}J_{0\xi}\left(\mathcal{F}_\nu Y_{01}-\sqrt{\mathcal{F}}\mathcal{K}_\nu Y_{11}\right)}{2\pi f(\mathcal{F}_\nu J_{01}-\sqrt{\mathcal{F}}\mathcal{K}_\nu J_{11})}+$$
$$+\frac{\ln\xi-\frac{\pi}{2}J_{0\rho}Y_{0\xi}}{2\pi f}\qquad 0\le\rho\le\xi \quad (4.16a)$$

$$G(\rho,\xi)=\frac{\mathcal{K}_\nu\left(J_{01}-J_{0\rho}-J_{0\xi}\right)+\frac{\pi}{2}J_{0\xi}J_{0\rho}\left(\mathcal{F}_\nu Y_{01}-\sqrt{\mathcal{F}}\mathcal{K}_\nu Y_{11}\right)}{2\pi f(\mathcal{F}_\nu J_{01}-\sqrt{\mathcal{F}}\mathcal{K}_\nu J_{11})}+$$

$$+\frac{\ln\rho-\frac{\pi}{2}J_{0\xi}Y_{0\rho}}{2\pi f}\qquad \xi\le\rho\le 1 \tag{4.16b}$$

In the formulae providing the last two Green functions

$$\mathcal{K}=\frac{R_o k_\gamma}{I_1E_1}\,,\qquad \mathcal{F}_\nu=\frac{\mathcal{F}}{1-\nu}\,,\qquad \mathcal{K}_\nu=1-\frac{\mathcal{K}}{1-\nu}\,. \tag{4.17}$$

It can be shown that (a) for $\mathcal{K}\to 0$ the Green function (4.16) coincides with the Green function (4.14) valid for the simply supported plate and (b) for $\mathcal{K}\to\infty$ the Green function (4.16) coincides with the Green function (4.12) valid for the clamped plate.

4.3. **Green functions for a tensile f.**

4.3.1. *General solution.* If the in-plane load is a tensile load

$$w(\rho)=c_1+c_2\ln\rho+c_3I_0\left(\sqrt{\mathcal{F}}\rho\right)+c_4K_0\left(\sqrt{\mathcal{F}}\rho\right) \tag{4.18}$$

is the general solution we need when determining the Green function – c_1, c_2, c_3 and c_4 are again undetermined constants of integration. With the knowledge of the general solution we assume that the Green function, which satisfies conditions (3.5), can be given in the following form

$$G(\rho,\xi)=A_1+A_3I_0(\sqrt{\mathcal{F}}\rho)\,,\qquad \rho<\xi\,, \tag{4.19a}$$

$$G(\rho,\xi)=B_1+B_2\ln\rho+B_3I_0(\sqrt{\mathcal{F}}\rho)+B_4K_0(\sqrt{\mathcal{F}}\rho)\,,\qquad \rho>\xi \tag{4.19b}$$

in which the integration constants are denoted in the same way as for the case of compressive f – however this may not cause any misunderstanding.

4.3.2. *Green function for the clamped plate.* When determining the Green function we need the following derivatives

$$G'(\rho,\xi)=A_3\sqrt{\mathcal{F}}I_1(\sqrt{\mathcal{F}}\rho)\qquad \rho<\xi\,, \tag{4.20a}$$

$$G'(\rho,\xi)=B_2\frac{1}{\rho}+B_3\sqrt{\mathcal{F}}I_1(\sqrt{\mathcal{F}}\rho)-B_4\sqrt{\mathcal{F}}K_1(\sqrt{\mathcal{F}}\rho)\qquad \rho>\xi\,, \tag{4.20b}$$

$$G''(\rho,\xi)=A_3\mathcal{F}\left(I_0\left(\sqrt{\mathcal{F}}\rho\right)-\frac{1}{\sqrt{\mathcal{F}}\rho}I_1\left(\sqrt{\mathcal{F}}\rho\right)\right)\qquad \rho<\xi\,, \tag{4.21a}$$

$$G''(\rho,\xi)=-B_2\frac{1}{\rho^2}+B_3\mathcal{F}\left(I_0\left(\sqrt{\mathcal{F}}\rho\right)-\frac{1}{\sqrt{\mathcal{F}}\rho}I_1\left(\sqrt{\mathcal{F}}\rho\right)\right)+$$

$$+B_4\mathcal{F}\left(K_0\left(\sqrt{\mathcal{F}}\rho\right)+\frac{1}{\sqrt{\mathcal{F}}\rho}K_1\left(\sqrt{\mathcal{F}}\rho\right)\right)\qquad \rho>\xi\,, \tag{4.21b}$$

$$G'''(\rho,\xi)=A_3\frac{\mathcal{F}^{3/2}}{4}\left[3I_1(\sqrt{\mathcal{F}}\rho)+I_3(\sqrt{\mathcal{F}}\rho)\right]=$$

$$= -A_3\mathcal{F}^{3/2}\left(\frac{1}{\sqrt{\mathcal{F}}x}I_2\left(\sqrt{\mathcal{F}}x\right) - I_1\left(\sqrt{\mathcal{F}}x\right)\right) \qquad \rho < \xi\,. \tag{4.22a}$$

$$\begin{aligned} G'''(\rho,\xi) &= -2B_2\frac{1}{\rho^3} + B_3\frac{\mathcal{F}^{3/2}}{4}\left[3I_1(\sqrt{\mathcal{F}}\rho) + I_3(\sqrt{\mathcal{F}}\rho)\right] - \\ &- B_4\frac{\mathcal{F}^{3/2}}{4}\left[3K_1(\sqrt{\mathcal{F}}\rho) + K_3(\sqrt{\mathcal{F}}\rho)\right] = \\ &= -2B_2\frac{1}{\rho^3} + B_3\mathcal{F}^{3/2}\left(\frac{1}{\sqrt{\mathcal{F}}x}I_2\left(\sqrt{\mathcal{F}}x\right) - I_1\left(\sqrt{\mathcal{F}}x\right)\right) \\ &- B_4\mathcal{F}^{3/2}\left[\frac{1}{\sqrt{\mathcal{F}}x}K_2\left(\sqrt{\mathcal{F}}x\right) + K_1\left(\sqrt{\mathcal{F}}x\right)\right] \qquad \rho > \xi \end{aligned} \tag{4.22b}$$

obtained by utilizing (A.2). Substituting the Green function and its derivatives into the continuity conditions (4.3a) and combining (4.3b) and (4.3c) we have

$$A_1 + A_3 I_0(\sqrt{\mathcal{F}}\xi) = B_1 + B_2\ln\xi + B_3 I_0(\sqrt{\mathcal{F}}\xi) + B_4 K_0(\sqrt{\mathcal{F}}\xi)\,, \tag{4.23a}$$

$$A_3\sqrt{\mathcal{F}}I_1(\sqrt{\mathcal{F}}\xi) = B_2\frac{1}{\xi} + B_3\sqrt{\mathcal{F}}I_1(\sqrt{\mathcal{F}}\xi) - B_4\sqrt{\mathcal{F}}K_1(\sqrt{\mathcal{F}}\xi)\,, \tag{4.23b}$$

$$A_3 I_0(\sqrt{\mathcal{F}}\xi) = B_3 I_0(\sqrt{\mathcal{F}}\xi) + B_4 K_0(\sqrt{\mathcal{F}}\xi)\,. \tag{4.23c}$$

By repeating the line of thought resulting in equation (4.10d) discontinuity condition (4.4) leads to the equation

$$B_2 = -1/2\pi f\,. \tag{4.23d}$$

The last two equations for the integration constants are provided again by the boundary conditions (4.6)

$$B_1 + B_3 I_0(\sqrt{\mathcal{F}}) + B_4 K_0(\sqrt{\mathcal{F}}) = 0\,, \tag{4.23e}$$

$$B_2 + B_3\sqrt{\mathcal{F}}I_1(\sqrt{\mathcal{F}}) - B_4\sqrt{\mathcal{F}}K_1(\sqrt{\mathcal{F}}) = 0\,. \tag{4.23f}$$

Let $I_{n\rho} = I_n(\sqrt{\mathcal{F}}\rho)$, $I_{n\xi} = I_n(\sqrt{\mathcal{F}}\xi)$, $I_{n1} = I_n(\sqrt{\mathcal{F}})$, $K_{n\rho} = K_n(\sqrt{\mathcal{F}}\rho)$, $K_{n\xi} = K_n(\sqrt{\mathcal{F}}\xi)$ and $K_{n1} = K_n(\sqrt{\mathcal{F}})$. Making use of the notations introduced equation system (4.23) can be cast into the following form:

$$\begin{bmatrix} 1 & I_{0\xi} & -1 & -\ln\xi & -I_{0\xi} & -K_{0\xi} \\ 0 & \sqrt{\mathcal{F}}J_{1\xi} & 0 & -\frac{1}{\xi} & -\sqrt{\mathcal{F}}I_{1\xi} & \sqrt{\mathcal{F}}K_{1\xi} \\ 0 & I_{0\xi} & 0 & 0 & -I_{0\xi} & -K_{0\xi} \\ 0 & 0 & 0 & 1 & 0 & 0 \\ 0 & 0 & 1 & 0 & I_{01} & K_{01} \\ 0 & 0 & 0 & 1 & \sqrt{\mathcal{F}}I_{11} & -\sqrt{\mathcal{F}}K_{11} \end{bmatrix} \begin{bmatrix} A_1 \\ A_3 \\ B_1 \\ B_2 \\ B_3 \\ B_4 \end{bmatrix} = \begin{bmatrix} 0 \\ 0 \\ 0 \\ -\frac{1}{2\pi f} \\ 0 \\ 0 \end{bmatrix} \tag{4.24}$$

With the integration constants $A_1,\ A_3,\ B_1,\ldots,B_4$ equation (4.19) yields the Green function as

$$G(\rho,\xi) = \frac{I_{11}\ln\xi + \frac{1}{\sqrt{F}}\left(I_{01} - I_{0\xi} - I_{0\rho}\right) + I_{0\rho}\left(I_{0\xi}K_{11} + K_{0\xi}I_{11}\right)}{2I_{11}\pi f} \qquad 0 < \rho \le \xi\,, \tag{4.25a}$$

$$G(\xi,\rho)=\frac{I_{11}\ln\rho+\frac{1}{\sqrt{F}}\left(I_{01}-I_{0\rho}-I_{0\xi}\right)+I_{0\xi}\left(I_{0\rho}K_{11}+K_{0\rho}I_{11}\right)}{2I_{11}\pi f}\qquad \xi\le\rho\le 1\ . \tag{4.25b}$$

4.3.3. *Green function for the simply supported plate.* We present the Green function without providing details concerning the paper and pencil calculations

$$G(\rho,\xi)=\frac{I_{0\xi}+I_{0\rho}-I_{01}-I_{0\rho}I_{0\xi}\left(\sqrt{\mathcal{F}}K_{11}+\mathcal{F}_\nu K_{01}\right)}{2\pi f(\mathcal{F}_\nu I_{01}-\sqrt{\mathcal{F}}I_{11})}+ \\ +\frac{\ln\xi+I_{0\rho}K_{0\xi}}{2\pi f}\qquad 0<\rho\le\xi\ , \tag{4.26a}$$

$$G(\rho,\xi)=\frac{I_{0\rho}+I_{0\xi}-I_{01}-I_{0\xi}I_{0\rho}\left(\sqrt{\mathcal{F}}K_{11}-\mathcal{F}_\nu K_{01}\right)}{2\pi f(\mathcal{F}_\nu I_{01}-\sqrt{\mathcal{F}}I_{11})}+ \\ +\frac{\ln\rho+I_{0\xi}K_{0\rho}}{2\pi f}\qquad \xi\le\rho\le 1\ . \tag{4.26b}$$

4.3.4. *Green function for the spring supported plate.* The Green function is given below again without presenting the calculations

$$G(\rho,\xi)=\frac{\mathcal{K}_\nu\left(I_{0\xi}+I_{0\rho}-I_{01}\right)-I_{0\rho}I_{0\xi}\left(\mathcal{F}_\nu K_{01}+\sqrt{\mathcal{F}}\mathcal{K}_\nu K_{11}\right)}{2\pi f(\mathcal{F}_\nu I_{01}-\sqrt{\mathcal{F}}\mathcal{K}_\nu I_{11})}+ \\ +\frac{\ln\xi+I_{0\rho}K_{0\xi}}{2\pi f}\qquad 0<\rho\le\xi\ , \tag{4.27a}$$

$$G(\xi,\rho)=\frac{\mathcal{K}_\nu(I_{0\rho}+I_{0\xi}-I_{01})-I_{0\xi}I_{0\rho}\left(\mathcal{F}_\nu K_{01}+\sqrt{\mathcal{F}}\mathcal{K}_\nu K_{11}\right)}{2\pi f(\mathcal{F}_\nu I_{01}-\sqrt{\mathcal{F}}\mathcal{K}_\nu I_{11})}+ \\ +\frac{\ln\rho+K_{0\rho}I_{0\xi}}{2\pi f}\qquad \xi\le\rho\le 1\ . \tag{4.27b}$$

If $\mathcal{K}\to 0$ (4.27) coincides with (4.25). Similarly if $\mathcal{K}\to\infty$ (4.27) coincides with (4.26).

4.4. **Solutions of statical boundary value problems.** Given the Green functions, the deflection due to an axisymmetric load $p_z(\rho)$ can always be calculated as

$$w(\rho)=2\pi R_o^2\int_0^1 G(\rho,\xi)p_z(\xi)\,\xi\,\mathrm{d}\xi\ . \tag{4.28}$$

5. Integral equation for the natural frequencies

5.1. **Integral equation of the problem.** Under the assumption of harmonic vibrations the amplitude $W(\rho)$ of the vibrations $w(\rho,t)$ should satisfy the differential equation

$$\left(\frac{\mathrm{d}^2}{\mathrm{d}\rho^2}+\frac{1}{\rho}\frac{\mathrm{d}}{\mathrm{d}\rho}\right)\left[\left(\frac{\mathrm{d}^2}{\mathrm{d}\rho^2}+\frac{1}{\rho}\frac{\mathrm{d}}{\mathrm{d}\rho}\right)W+\mathcal{F}W\right]=\frac{R_o^4}{I_1E_1}\frac{\gamma}{g}\alpha^2W \tag{5.1}$$

where γ is the plate weight for the unit area of the middle surface and g is the gravitational acceleration. The eigenvalue problems defined by equation (5.1) and boundary conditions (3.2), (3.3) and (3.4) are all self adjoint. Since $\alpha^2\gamma W/g$ corresponds to p_z in equation (3.1) it follows from equation (4.28) that the amplitude $W(\rho)$ should satisfy the integral equation

$$W(\rho)=\lambda\int_0^1\hat{G}(\rho,\xi)\,W(\xi)\,\xi\,\mathrm{d}\xi\quad\text{where}\quad\lambda=\frac{\gamma}{g}\alpha^2\,,\qquad\hat{G}(\rho,\xi)=2\pi R_o^2G(\rho,\xi)\,, \tag{5.2}$$

which can be manipulated into the following form:

$$W(\rho)=\frac{\gamma}{g}\alpha^2\int_0^1\frac{R_o^2}{f}\tilde{G}(\rho,\xi)\,W(\xi)\,\xi\,\mathrm{d}\xi=\underbrace{\frac{\gamma}{g}\frac{\alpha^2R_o^4}{I_1E_1}}_{\mathcal{A}}\int_0^1\underbrace{\frac{1}{\frac{fR_o^2}{I_1E_1}}}_{\mathcal{F}}\tilde{G}(\rho,\xi)\,W(\xi)\,\xi\,\mathrm{d}\xi\,. \tag{5.3}$$

Here $\mathcal{A}$ and $\mathcal{F}$ are dimensionless quantities: $\mathcal{A}$ is proportional to the square of a natural frequency, $\mathcal{F}$ is proportional to the load. If we introduce a new unknown function

$$y(\rho)=\sqrt{\rho}W(\rho) \tag{5.4}$$

then we have

$$\underbrace{\sqrt{\rho}W(\rho)}_{y(\rho)}=\mathcal{A}\int_0^1\underbrace{\sqrt{\rho}\frac{\tilde{G}(\rho,\xi)}{\mathcal{F}}\sqrt{(}\xi)}_{\mathcal{G}(\rho,\xi)}\underbrace{\sqrt{\xi}W(\xi)}_{y(\xi)}\mathrm{d}\xi\,,labelVibr50 \tag{5.5}$$

that is

$$y(\rho)=\mathcal{A}\int_0^1\mathcal{G}(\rho,\xi)y(\xi)\mathrm{d}\xi\,. \tag{5.6}$$

The above equation is a homogenous Fredholm integral equation with a symmetric kernel. At the same time this equation is an eigenvalue problem with $\mathcal{A}$ as an eigenvalue, which is a function of the dimensionless in-plane load $\mathcal{F}$.

5.2. **Computational algorithm.** A numerical solution to the eigenvalue problem (5.6) can be sought by quadrature methods [17]. Consider the integral formula

$$J(\phi)=\int_0^1\phi(\xi)\mathrm{d}\xi\equiv\sum_{j=0}^{n}w_j\phi(\xi_j)\,,\qquad\xi_j\in[0,1]\,,\quad j=0,1,\ldots,n\,, \tag{5.7}$$

where $\phi(\xi)$ is a scalar and the weights w_j are known. Making use of the above equation we obtain from (5.6) that

$$\sum_{j=0}^{n} w_j \mathcal{G}(\rho, \xi_j)\, y(\xi_j) = \chi y(\rho)\,, \qquad \chi = 1/\mathcal{A}\,, \quad x \in [0,1]\,, \quad j = 0, 1, \ldots, n \tag{5.8}$$

the solution of which yields an approximate eigenvalue $\mathcal{A} = 1/\chi$ and an approximate eigenfunction $y(\rho)$. After setting ρ to ρ_i $(i = 0, 1, 2, \ldots, n)$ we have

$$\sum_{j=0}^{n} w_j \mathcal{G}(\rho_i, \xi_j)\, y\,(\xi_j) = \chi y(\rho_i) \quad \chi = 1/\mathcal{A} \qquad x \in [0,1] \tag{5.9}$$

or

$$\boldsymbol{\mathcal{G}} \mathcal{D} \tilde{y} = \chi\, \tilde{y}\,, \tag{5.10a}$$

where $\boldsymbol{\mathcal{G}} = [G(\rho_i, \xi_j)]$ is symmetric,

$$\mathcal{D} = \operatorname{diag}(w_0 | \ldots | w_k | \ldots | w_n|) \quad \text{and} \quad \tilde{y}^T = [y(x_0)|y(x_1)|\ldots|y(x_n)]. \tag{5.10b}$$

After solving the algebraic eigenvalue problem (5.10) we have the approximate eigenvalues χ_r and eigenvectors $\tilde{y}_r$ $(r = 0, 1, \ldots, n)$. The corresponding eigenfunction is obtained by substituting back into equation (5.8):

$$y(\rho) = \frac{1}{\chi_r} \sum_{j=0}^{n} w_j \mathcal{G}(\rho, \xi_j)\, y(\xi_j)\,. \tag{5.11}$$

Divide the interval $[0, 1]$ into equidistant subintervals of length h and apply the integration formula to each subinterval. By repeating the line of thought leading to equation (5.10) one can show that the algebraic eigenvalue problem obtained is of the same structure as that of equation (5.10).

It is also possible to attack the integral equation (5.1) as a boundary integral equation and to apply isoparametric approximation in the subintervals, i.e., on the elements. If this is the case one can approximate the eigenfunction on the e-th element (on the e-th subinterval which is mapped onto the interval $\eta \in [-1, 1]$ and is denoted by L_e) as

$$\overset{e}{y}(\eta) = [N_1(\eta)|N_2(\eta)|N_3(\eta)] \begin{bmatrix} \overset{e}{y}_1 \\ \overset{e}{y}_2 \\ \overset{e}{y}_3 \end{bmatrix}\,, \tag{5.12}$$

where quadratic local approximations are assumed,

$$N_1 = 0.5\eta(\eta - 1),\ N_2 = 1 - \eta^2,\ N_3 = 0.5\eta(\eta + 1)\,,$$

and $\overset{e}{y}_i$ is the value of the eigenfunction $y(\rho)$ at the left endpoint, the midpoint and the right endpoint of the element, respectively. Substituting equation (5.12) into equation (5.6) we have

$$y(\rho) = \mathcal{A} \sum_{e=1}^{n_{be}} \int_{\mathfrak{L}_e} \mathcal{G}\,[\rho, \xi\,(\eta)]\,[N_1(\eta)|N_2(\eta)|N_3(\eta)] \mathcal{J}(\eta) d\eta \begin{bmatrix} \overset{e}{y}_1 \\ \overset{e}{y}_2 \\ \overset{e}{y}_3 \end{bmatrix}\,, \tag{5.13}$$

where n_{be} is the number of elements (subintervals), $\mathcal{J}(\eta)$ is the Jacobian. Using equation (5.13) as our point of departure and repeating the line of thought leading to (5.10) we shall arrive again at an algebraic eigenvalue problem. A program has been developed in Fortran 90 which solves the algebraic eigenvalue problem formulated in this way.

6. Computational results

6.1. **Clamped plate.** Let us introduce the following dimensionless quantities

$$\mathcal{A}_{oi} = \frac{\gamma}{g}\frac{R_o^2}{I_1 E_1}\alpha_{oi}^2 , \qquad \mathcal{A}_i = \frac{\gamma}{g}\frac{R_o^2}{I_1 E_1}\alpha_i^2 \tag{6.1a}$$

and

$$\mathcal{F}_{o1} = \frac{\gamma}{g}\frac{R_o^2}{I_1 E_1} f_1 . \tag{6.1b}$$

where α_{oi} and α_i are the i-th ($i = 1, 2, \ldots$) natural frequencies of the unloaded and loaded plates, while f_1 is the first critical load. The computational results for $i = 1$ are presented in Table 1.

Table 1

$\mathcal{F}/\mathcal{F}_{o1}$	0.068	0.136	0.204	0.272	0.341	0.409	0.477
$\mathcal{A}/\mathcal{A}_{o1}$ – compression	0.929	0.863	0.796	0.730	0.663	0.595	0.528
$\mathcal{A}/\mathcal{A}_{o1}$ – tension	1.061	1.127	1.193	1.258	1.324	1.389	1.454
$\mathcal{F}/\mathcal{F}_{o1}$	0.545	0.613	0.681	0.749	0.817	0.886	0.954
$\mathcal{A}/\mathcal{A}_{o1}$ – compression	0.460	0.392	0.324	0.255	0.186	0.117	0.048
$\mathcal{A}/\mathcal{A}_{o1}$ – tension	1.5189	1.584	1.648	1.713	1.777	1.841	1.906

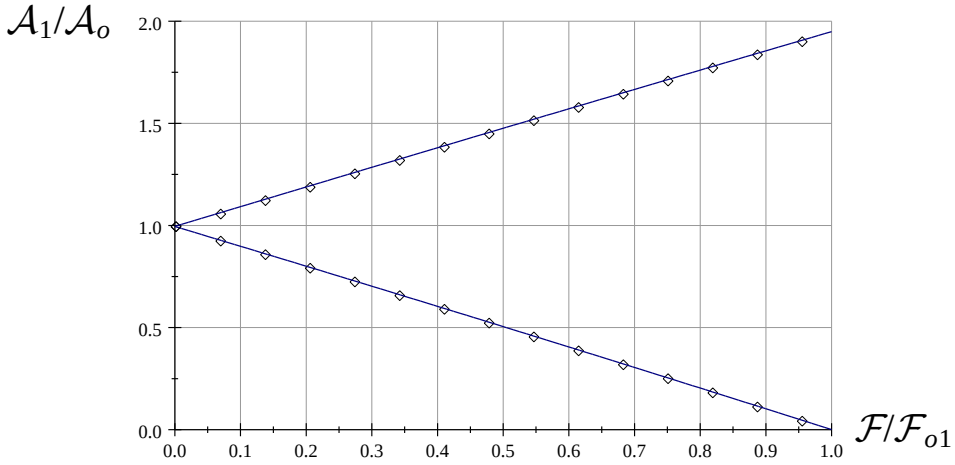

Figure 2.

With the knowledge of computational results we have fitted the following curves onto the discrete points – these are denoted by diamonds in Figure 2 ($\mathcal{A}_{o1} = 104.85$, $\mathcal{F}_{o1} = 14.68$)

$$\frac{\mathcal{A}_1}{\mathcal{A}_{o1}} = 0.994\,99 - 0.965\,94\frac{\mathcal{F}}{\mathcal{F}_{o1}} - 2.851\,4 \times 10^{-2}\left(\frac{\mathcal{F}}{\mathcal{F}_{o1}}\right)^2 \tag{6.2a}$$

$$\frac{\mathcal{A}_1}{\mathcal{A}_{o1}} = 0.995\,61 + 0.968\,14\frac{\mathcal{F}}{\mathcal{F}_{o1}} - 1.474\,2 \times 10^{-2}\left(\frac{\mathcal{F}}{\mathcal{F}_{o1}}\right)^2 \tag{6.2b}$$

Observe that the approximate solution (6.2) is practically linear in the interval $\mathcal{F}/\mathcal{F}_{o1} \in [0, 1]$.

6.2. **Simply supported plate.** For a simply supported plate the computational results are presented in Table 2 under the assumption that $i = 1$. These are denoted by diamonds in Figure 3.

TABLE 2

$\mathcal{F}/\mathcal{F}_{o1}$	0.070	0.140	0.210	0.280	0.350	0.420	0.490
$\mathcal{A}/\mathcal{A}_{o1}$ – compression	0.930	0.860	0.790	0.720	0.650	0.580	0.510
$\mathcal{A}/\mathcal{A}_{o1}$ – tension	1.071	1.141	1.211	1.281	1.351	1.421	1.491
$\mathcal{F}/\mathcal{F}_{o1}$	0.560	0.630	0.700	0.770	0.817	0.840	0.910
$\mathcal{A}/\mathcal{A}_{o1}$ – compression	0.440	0.370	0.300	0.230	0.159	0.089	0.019
$\mathcal{A}/\mathcal{A}_{o1}$ – tension	1.561	1.631	1.701	1.771	1.841	1.911	1.981

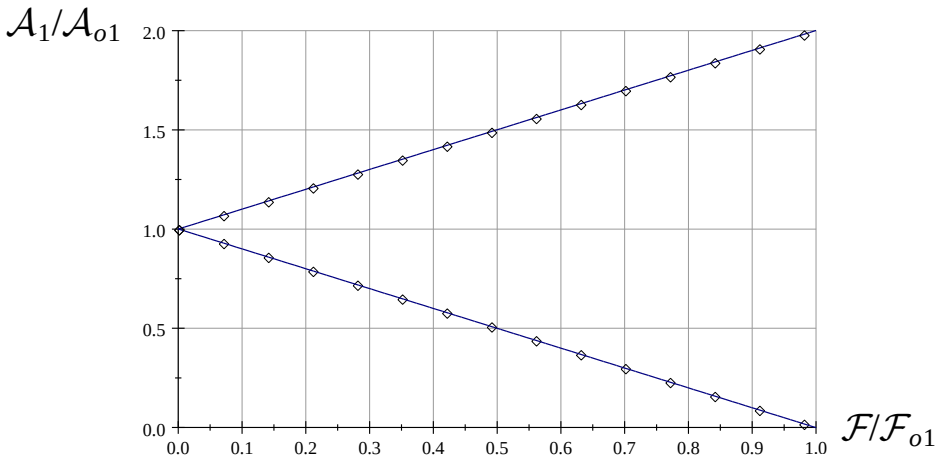

Figure 3.

The approximate solutions obtained again by fitting a curve onto the computational results are practically linear functions. These are are also shown in Figure 3 ($\mathcal{A}_{o1} = 24.838$, $\mathcal{F}_{o1} = 4.285$).

$$\frac{\mathcal{A}_1}{\mathcal{A}_{o1}} = 1.0004 - 1.0007\frac{\mathcal{F}}{\mathcal{F}_{o1}} \simeq 1.000 - 1.000\frac{\mathcal{F}}{\mathcal{F}_{o1}} \tag{6.3a}$$

$$\frac{\mathcal{A}_1}{\mathcal{A}_{o1}} = 1.0004 + 1.0007\frac{\mathcal{F}}{\mathcal{F}_{o1}} \simeq 1.000 + 1.000\frac{\mathcal{F}}{\mathcal{F}_{o1}} \tag{6.3b}$$

The square of the first natural frequency of the plate when unloaded and the first critical load can be calculated by using equation (6.1a).

6.3. **Spring supported plate.** For a spring supported plate the results depend on the dimensionless spring constant $\mathcal{K}$ as well. If $i = 1$ the table below shows the results we have obtained for $\mathcal{A}_{o1}(\mathcal{K})$ and $\mathcal{F}_{o1}(\mathcal{K})$.

TABLE 3

$\mathcal{K}$	0.0	1.00	5.00	10.00	50.00	100.00	1000.00	$\mathcal{K} \to \infty$
$\mathcal{A}_{o1}$	24.838	37.36	63.118	76.677	96.791	100.41	103.97	104.85
$\mathcal{F}_{o1}$	4.285	6.498	10.481	12.182	14.115	14.397	14.657	14.68

Observe that for $\mathcal{K} = 0$ and $\mathcal{K} \to \infty$ Table 3 contains the values valid for simply supported and clamped plates. For a compressive f the following curves can be fitted onto the results obtained:

$$\mathcal{K} = 1.00 \qquad \frac{\mathcal{A}_1}{\mathcal{A}_{o1}} = 0.9937 - 1.0067\frac{\mathcal{F}}{\mathcal{F}_{o1}} \tag{6.4a}$$

$$\mathcal{K} = 5.00 \qquad \frac{\mathcal{A}_1}{\mathcal{A}_{o1}} = 1.000 - 0.99119\frac{\mathcal{F}}{\mathcal{F}_{o1}} - 8.786\,3 \times 10^{-3}\left(\frac{\mathcal{F}}{\mathcal{F}_{o1}}\right)^2 \tag{6.4b}$$

$$\mathcal{K} = 10.00 \qquad \frac{\mathcal{A}_1}{\mathcal{A}_{o1}} = 1.000 - 0.982\,23\frac{\mathcal{F}}{\mathcal{F}_{o1}} - 1.776\,3 \times 10^{-2}\left(\frac{\mathcal{F}}{\mathcal{F}_{o1}}\right)^2 \tag{6.4c}$$

$$\mathcal{K} = 50.00 \qquad \frac{\mathcal{A}_1}{\mathcal{A}_{o1}} = 1.000 - 0.972\,1\frac{\mathcal{F}}{\mathcal{F}_{o1}} - 2.783\,9 \times 10^{-2}\left(\frac{\mathcal{F}}{\mathcal{F}_{o1}}\right)^2 \tag{6.4d}$$

$$\mathcal{K} = 100.00 \qquad \frac{\mathcal{A}_1}{\mathcal{A}_{o1}} = 1.000 - 0.9712\frac{\mathcal{F}}{\mathcal{F}_{o1}} - 2.82 \times 10^{-2}\left(\frac{\mathcal{F}}{\mathcal{F}_{o1}}\right)^2 \tag{6.4e}$$

$$\mathcal{K} = 1000.00 \qquad \frac{\mathcal{A}_1}{\mathcal{A}_{o1}} = 0.999\,97 - 0.971\,08\frac{\mathcal{F}}{\mathcal{F}_{o1}} - 2.\,882\,7 \times 10^{-2}\left(\frac{\mathcal{F}}{\mathcal{F}_{o1}}\right)^2 \tag{6.4f}$$

For a tensile f equations (6.5) are the polynomials we have fitted onto the computational results.

$$\mathcal{K} = 1.00 \qquad \frac{\mathcal{A}_1}{\mathcal{A}_{o1}} = 0.993\,64 + 1.006\,8\frac{\mathcal{F}}{\mathcal{F}_{o1}} \tag{6.5a}$$

$$\mathcal{K} = 5.00 \qquad \frac{\mathcal{A}_1}{\mathcal{A}_{o1}} = 1.000\,2 + 0.992\,03\frac{\mathcal{F}}{\mathcal{F}_{o1}} - 4.511 \times 10^{-3}\left(\frac{\mathcal{F}}{\mathcal{F}_{o1}}\right)^2 \tag{6.5b}$$

$$\mathcal{K} = 10.00 \qquad \frac{\mathcal{A}_1}{\mathcal{A}_{o1}} = 1.000\,4 + 0.983\,59\frac{\mathcal{F}}{\mathcal{F}_{o1}} - 8.652\,4 \times 10^{-3}\left(\frac{\mathcal{F}}{\mathcal{F}_{o1}}\right)^2 \tag{6.5c}$$

$$\mathcal{K}=50.00 \qquad \frac{\mathcal{A}_1}{\mathcal{A}_{o1}} = 1.000\,6 + 0.974\,11\frac{\mathcal{F}}{\mathcal{F}_{o1}} - 1.400\,3\times 10^{-2}\left(\frac{\mathcal{F}}{\mathcal{F}_{o1}}\right)^2 \tag{6.5d}$$

$$\mathcal{K}=100.00 \qquad \frac{\mathcal{A}_1}{\mathcal{A}_{o1}} = 1.000\,6 + 0.973\,60\frac{\mathcal{F}}{\mathcal{F}_{o1}} - 1.454\,6\times 10^{-2}\left(\frac{\mathcal{F}}{\mathcal{F}_{o1}}\right)^2 \tag{6.5e}$$

$$\mathcal{K}=1000.00 \qquad \frac{\mathcal{A}_1}{\mathcal{A}_{o1}} = 1.004\,7 + 0.945\,10\frac{\mathcal{F}}{\mathcal{F}_{o1}} + 1.868\,7\times 10^{-2}\left(\frac{\mathcal{F}}{\mathcal{F}_{o1}}\right)^2 \tag{6.5f}$$

Observe that functions (6.4) and (6.5) are almost linear functions. For this reason Table 4 presents the computational results if $\mathcal{K} = 100.0$ only.

TABLE 4

$\mathcal{F}/\mathcal{F}_{o1}$	0.069	0.139	0.208	0.278	0.347	0.417	0.486
$\mathcal{A}/\mathcal{A}_{o1}$ – compression	0.933	0.865	0.796	0.729	0.659	0.590	0.521
$\mathcal{A}/\mathcal{A}_{o1}$ – tension	1.068	1.136	1.203	1.270	1.337	1.404	1.471
$\mathcal{F}/\mathcal{F}_{o1}$	0.556	0.625	0.695	0.764	0.834	0.903	0.972
$\mathcal{A}/\mathcal{A}_{o1}$ – compression	0.452	0.382	0.312	0.241	0.171	0.100	0.028
$\mathcal{A}/\mathcal{A}_{o1}$ – tension	1.537	1.604	1.670	1.736	1.802	1.868	1.934

Figure 4 shows function (6.4e) and (6.5e) fitted onto the above results.

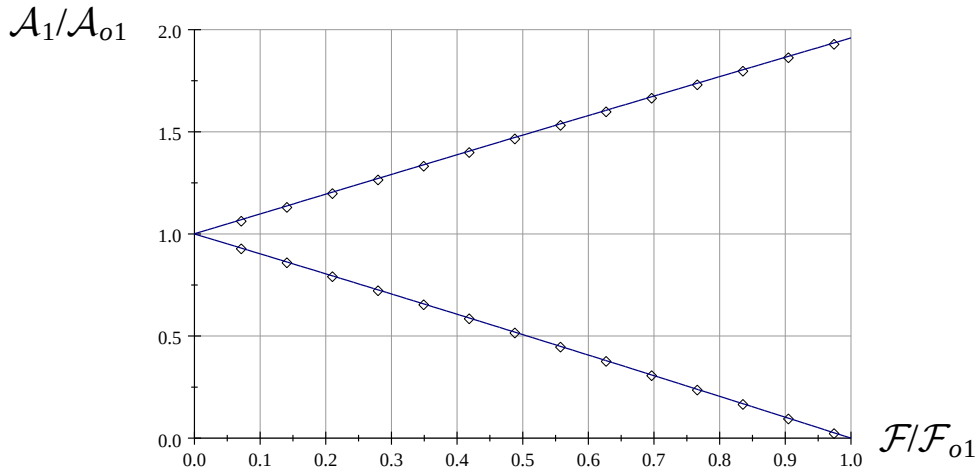

Figure 4.

7. Concluding remarks

We have dealt with the vibrations of circular plates subjected to a constant radial load in its plane on the outer boundary. The load can be either compressive or tensile. When solving the problem we have assumed that the deformations due to the load are also axisymmetric.

(a) We have determined the Green functions for three support arrangements – a clamped plate, a simply supported plate and a plate supported by a torsional spring on its outer boundary – and for tensile and compressive in-plane loads as well. With the Green functions, the self adjoint eigenvalue problems giving the natural frequencies of the vibrations for the circular plates and loads considered have been replaced by six eigenvalue problems each of which is governed by a Fredholm integral equation.

(b) If the plate is subjected to a load perpendicular to the middle plane the deflections can be determined by integration – see equation (4.28).

(c) The eigenvalue problems governed by the Fredholm integral equations are reduced to algebraic eigenvalue problems and the eigenvalues as functions of the load are computed using the boundary element method and the QZ algorithm. According to the results the square of the first natural frequency can be approximated with good accuracy (or accurately for a simply supported plate) by linear functions of the load for the parameters (material constants and geometrical data) considered.

(d) Though in Section 6 we have presented the computational results for the first eigenvalues only, it seems probable on the basis of the computational results that equation

$$\frac{\mathcal{A}_i}{\mathcal{A}_{oi}} \approx 1.000 - 1.000 \frac{\mathcal{F}}{\mathcal{F}_{oi}} \tag{7.1}$$

provides a very good approximation if $i > 1$.

Finally we remark that investigations for annular plates are in progress. Some preliminary results for compressive loads were presented earlier [18, 2005], [19, 2005].

Appendix A. Bessel functions – fundamental relations

Let us denote $J_n(x)$ and $Y_n(x)$ uniformly by $H_n(x)$. The following relations hold

$$\frac{dH_0(x)}{dx} = -H_1(x) \ , \tag{A.1a}$$

$$\frac{dH_1(x)}{dx} = \frac{1}{x}\left(H_0(x)\, x - H_1(x)\right) = H_0(x) - \frac{1}{x} H_1(x) = \frac{1}{2}\left(H_0(x) - H_2(x)\right) \ , \tag{A.1b}$$

$$\frac{dH_n(x)}{dx} = \frac{1}{2}\left(H_{n-1}(x) - H_{n+1}(x)\right) \ , \tag{A.1c}$$

$$\frac{2n}{x} H_n(x) = H_{n-1}(x) + H_{n+1}(x) \ , \tag{A.1d}$$

and

$$Y_n(x) J_{n+1}(x) - Y_{n+1}(x) J_n(x) = \frac{2}{\pi x} \ . \tag{A.1e}$$

See [20, 1977a] for more details.

As regards the Bessel functions $I_n(x)$ and $K_n(x)$, use has been made of the following relations

$$\frac{dI_0(x)}{dx} = I_1(x) \ , \qquad \frac{dK_0(x)}{dx} = -K_1(x) \ , \tag{A.2a}$$

$$\frac{dI_1(x)}{dx} = \frac{1}{x}\left(xI_0(x) - I_1(x)\right) = I_0(x) - \frac{1}{x} I_1(x) = \frac{1}{2}\left(I_0(x) + I_2(x)\right) \ , \tag{A.2b}$$

$$\frac{dI_n(x)}{dx} = \frac{1}{2}\left(I_{n-1}(x) + I_{n+1}(x)\right) \ , \tag{A.2c}$$

$$\frac{2n}{x} I_n(x) = I_{n-1}(x) - I_{n+1}(x) \ , \tag{A.2d}$$

$$\frac{dK_1(x)}{dx} = -\frac{1}{x}\left(xK_0\left(x\right) + K_1\left(x\right)\right) = -K_0\left(x\right) - \frac{1}{x}K_1\left(x\right) = -\frac{1}{2}\left(K_0(x) + K_2(x)\right) \ , \tag{A.2e}$$

$$\frac{dK_n(x)}{dx} = -\frac{1}{2}\left(K_{n-1}(x) + K_{n+1}(x)\right) \ , \tag{A.2f}$$

$$-\frac{2n}{x} I_n(x) = K_{n-1}(x) - K_{n+1}(x) \ , \tag{A.2g}$$

and

$$I_n(x)K_{n+1}(x) + I_{n+1}(x)K_n(x) = \frac{1}{x} \ . \tag{A.2h}$$

See [20, 1977b] for more details.

Appendix B. Clamped plate – calculation of the integration constants

After solving equation system (4.10) we have

$$A_1 = \frac{1}{2\pi f}\left(\ln\xi - \frac{J_{01} - J_{0\xi}}{\sqrt{\mathcal{F}}J_{11}}\right) \ , \qquad A_3 = \frac{1}{4f}\left(\frac{2}{\pi\sqrt{\mathcal{F}}J_{11}} - Y_{0\xi} + \frac{Y_{11}J_{0\xi}}{J_{11}}\right) \ , \tag{B.1a}$$

$$B_1 = \frac{1}{2\pi f}\frac{J_{0\xi} - J_{01}}{\sqrt{\mathcal{F}}J_{11}} \ , \ , \qquad B_2 = \frac{1}{2\pi f} \ , \qquad B_3 = \frac{1}{2\pi f}\left(\frac{1}{\sqrt{\mathcal{F}}J_{11}} + \frac{\pi Y_{11}J_{0\xi}}{2J_{11}}\right) \tag{B.1b}$$

and

$$B_4 = -\frac{1}{2f\pi}\frac{\pi J_{0\xi}}{2} \ . \tag{B.1c}$$

Substitution of the solutions above into (4.2) yields the Green function for the clamped plate.

References

1. R. Lawther: On the straightness of eigenvalue iterations. *Computational Mechanics*, **37**, (2006), 362–368.
2. S. Syngellakis and A. Elzein: Plate buckling loads by the the boundary element method. *International Journal for Numerical Methods in Engineering*, **37**, (1994), 1763–1778.
3. M. S. Nerantzaki and J. T. Katsikadelis: Buckling of plates with variable thickness – an analog solution. *Engineering Analysis with Boundary elements*, **18**, (1996), 149–154.
4. J. Lin, R. C. Duffield and H. Shih: Buckling analysis of elastic plates by boundary element method. *Engineering Analysis with Boundary Elements*, **23**, (1999), 131–137.
5. P. H. Wen, M. H. Aliabadi and A. Young: Application of dual reciprocity method to plates and shells. *Engineering Analysis with Boundary elements*, **24**, (2000), 583–590.
6. J. Purbolaksono and M. H. Aliabadi: Buckling analysis of shear deformable plates by boundary element method. *International Journal for Numerical Methods in Engineering*, **62**, (2005), 537–563.

7. C.D. Mote Jr: Free vibrations of initially stressed circular disks. *Journal of Engineering for Industry*, **87**, (1965), 258–364.
8. G. C. Pardoen: Vibration and buckling analysis of axisymmetric polar orthotropic circular plates. *Computers & Structures*, **4**, (1974), 951–960.
9. D. Chotova: Vibrations of circular plates subjected to an in plane load. Master thesis (in Hungarian), Department of Mecahnics, University of Miskolc, Hungary, 1980.
10. L. W. Chen and J. L. Dong: Large amplitude vibration of an initially stressed hick circular plate. *AIAA*, **21**, (1983), 1317–1324.
11. L. W. Chen and J. L. Dong: Vibrations of an initially stressed transversely isotropic circular thick plate. *International Journal of Mechanical Sciences*, **26**(4), (1984), 253–263.
12. A. Tylikowskia and K. Frischmuthb: Stability and stabilization of circular plate parametric vibrations. *International Journal of Solids and Structures*, **40**, (2003), 5187–5196.
13. D. Younesian and M. H. Aleghafourian: A direct formulation and numerical solution of the general transient elastodynamic problem. *International Journal of Civil Engineering and Building Materials*, **2**(4), (2012), 167–174.
14. N. Szűcs: Vibrations of circular plates subjected to an in-plane load. *GÉP*, **LVIII**(5-6), (2007), 41–47. (in Hungarian).
15. P. Zdeněk Bažant and L. Cedolin: *Stability of structures, Elastic, Inelastic, Fracture, and Damage Theories* (2nd edition). Dover Publications, Inc. Mineola, New York, 2003, p. 427.
16. I. Kozák: *Strength of materials V. – Thin walled structures and the theory of plates and shells*. Tankönyvkiadó (Publisher of Textbooks), Budapest, Hungary, 1967, pp. 287-291. (in Hungarian).
17. C. T. H. Baker: *The Numerical Treatment of Integral Equations – Monographs on Numerical Analysis*. Clarendon Press, Oxford, 1977.
18. G. Szeidl, D. Georgieva and N. Szűcs: Vibration of a circular plate with a hole subjected to a radial uniform load in its plane. In *Section G: Applied Mechanics, Modern Numerical Methods*, pages 149–154, microCAD 2005, University of Miskolc, March 10-11, 2005.
19. G. Szeidl, N. Szűcs and B. Tóth: Vibration of circular plates subjected to uniform loads in their plane. In V. Kompis, editor, *Numerical Methods on Continuum Mechanics and 4th Workshop on Trefftz Methods*, Slovakia, August 23-26, 2005., Extended six page abstract on the conference CD.
20. E. Janke, F. Emde and F. Lösch: *Tafelen Höheren Funktionen*. Nauka, Moscow, 1977, (a) p. 241-242 and (b) 245-246. (Russian edition.)

Notes for Contributors

to the Journal of Computational and Applied Mechanics

Aims and scope. The aim of the journal is to publish research papers on theoretical and applied mechanics. Special emphasis is given to articles on computational mechanics, continuum mechanics (mechanics of solid bodies, fluid mechanics, heat and mass transfer) and dynamics. Review papers on a research field and materials effective for teaching can also be accepted and are published as review papers or classroom notes. Papers devoted to mathematical problems relevant to mechanics will also be considered.

Frequency of the journal. Two issues a year (approximately 80 pages per issue).

Submission of Manuscripts. Submission of a manuscript implies that the paper has not been published, nor is being considered for publication elsewhere. Papers should be written in standard grammatical English. The manuscript is to be submitted in electronic, preferably in pdf, format. The text is to be 130 mm wide and 190 mm long and the main text should be typeset in 10pt CMR fonts. Though the length of a paper is not prescribed, authors are encouraged to write concisely. However, short communications or discussions on papers published in the journal must not be longer than 2 pages. Each manuscript should be provided with an English Abstract of about 50–70 words, reporting concisely on the objective and results of the paper. The Abstract is followed by the Mathematical Subject Classification – in case the author (or authors) give the classification codes – then the keywords (no more than five). References should be grouped at the end of the paper in numerical order of appearance. Author's name(s) and initials, paper titles, journal name, volume, issue, year and page numbers should be given for all journals referenced.

The journal prefers the submission of manuscripts in LaTeX. Authors should prefer the $\mathcal{AMS}$-LaTeX article class and are not recommended to define their own LaTeX commands. Visit our home page for further details concerning how to edit your paper.

For the purpose of refereeing the manuscripts should be sent either to Balázs Tóth (Balazs.TOTH@uni-miskolc.hu) or György SZEIDL (Gyorgy.SZEIDL@uni-miskolc.hu).

The eventual supply of an accepted for publication paper in its final camera-ready form will ensure more rapid publication. Format requirements are provided by the home page of the journal from which sample LaTeX files can be downloaded:

http://www.mech.uni-miskolc.hu/jcam

These sample files can also be obtained directly (via e-mail) from Balázs TÓTH (Balazs.TOTH@uni-miskolc.hu), upon request.

One issue of the journal and ten offprints will be provided free of charge and mailed to the correspondent author. Since JCAM is an open access journal each paper can be downloaded freely from the homepage of the journal.

The Journal of Computational and Applied Mechanics is abstracted in Zentralblatt für Mathematik and in the Russian Referativnij Zhurnal.

Secretariat of the Vice-Rector for Research and International Relations, University of Miskolc
Responsible for publication: Prof. Dr. Tamás Kékesi
Published by the Miskolc University Press under the leadership of Attila Szendi
Responsible for duplication: Works manager Erzsébet Pásztor
Number of copies printed: 75
Put to the Press on June 30, 2017
Number of permission: TNRT. 2017-240.ME **HU ISSN 1586–2070**

A Short History of the Publications of the University of Miskolc

The University of Miskolc (Hungary) is an important center of research in Central Europe. Its parent university was founded by the Empress Maria Teresia in Selmecbánya (today Banska Štiavnica, Slovakia) in 1735. After the first World War the legal predecessor of the University of Miskolc moved to Sopron (Hungary) where, in 1929, it started the series of university publications with the title *Publications of the Mining and Metallurgical Division of the Hungarian Academy of Mining and Forestry Engineering* (Volumes I.-VI.). From 1934 to 1947 the Institution had the name Faculty of Mining, Metallurgical and Forestry Engineering of the József Nádor University of Technology and Economic Sciences at Sopron. Accordingly, the publications were given the title *Publications of the Mining and Metallurgical Engineering Division* (Volumes VII.-XVI.). For the last volume before 1950 – due to a further change in the name of the Institution – *Technical University, Faculties of Mining, Metallurgical and Forestry Engineering, Publications of the Mining and Metallurgical Divisions* was the title.

For some years after 1950 the Publications were temporarily suspended.

After the foundation of the Mechanical Engineering Faculty in Miskolc in 1949 and the movement of the Sopron Mining and Metallurgical Faculties to Miskolc, the Publications restarted with the general title *Publications of the Technical University of Heavy Industry* in 1955. Four new series - Series A (Mining), Series B (Metallurgy), Series C (Machinery) and Series D (Natural Sciences) - were founded in 1976. These came out both in foreign languages (English, German and Russian) and in Hungarian.

In 1990, right after the foundation of some new faculties, the university was renamed to University of Miskolc. At the same time the structure of the Publications was reorganized so that it could follow the faculty structure. Accordingly three new series were established: Series E (Legal Sciences), Series F (Economic Sciences) and Series G (Humanities and Social Sciences). The latest series, i.e., the series H (European Integration Studies) was founded in 2001. The eight series are formed by some periodicals and such publications which come out with various frequencies.

Papers on computational and applied mechanics were published in the

Publications of the University of Miskolc, Series D, Natural Sciences.

This series was given the name Natural Sciences, Mathematics in 1995. The name change reflects the fact that most of the papers published in the journal are of mathematical nature though papers on mechanics also come out.

The series

Publications of the University of Miskolc, Series C, Fundamental Engineering Sciences

founded in 1995 also published papers on mechanical issues. The present journal, which is published with the support of the Faculty of Mechanical Engineering and Informatics as a member of the Series C (Machinery), is the legal successor of the above journal.

Journal of Computational and Applied Mechanics

Volume 12, Number 1 (2017)

Contents

Contributed Papers

István ECSEDI and Attila BAKSA: A half circular beam bending by radial loads 3–18

László Péter KISS: Green's functions for nonhomogeneous curved beams with applications to vibration problems 19–41

Ákos József LENGYEL: Dynamic analysis of composite beams with weak shear connection subjected to an axial load 43–55

Nóra SZŰCS and György SZEIDL: Vibration of circular plates subjected to constant radial load in their plane 57–76